(2)

AD

AMMRC TR 85-2

LOW-COST, NET-SHAPE CERAMIC RADIAL TURBINE PROGRAM

May 1985

D.W. RICHERSON and J.R. SMYTH
GARRETT TURBINE ENGINE CO.
A Division of The Garrett Corporation
111 S. 34th St., P.O. Box 5217
Phoenix, AZ 85010

FINAL TECHNICAL REPORT for the Period
February 1981 — December 1984

Prepared for

ARMY MATERIALS AND MECHANICS RESEARCH CENTER
Watertown, Massachusetts 02172

The findings in this report are not to be construed as an official Department of the Army position, unless so designated by other authorized documents.

Mention of any trade names or manufacturers in this report shall not be construed as advertising nor as an official indorsement or approval of such products or companies by the United States Government.

DISPOSITION INSTRUCTIONS

Destroy this report when it is no longer needed.
Do not return it to the originator.

UNCLASSIFIED

SECURITY CLASSIFICATION OF THIS PAGE (When Data Entered)

REPORT DOCUMENTATION PAGE	READ INSTRUCTIONS BEFORE COMPLETING FORM
1. REPORT NUMBER	2. GOVT ACCESSION NO. AD-A157532	3. RECIPIENT'S CATALOG NUMBER
4. TITLE (and Subtitle) LOW-COST, NET-SHAPE CERAMIC RADIAL TURBINE PROGRAM FINAL TECHNICAL REPORT	5. TYPE OF REPORT & PERIOD COVERED Final Report Feb 1981 - Dec 1984
	6. PERFORMING ORG. REPORT NUMBER 21-5541
7. AUTHOR(s) D. Richerson J. Smyth	8. CONTRACT OR GRANT NUMBER(s) DAAG46-81-C-0006
9. PERFORMING ORGANIZATION NAME AND ADDRESS Garrett Turbine Engine Company 111 South 34th Street, P.O. Box 2517 Phoenix, Arizona 85010	10. PROGRAM ELEMENT, PROJECT, TASK AREA & WORK UNIT NUMBERS
11. CONTROLLING OFFICE NAME AND ADDRESS U.S. Army Materials and Mechanics Research Center Arsenal Street Watertown, Massachusetts 07172	12. REPORT DATE May 1985
	13. NUMBER OF PAGES 161
14. MONITORING AGENCY NAME & ADDRESS(if different from Controlling Office) U.S. Army Materials and Mechanics	15. SECURITY CLASS. (of this report) Unclassified
	15a. DECLASSIFICATION/DOWNGRADING SCHEDULE

16. DISTRIBUTION STATEMENT (of this Report)

Approved for public release; distribution unlimited.

17. DISTRIBUTION STATEMENT (of the abstract entered in Block 20, if different from Report)

18. SUPPLEMENTARY NOTES

(author(s))

19. KEY WORDS (Continue on reverse side if necessary and identify by block number)

Ceramic engine; Ceramics; Brittle material design; Component design; Silicon nitride; Injection molding; Low cost; Mechanical properties; Net shape; Processing;

20. ABSTRACT (Continue on reverse side if necessary and identify by block number)

This program's technical objective was to establish

The AMMRC/Garrett Low-Cost, Net-Shape Ceramic Radial Turbine Rotor Program was begun in 1981 with the objective establishing an injection-molded sintered silicon nitride manufacturing process to produce net-shape ceramic radial turbine rotors with high-temperature properties suitable for operation at tip speeds of 2000 feet per second and turbine inlet temperatures of 2500F.

DD FORM 1 JAN 73 1473 EDITION OF 1 NOV 65 IS OBSOLETE

UNCLASSIFIED

SECURITY CLASSIFICATION OF THIS PAGE (When Data Entered)

Block No. 20

ABSTRACT

The three-phase program consisted of: 1) screening 14 different sintered Si_3N_4 compositions; 2) process optimization and rotor fabrication; and 3) rotor stress analysis and rotor spin testing.

A composition of 92 percent Si_3N_4 - 6 percent Y_2O_3 - 2 percent Al_2O_3 was developed with room temperature strength in excess of the 90 ksi program goal. A second composition (94 percent Si_3N_4 - 6 percent Y_2O_3) was developed with room temperature and 2250F strength in excess of the 90 ksi and 80 ksi program goals respectively.

T02 turbocharger rotors were fabricated from the improved materials and exhibited burst speeds during spin testing up to 212,000 rpm. The burst speeds were lower than were predicted analytically based on the test bar strength data. Surface defects such as knit lines and cracks were consistently present in the rotors and possibly contributed to the low burst speed.

EXECUTIVE SUMMARY

The technical objective of the program was to establish an injection molded sintered silicon nitride manufacturing process to produce net-shape ceramic radial turbine rotors with properties suitable for operation at tip speeds of 2000 feet per second and material temperatures of 2250F (corresponding to turbine inlet temperatures of approximately 2500F). Specific goals to demonstrate achievement of this objective included:

- Increase in room temperature flexural strength of test bars to 90 ksi
- Increase in 2250F test bar flexural strength to 80 ksi
- Fabrication of injection molded radial rotors with existing tooling
- Achievement of high strength in test bars machined from radial rotors
- Spin testing of injection molded radial rotors to 2000 feet per second tip speed.

The program was conducted in three phases, as shown in Figure 1. Phase I involved the screening of 14 different sintered Si_3N_4 compositions. Test bars were fabricated and evaluated with promising compositions selected for more detailed process optimization in Phase II. In addition to this process optimization, Phase II involved rotor fabrication, rotor stress analysis, and spin testing. Phase III involved continued iterations of rotor injection molding and spin testing. Several no-additional-cost time extensions were granted by AMMRC to permit additional material processing iterations.

Program management and materials characterization were conducted at Garrett Turbine Engine Company (GTEC), test bar and rotor fabrication were accomplished at AiResearch Casting

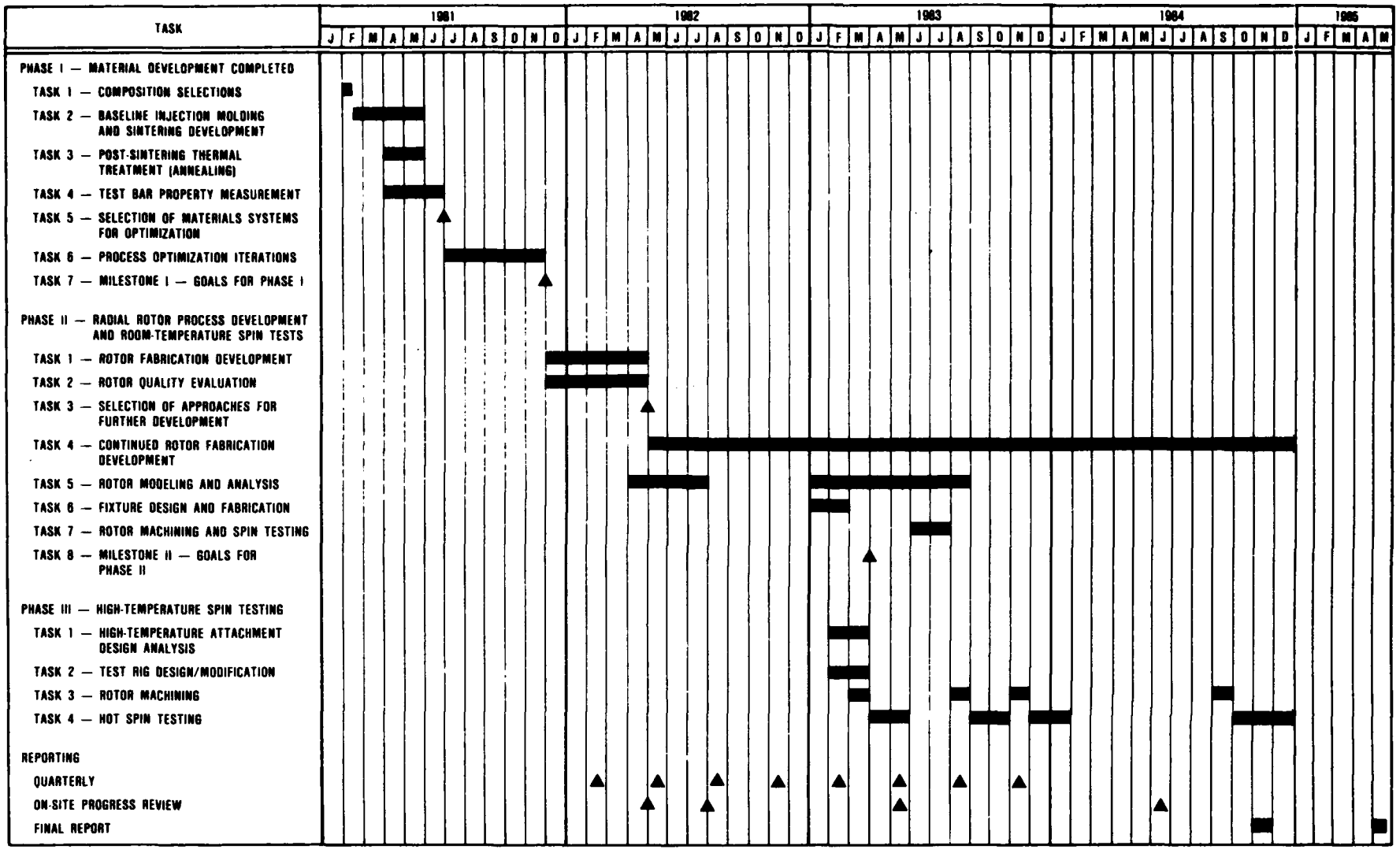

Figure 1. Schedule for Low-Cost, Net-Shape Ceramic Radial Turbine Program.

Company (ACC), and rotors were integrated into turbochargers and spin tested at Garrett Automotive Products Company (GAPCO).

Some of the ACC and GAPCO efforts were performed under company funding as a cost share. Additional efforts were conducted at no cost to the program at AMMRC, NASA Lewis Research Center, Ford Motor Company, and the General Electric Company. These efforts consisted primarily of sintering runs conducted with program specimens in a variety of nitrogen overpressure furnaces. In addition, AMMRC performed a series of stress rupture tests on program specimens.

Room Temperature Strength Increase

The improvements accomplished in room temperature flexure strength of sintered Si_3N_4 are illustrated as a function of time in Figure 2. The baseline sintered Si_3N_4 had a room temperature flexure strength of about 72 ksi. Fractography indicated that the strength was limited largely by molding flaws, i.e., flow lines, voids, and shrinkage cracks, by general porosity due to incomplete densification, and by surface flaws due to dissociation during sintering.

Molding flaws were reduced by modifying binder content, material and die temperature, and molding pressure. Iterative changes of these parameters resulted in increasing the room temperature strength to 88 ksi, as measured in the as-sintered condition. At this point in the development, molding flaws had largely been eliminated, and fractures were initiating at surface defects caused by dissociation during sintering.

The slight drop in the curve in Figure 2 in May 1982 resulted from a change in composition in which the Y_2O_3 was reduced from 8 to 6 percent, and the Al_2O_3 was reduced from 4 to 2 percent. This reduction in additives was made to improve

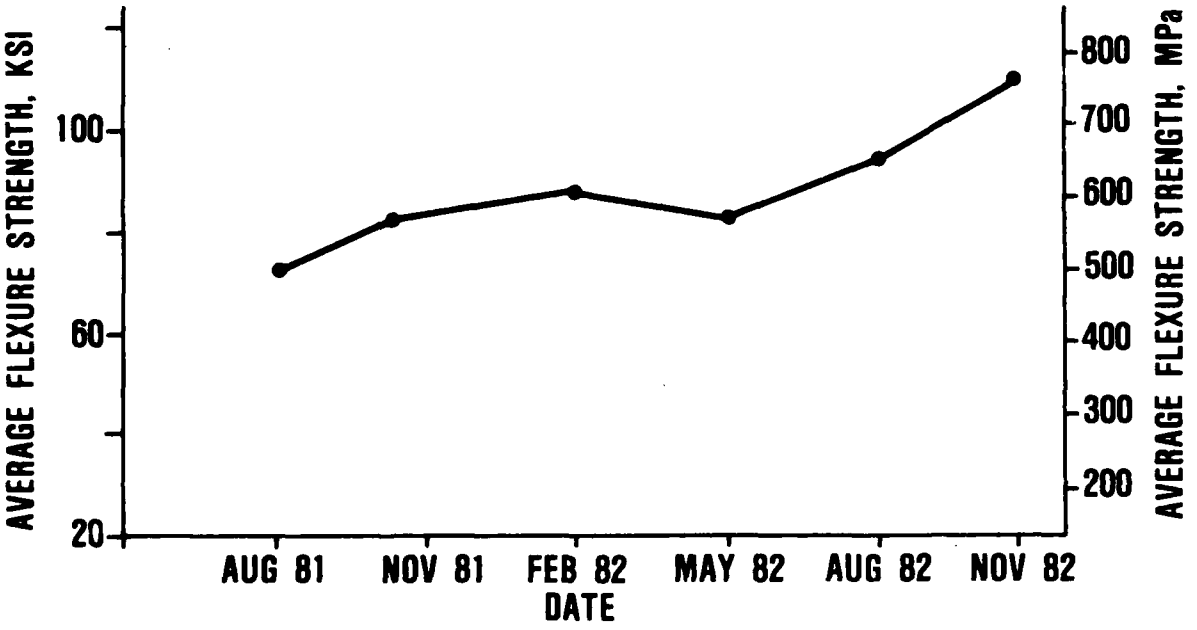

Figure 2. Room Temperature Strength Improvement for Injection-Molded Sintered Si_3N_4 Met Program Goals.

the high temperature strength, but also required modification of the sintering parameters to maintain the room temperature strength achieved with the prior composition. The major modifications involved increases in the temperature and nitrogen pressure during sintering. The last two data points, in which average strengths of 93 ksi and 111 ksi were obtained on machined test bars reflect, the results of these modifications. The 111 ksi average is for a 6 percent Y_2O_3 - 0 percent Al_2O_3 composition. These room temperature strengths exceeded the program goals.

High Temperature Strength Improvement

The improvements in the high temperature strength of injection molded Si_3N_4 achieved through iterative process development are illustrated in Figure 3. The baseline sintered Si_3N_4 had an average 2250F flexure strength of 52 ksi in the as-sintered condition.

High temperature strength improvements were achieved through reductions in the quantity of Y_2O_3 and Al_2O_3 sintering aids accompanied by increases in the temperature and nitrogen pressure during sintering. A high nitrogen pressure furnace was not available initially, which explains why no improvements were obtained between August 1981 and May 1982. However, hot isostatic pressing (HIP) of glass-encapsulated specimens was conducted during this time to screen compositions and pick one which, if fully densified, would meet the program objectives. Sintering trials were then pursued with this and other compositions in high nitrogen pressure sintering runs conducted by AMMRC, Ford, and NASA.

The August 1982 strength data in Figure 3 is for the 6 percent Y_2O_3 - 2 percent Al_2O_3 composition, and the last two points are for a 6 percent Y_2O_3 - 0 percent Al_2O_3 composition.

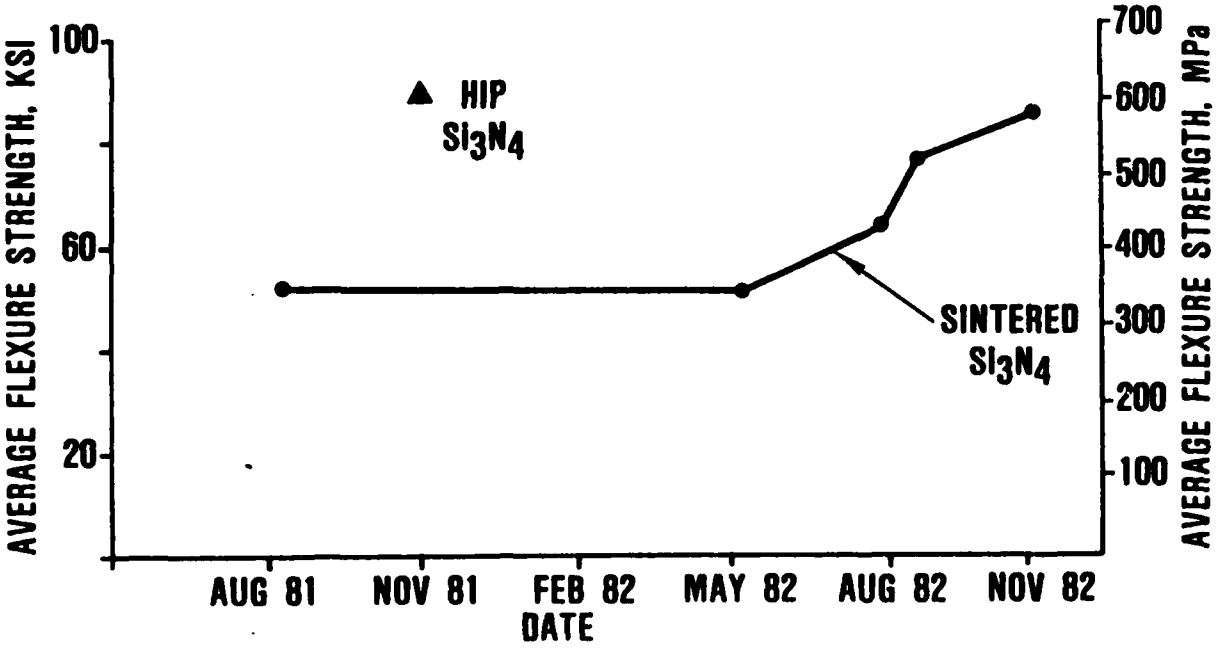

Figure 3. Room Temperature Strength Improvement for Injection-Molded Sintered Si_3N_4 Met Program Goals.

Data for all three were measured on machined test bars, and the final data met program goals. The hot-isostatic-pressing (HIP) strength data point was also obtained on a 6 percent Y_2O_3 - 0 percent Al_2O_3 composition and was measured on as-HIPed test bars.

Radial Rotor Fabrication

Initial rotor fabrication studies utilized tooling for a Garrett TO4 size radial turbocharger rotor. This tooling, selected because of its availability at the start of the program, was constructed of aluminum and had previously been used to injection mold wax patterns for metal rotor fabrication by the investment casting technique.

Figure 4 compares an as-injected TO4 size Si_3N_4 rotor with one after binder removal and sintering. The maximum tip diameter of the as-injected rotor was 3 inches and the length (including the shaft) was 5 inches. Rotors were fabricated with the TO4 tooling using both the direct sintering approach with Code 1 (88 percent Si_3N_4 - 8 percent Y_2O_3 - 4 percent Al_2O_3) and Code 2 (92 percent Si_3N_4 - 6 percent Y_2O_3 - 2 percent Al_2O_3) compositions and the sintered reaction-bonded Si_3N_4 (SRBN) approach with the Code 7 (Si plus 6 percent Y_2O_3 -2 percent Al_2O_3 - 1 percent Fe_2O_3) composition.

Significant problems were encountered in fabricating rotors with the TO4 tool. These problems manifested themselves as cracks and shrink voids in the rotors. Improvements were achieved through process modifications, but no defect-free rotors were obtained. A major problem was judged to be the TO4 tooling, since it was not designed for ceramics and had limitations such as sharp radii at edges and inadequate contouring to transition from the hub to the blades.

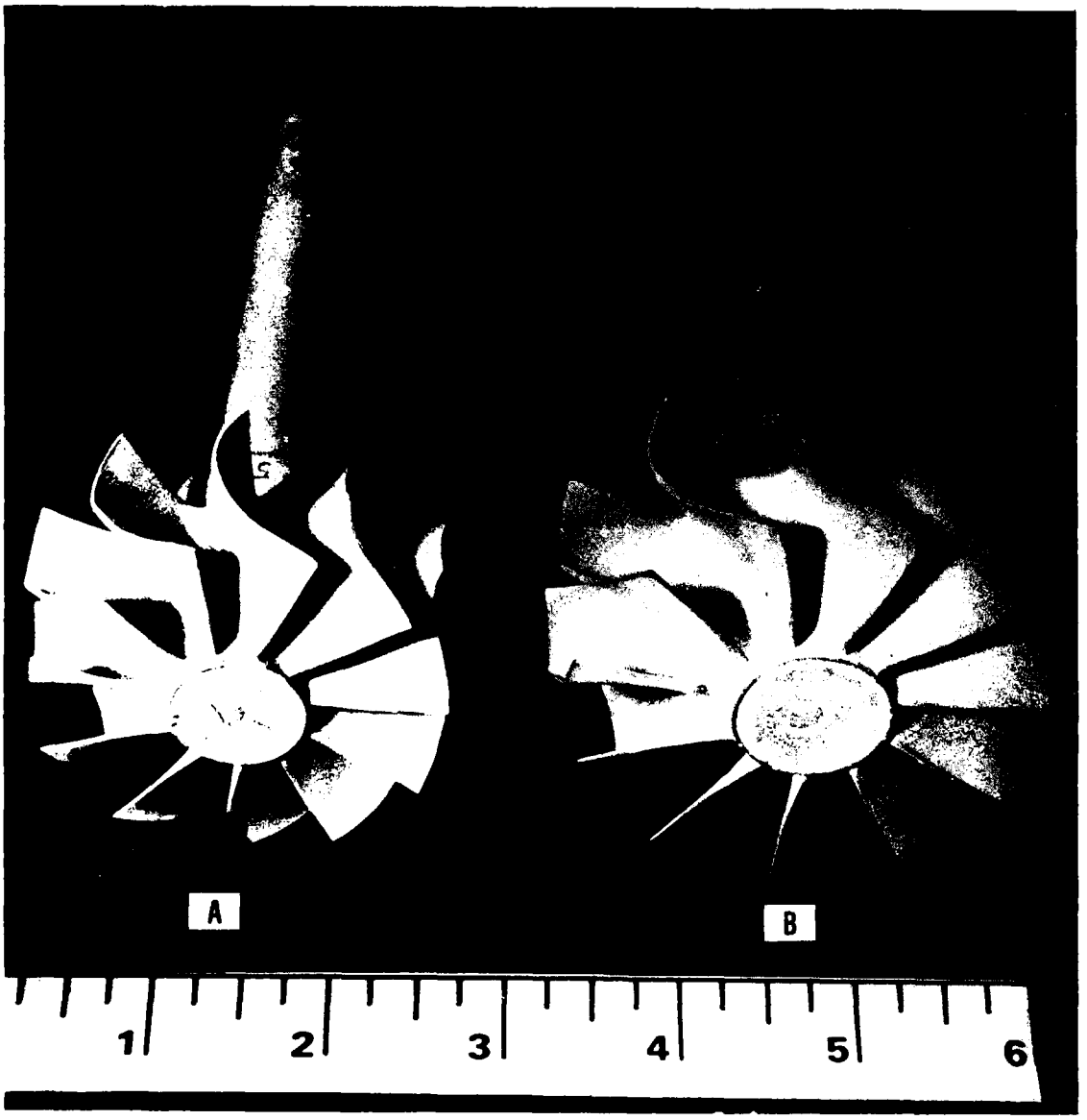

Figure 4. TO4 Rotor--A) As sintered B) As Injection-Molded.

Parallel to this program, ACC and GAPCO conducted an in-house effort to develop a TO2 size (smaller than TO4) ceramic radial turbocharger rotor. This effort included fabrication of a steel injection molding tool designed specifically for ceramics. Garrett and AMMRC jointly agreed to discontinue studies with the TO4 tool and switch to the new TO2 tool. This change would take advantage of the improved tool design as well as benefit from molding technology being developed under the Garrett in-house program.

TO2 rotors of several different compositions were injection-molded free of internal defects as determined by X-ray radiography and intermittently verified by fracturing or sectioning molded rotors. However, by the time the binder was removed and the rotors were sintered to near-theoretical density, varying degrees of surface defects appeared on each rotor. These defects were primarily of two types: (1) flow lines (cracks) in the hub and shaft area, and (2) cracks at the blade-hub transition at the exducer end of the rotor. The TO2 tool was improved to provide a larger radius at the blade root and additional processing iterations were conducted with the modified tool. Some as-molded rotors and some rotors after binder removal (dewaxed) are shown in Figure 5.

Strength of Test Bars Machined From Rotors

Test bars were machined from the interior of injection molded sintered rotors fabricated at ACC and the flexural strength measured both at room temperature and at 2250F. The room temperature results are listed in Table 1, along with similar measurements obtained by Garrett on TO2 ceramic turbocharger rotors from NGK Insulators* and Kyocera**. Although

*Nagoya, Japan
**Kyoto, Japan

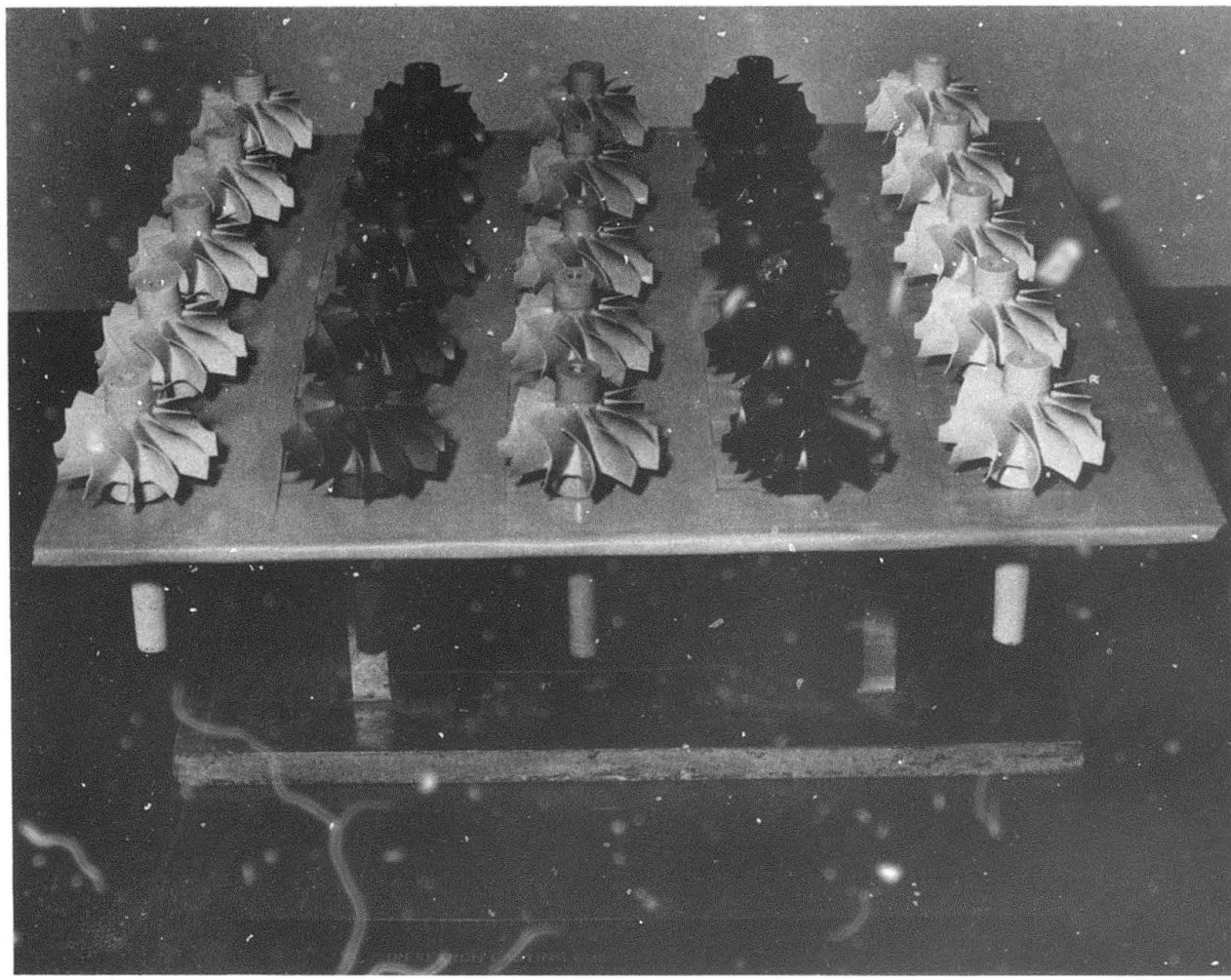

Figure 5. Codes 2 and 7 Molded and Dewaxed T02 Rotors (Row 1-Code 2 Dewaxed; Row 2-Code 7 Dewaxed; Row 3-Code 2 Molded; Row 4-Code 7 Molded; Row 5-Code 2 Dewaxed).

MP-86605

TABLE 1. ROOM TEMPERATURE STRENGTH OF TEST BARS CUT FROM ROTORS

Specimen No.	Flexure Strength[a] (ksi)	Fracture Origin[b]
Code 2		
12063-5	104.1	---
12063-6	83.8	---
12063-9	83.8	---
12063-11	97.9	---
12063-18	45.6	Flow line
12063-21	30.9	Large low density area
Code 7		
09143-5	80.1	---
09143-6	70.3	---
10033-4	87.2	---
10033-14	54.0	Large internal void
10033-16	57.4	Internal flow line
10033-17	68.6	Subsurface porous area
NGK SN50		
N 116A	68.7	Large Grain or Agglomerate
N 133A	52.1	Large Grain or Agglomerate
N 133B	63.5	Large Grain or Agglomerate
N 136A	54.2	Large Grain or Agglomerate
N 136B	62.5	Large Grain or Agglomerate
N 141A	54.2	Large Grain or Agglomerate
N 141B	46.9	Large Grain or Agglomerate
N 141A	53.6	Large Grain or Agglomerate
N 141B	58.3	Large Grain or Agglomerate
N 150A	46.9	Large Grain or Agglomerate
Kyocera SN220		
14767	124.4	Tensile Face
14768	100.8	Inclusion
14769	112.3	Tensile Face
14770	91.6	Tensile Face

[a]4-point bend
[b]10-40X

limited, the data indicate that the AMMRC turbocharger rotors are comparable to other state-of-the-art rotors, but that process improvements are still required.

Rotor Spin Testing

The original program plan was to attach ceramic rotors to metal shafts and spin them in an evacuated whirlpit to failure. Evaluation during the program determined that the speed of available whirlpit hardware was not high enough to accomplish the room temperature burst tests. The decision was then made to conduct all the rotor tests in actual turbochargers operating at 1750F. The results are summarized in Table 2 and compared with the results obtained on rotors procured from NGK Insulators and Kyocera. The Code 2 rotors failed due to flaws that had been identified prior to test.

Silicon Nitride Wettability Study

A subcontract was issued to the University of Washington to study the wettability of Y_2O_3-Al_2O_3-SiO_2 compositions on Si_3N_4 substrates. The main tasks of this study were the measurement of the contact angle of sessile drops of various Y_2O_3-Al_2O_3-SiO_2 compositions on CVD Si_3N_4 and the compilation of data on the Si_3N_4-Y_2O_3-Al_2O_3-SiO_2 phase system.

This sessile drop study was conducted to better understand the wetting behavior of Y_2O_3-Al_2O_3-SiO_2 liquids on Si_3N_4 as a function of composition and temperature, and to use this information to aid in optimizing the system for pressureless sintering of Si_3N_4.

A camera mounted telescope was used to observe and record the sessile drop behavior in a graphite tube furnace under flowing N_2. Polished CVD α-Si_3N_4 was used as the substrate

TABLE 2. ROTOR SPIN TEST RESULTS AT 1750F

Material	Rotors	Burst Speed (krpm)
Code 2 (This Program)	1	212
	2	157
	3	160
	4	148
	5	197
	6	143
	7	142
	8	168
	9	154
SN220 (Kyocera)	1	201
	2	189
	3	157
	4	197
	5	190
	6	180
	7	177
	8	155
SN50 (NGK)	1	238
	2	216
	3	188
	4	177
	5	206
	6	187
	7	174
	8	152
	9	140

material because of its high purity and theoretical density. All compositions eventually wet the CVD Si_3N_4 as the temperature increased, but many showed strong reactivity and gas evolution at the increased temperatures.

Summary Conclusions

- Room temperature and high temperature strengths of test bars of sintered injection-molded Si_3N_4 were significantly improved through iterative process modification and composition changes. The program goals were met with a composition containing 6 percent Y_2O_3 which had room temperature and 2250F strengths in excess of 100 ksi and 80 ksi respectively. However, a high nitrogen pressure sintering furnace was required to densify this composition. A second composition containing 6 percent Y_2O_3 and 2 percent Al_2O_3 was developed which could be densified in a conventional furnance and exhibited room temperature and 2250F strengths in excess of 90 ksi and 60 ksi respectively. Based on these results, ACC has replaced the baseline material that existed at the start of the program (an 8 percent Y_2O_3 - 4 percent Al_2O_3 composition with room temperature and 2250F strengths of 76 ksi and 53 ksi respectively) with the lower additive composition.

- T02 turbocharger rotors were fabricated from the improved materials. Test bars cut from the interior of these rotors had strengths comparable to those of the injection-molded test bars.

- The 3-D finite element analysis based on strength data predicted a capability of 380,000 rpm with a 0.1 percent probability of failure. The target for TO2

turbocharger production is 190,000 rpm with a 0.1 percent probability of failure. However, surface defects such as knit lines and cracks were consistently present in the rotors and contributed to a lower burst speed during spin testing than was predicted based on the test bar strength data.

- The maximum burst speed during spin testing exhibited by rotors fabricated from the improved materials was 212,000 rpm. Rotors from other sources spin tested at GAPCO had similar results: 238,000 rpm maximum for TO2 rotors from NGK insulators, and 201,000 rpm maximum for TO2 rotors from Kyocera.

- Further fabrication development is necessary to eliminate the source of surface defects that limit rotor speed. Additional effort is also necessary to assess rotor dynamics and vibration to determine whether the turbocharger system design is influencing the spin test results.

- Since the 6 percent Y_2O_3 - 2 percent Al_2O_3 materials is an easily sintered composition with improved properties, it is replacing the earlier baseline composition in several ceramic turbocharger and automotive gas turbine engine rotor development efforts at ACC.

PREFACE

This is the final technical report of the Low-Cost, Net-Shape Ceramic Radial Turbine Program initiated through the Army Advanced Concepts Division. The program was funded under Contract Number DAAG46-81-C-0006 and was monitored by Dr. R. N. Katz for the Army Materials and Mechanics Research Center.

The authors would like to thank the following people for contributions to the program:

GTEC
- Dr. James Wimmer, who was the Principal Investigator early in the program, for his helpful discussion and technical contributions
- Laura Lindberg for her assistance with the fractographic analyses
- Karl Johnson, who was Program Manager during a majority of the program

ACC
- Karsten Styhr, Ed Hodge, and Hun Yeh for their direction of the test bar and rotor fabrication effort
- Lonnie Anderson and Steve Haynes for their assistance in the experimental work

GAPCO
- Mark Lasker, Joe Byrne, Harold Cox, and Ho Fang for their assistance in the machining and elevated temperature spin testing effort

AMMRC
- Dr. R.N. Katz, the AMMRC Program Manager, for his support throughout the program

- George Gazza for conducting high pressure sintering studies
- George Quinn for conducting the stress-rupture experiments

Ford Motor Co. - John Mangels for conducting high pressure sintering studies

NASA-Lewis R.C. - William Sanders for conducting high pressure sintering studies

General Electric Co. - Dr. Charles Greskovich for providing the $BeSiN_2$ sintering aid and for conducting sintering studies

AFWAL - Ron Kearns for conducting chemical analysis of the starting and processed powders

TABLE OF CONTENTS

LIST OF TABLES

LIST OF TABLES (Contd)

LIST OF ILLUSTRATIONS

LIST OF ILLUSTRATIONS (Contd)

LIST OF ILLUSTRATIONS (Contd)

LIST OF ILLUSTRATIONS (Contd)

1. INTRODUCTION

This document, submitted by the Garrett Turbine Engine Company, presents the final technical report for the Low-Cost, Net-Shape Ceramic Radial Turbine Program. The program was conducted for the Army Materials and Mechanics Research Center (AMMRC) under Contract No. DAAG46-81-C-0006. Submitted in response to CDRL Sequence Number A003, this report covers the period from February 1, 1981, through December 31, 1984.

1.1 Overall Program Description

The objective of the 47-month program was to establish an injection-molded, sintered silicon nitride manufacturing process to produce net-shape ceramic radial turbine rotors with high temperature properties suitable for operation at tip speeds of 2000 feet per second and material temperatures of 2250F (corresponding to turbine inlet temperatures of approximately 2500F). As shown in Figure 6, the program consisted of three phases:

- Phase I - Material Development
- Phase II - Radial Rotor Process Development and Room Temperature Spin Testing
- Phase III - High-Temperature Spin Testing

The objective of Phase I was to develop an injection-molded, sintered silicon nitride having the required high temperature strength and to demonstrate that this material could be injection molded into a radial rotor configuration. The Phase I goal was the retention of 70 ksi strength up to 2250F. Existing turbocharger rotor tooling, for the Garrett T04 configuration, was utilized for the demonstration of shape forming capability.

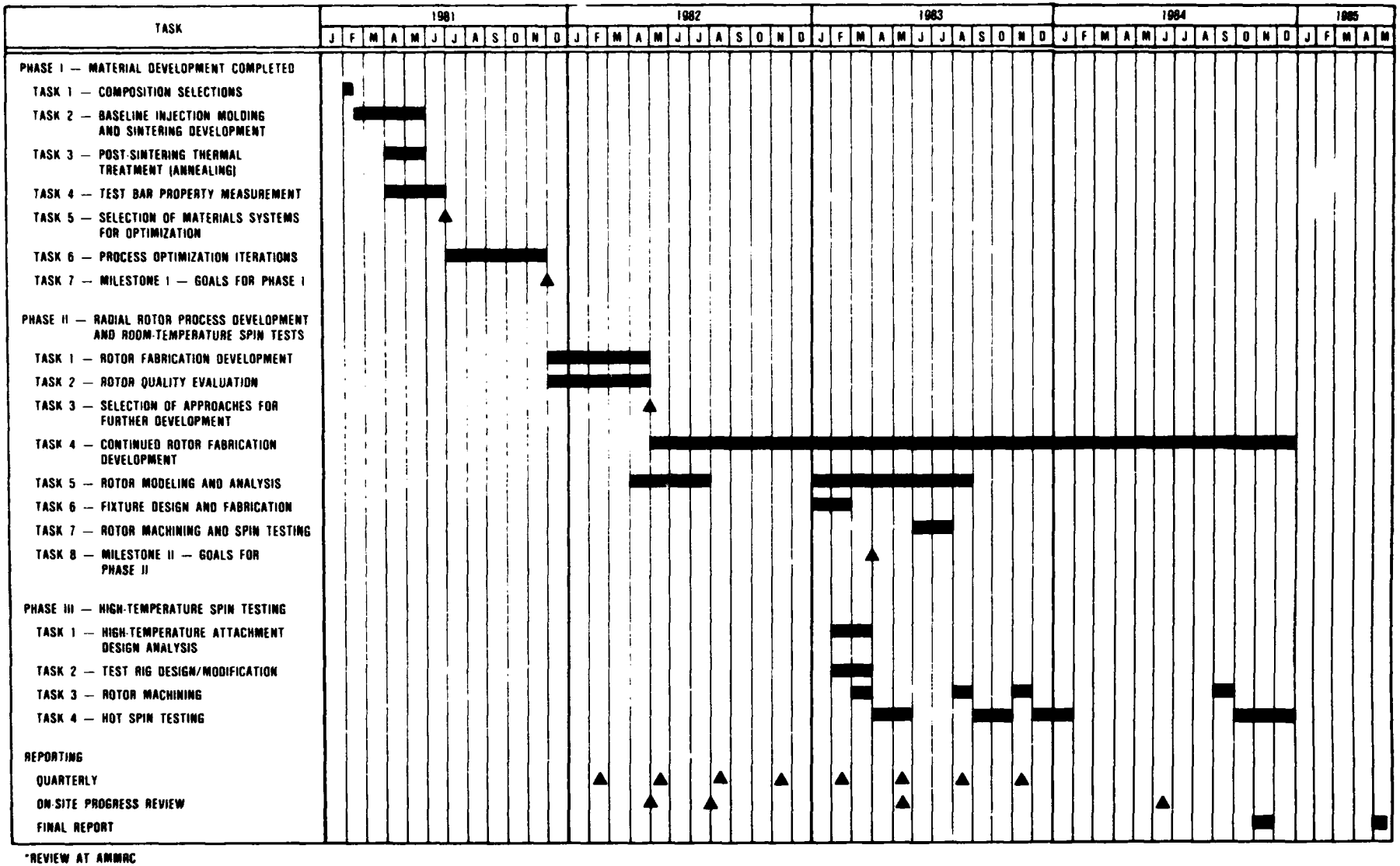

*REVIEW AT AMMRC

G3-0100-74A

Figure 6. Schedule for Low-Cost, Net-Shape Ceramic Radial Turbine Program.

Phase II continued material development, but primarily concentrated on rotor fabrication process development and on demonstrating that test-bar properties could be achieved in sintered rotors.

Phase III concentrated on accomplishing the final high-temperature material property goals of 80 ksi and on demonstrating rotor integrity through elevated temperature spin testing of sintered rotors.

Three Garrett divisions teamed to conduct the program: Garrett Turbine Engine Company (GTEC) in Phoenix, Arizona; AiResearch Casting Company (ACC) in Torrance, California; and the AiResearch Industrial Division (AID) of Garrett Automotive Products Company (GAPCO) in Lomita, California.

The AiResearch Casting Company (ACC) was responsible for the iterative process development of injection-molded, sintered silicon-nitride compositions and demonstrating that these compositions and processes are applicable to the injection-molding of net-shape ceramic radial turbine rotors of the selected turbocharger configuration.

ACC also produced test bars for process and property evaluation and was responsible for powder characterization in the "as received" and "processed" conditions.

GTEC was responsible for overall program direction and for test bar and rotor evaluation. Test bar evaluation included room- and elevated-temperature flexural testing, fractography, microstructure, X-ray diffraction phase analysis, stress ruptures, and the assessment of oxidation behavior. Rotor evaluation included determination of density and strength variation

within rotors, X-ray radiography, spin testing, and fractography. Garrett was also responsible for rotor modeling, analysis, and room temperature spin testing.

The AiResearch Industrial Division of Garrett was responsible for rotor machining, shaft attachment, balancing, and elevated-temperature spin testing.

1.2 Program Goals

The Phase I goal was to obtain a strength of 70 ksi at both room temperature and 2250F.

The Phase II goals were: (1) to obtain a room-temperature strength of 90 ksi and a 2250F strength of 80 ksi with a minimum Weibull modulus of 10 at both temperatures as measured on test bars machined from fully processed rotors; and (2) to correlate spin test results with measured test bar properties.

The Phase III goals were a further demonstration of the achievement of Phase II goal properties through elevated-temperature spin testing.

2. MATERIAL SELECTION AND DEVELOPMENT

The initial effort under the program was to select a variety of starting materials and compositions to be fabricated by injection molding into test bars 2.0 inch long by 0.125 inch thick by 0.25 inch wide. These test bars would then be strength tested in four point flexure at room temperature and 2250F using self-aligning test fixtures with an outer span of 1.5 inch and an inner span of 0.75 inch. Additional oxidation, heat treatment, and stress rupture tests would be conducted on selected specimens. Based upon all these tests plus measurements of density and examination of starting powder characteristics, injection molding characteristics, and final microstructure, candidate compositions would be selected for further development.

The following sections describe the results of the material selection, development, and testing efforts.

2.1 Selection of Material Compositions

Seven starting powders were selected and are identified as Powder Codes A through G in Table 3. Four of the powders were essentially alpha-phase silicon nitride to which sintering aids were required to achieve densification. One of these, LUCAS 373, was a "complete system as received" and consisted of silicon-nitride powder containing sintering aids ready to be formed and sintered in accordance with a proprietary schedule. The other two powders selected were silicon, one a commercial grade and the other a high purity electronic grade. Nitriding and sintering aids as well as a nitridation step and sintering step were required to produce a dense silicon-nitride from these powders.

TABLE 3. POWDERS SELECTED AS RAW MATERIALS

Powder Code	Name	Type
A	GTE SN 502	Alpha silicon nitride
B	STARCK LC-10	Alpha silicon nitride
C	LUCAS 373	Silicon nitride system - complete
D	KBI 21-2000	Silicon powder (98.5%)
E	Dow Corning S00090	Silicon chips (99.99%)
F	Toshiba	Alpha silicon nitride
G	STARCK LC-12	Alpha silicon nitride
V	G.E. Sintering Aid	Beryllium silicon nitride
W	MCB, CB 385	Iron oxide
X	Linde A, A 807	Aluminum oxide
Y	Molycorp, 1157	Yttrium oxide
Z	J.T. Baker, 5-1616	Chromium oxide

Five sintering and nitriding aids were selected for use with the seven silicon/silicon nitride powders. These are listed in Table 3, identified as Codes V through Z. The Code V sintering aid raw material was made available to the program through the courtesy of the General Electric Corporate Research and Development Center. This material, the compound Beryllium Silicon Nitride ($BeSiN_2$), was synthesized at the G.E. Laboratories. G.E. processed powder was molded and dewaxed at ACC. G.E. added the necessary SiO_2 by a controlled oxidation exposure and conducted the sintering required for full densification.

Fifteen combinations of the seven silicon-based powders and the five additive powders were selected by a technical team composed of AMMRC, GTEC, and ACC personnel. These compositions are listed in Table 4. A sixteenth composition employing other sintering aids was recommended by GTEC and ACC, however, work on that composition (Code 15) was not authorized by AMMRC.

Codes 2, 4, 7, 11, and 12, in which the same 6 percent Y_2O_3 - 2 percent Al_2O_3 additive was used, provided a means of comparing silicon nitride derived from five different sources.

One selected composition, Code 13, was judged to be sufficiently similar to another, Code 6, to be eliminated so that development resources might better be spent on other compositions. The only difference between the two was a small quantity of a nitriding aid; chrome oxide in the case of Code 6, and iron oxide in the case of Code 13. Earlier IR&D results at ACC showed a statistically insignificant difference between the two but slightly favored the chrome oxide.

A total of 14 compositions were therefore evaluated in the screening task of Phase I. The effort involved processing at least one batch (generally about 6 pounds) of each selected

TABLE 4. COMPOSITION SELECTION

Code	Powder	Additives[a]
1	GTE SN 502	8% Y_2O_3, 4% Al_2O_3
2	GTE SN 502	6% Y_2O_3, 2% Al_2O_3
3	STARCK LC-10	8% Y_2O_3, 4% Al_2O_3
4	STARCK LC-10	6% Y_2O_3, 2% Al_2O_3
5	LUCAS 373	System complete as received
6	KBI - 21 - 2000	8% Y_2O_3, 4% Al_2O_3, 1% Cr_2O_3[b]
7	KBI - 21 - 2000	6% Y_2O_3, 2% Al_2O_3, 1% Fe_2O_3[b]
8	KBI - 21 - 2000	8% Y_2O_3, (adjusted to 1.4 g/cc density)[b]
9	KBI - 21 - 2000	6% Y_2O_3, 1% Fe_2O_3[b]
10	DOW S00090	6% Y_2O_3, 1% Fe_2O_3[b]
11	Toshiba	6% Y_2O_3, 2% Al_2O_3
12	STARCK LC-12	6% Y_2O_3, 2% Al_2O_3
13	KBI - 21 - 2000	8% Y_2O_3, 4% Al_2O_3, 1% Fe_2O_3[b]
14	GTE SN 502	7% $BeSiN_2$, 7% SiO_2
15	GTE SN 502	4% MgO, 1% $SrTiO_2$, 5% CeO_2
16	KBI - 21 - 2000	6% Y_2O_3[b]

[a]Percent by Weight

[b]Based on final Si_3N_4 composition

composition. Although processing steps were similar, involving analysis, weighing, mixing, milling, blending with binder, pelletizing, injection molding, NDE, binder removal, and multiple heat treat/sintering cycles, the behavior of each composition was sufficiently different that each will be described individually in subsection 2.3.

2.2 Characterization of Starting Materials

Characterization of powders consisted of chemical analysis, particle size distribution, particle morphology, and X-ray diffraction.

Chemical analysis was conducted at Coors Spectrochemical Laboratory*, Air Force Wright Aeronautical Laboratory**, and Ledoux Inc.*** on starting powders and on various batch mixes. The results are summarized in Tables 5 through 7. There were discrepancies between the analyses and in comparison with batch compositions suggesting the need for refinement of analysis techniques or standards.

Oxygen content was determined by IRT Corporation**** and AMMRC using neutron activation. The results are summarized in Table 8.

Particle size distributions were performed at AMMRC using X-ray sedimentation. Examples of particle size distributions are illustrated in Figures 7 and 8. All the powders had an average size under about 6μm. The Si_3N_4 powders appeared finest, the Si powders coarsest, and the Al_2O_3 and Y_2O_3 in between.

*Golden, CO
**Wright-Patterson AFB, OH
***Teaneck, NJ
***San Diego, CA

TABLE 5. COMPARISON OF CHEMICAL ANALYSIS BY COORS AND AFML (WEIGHT PERCENT)

Specimen	14		2		5		8	
	Coors*	AFWAL**	Coors	AFWAL	Coors	AFWAL	Coors	AFWAL
Ca	0.03	0.015	0.03	0.001	0.4[a]	0.02	0.03	0.015
Fe	0.5	0.87	0.005	0.002	0.05	0.07	0.02	0.055
Co	0.01	0.002	0.01	0.002	0.01	0.002	0.01	0.002
V	0.03	0.06	0.005	-	0.005	-	0.005	-
Ni	0.01	0.06	0.01	-	0.01	-	0.01	-

[a]The Ca may have been introduced during analysis

*Coors Spectrochemical Laboratory, Golden, CO
**Air Force Wright Aeronautical Laboratory, Wright-Patterson AFB, OH

TABLE 6. COMPARISON OF Al AND Y AMOUNTS BETWEEN BATCHED COMPOSITION AND AFML ANALYSIS (WEIGHT PERCENT)

Specimen	2		5		8		X	
	ACC	AFWAL	ACC	AFWAL	ACC	AFWAL	ACC	AFWAL
Al	2.1	1.8	2.1	1.8	1.1	1.2	1.1	1.0
Y	6.3	5.7	6.3	5.6	4.7	4.4	4.7	4.5

Specimens[b]	1			2			3		
Elements	Ledoux*	Coors	AFWAL	Ledoux	Coors	AFWAL	Ledoux	Coors	AWAL
Al	--	--	--	1.62	3.7±0.2	1.9	1.42	3.6±0.2	1.6
Ca	0.002	0.003	0.006	0.001	0.03	0.0002	0.002	0.03	0.005
Cr	0.001	0.003	0.01	0.001	0.003	0.01	0.001	0.005	0.01
Fe	0.002	0.008	0.015	0.002	0.008	0.01	0.14	0.08	0.1
Mg	0.002	0.002	0.0015	0.001	0.001	0.0002	0.001	0.002	0.002
Mn	0.001	0.001	0.002	0.001	0.001	0.002	0.001	0.005	0.002
Mo	0.001	0.01	0.002	0.03	0.03	0.02	0.015	0.02	0.015
Ni	0.001	0.01	0.002	0.001	0.01	0.002	0.001	0.01	0.002
Ti	0.001	0.001	0.005	0.001	0.001	0.001	0.001	0.001	0.01
V	0.001	0.005	0.002	0.001	0.005	0.002	0.001	0.005	0.002
Zn	0.003	0.08	0.02	0.003	0.08	0.02	0.003	0.08	0.02
Y	--	--	--	6.79	8.0±0.2	4.6	6.65	5.6±0.2	4.6

[a]Semiquantitative emission spectroscopy except for Al and Y in specimens 2 and 3. The Al and Y concentrations in specimens 2 and 3 were determined by wet chemical analysis.

[b]Key to specimens:

1. Toshiba Si_3N_4 as received
2. Code 1 Mill Batch 50-94
3. Code 1 Test Bar S/N 10774/10775

*Teaneck, N.J.

TABLE 8. OXYGEN NEUTRON ACTIVATION ANALYSIS (W/O OXYGEN)

Additives	IRT*	AMMRC
Al_2O_3	44.4	47.38
Y_2O_3, Lot 1	18.1	16.81
Y_2O_3, Lot 2	19.0	
SN502, Lot 1	0.929	1.67
SN502, Lot 2	1.64	
SN502, Lot 3	1.33	
Code 1, Milled	3.870	5.48
Code 1, Molded	4.96	
Code 1, Dewaxed	4.71	
Code 1, Sintered	4.43	
Code 2, Milled	3.16	
Code 2, Dewaxed	3.59	
LC 10, Lot 1	1.47	2.04
LC 10, Lot 2	2.29	2.18
Code 4, Milled	3.97	
KBI 21-2000	0.316	0.32
Code 6, Molded	6.66	
Code 6, Dewaxed	5.850	
Code 7, Milled	5.12	5.71
Code 7, Molded	4.86	
Code 7, Dewaxed	5.49	
Code 7, Nitrided	3.40	
Code 9, Milled	2.44	
Code 9, Molded	3.40	
Dow Corning 500090, Lot 1	0.0479	0.05
Dow Corning 500090, Lot 2	0.0616	
Code 10, Milled	--	2.61
Code 10, Nitrided	2.04	
Code 10, Sintered	2.24	
Toshiba Powder, Lot 1	2.16	2.08
Toshiba Powder, Lot 2	1.71	
LC12, Lot 1	2.50	
LC12, Lot 2	2.50	2.08
Code 12, Milled (34 Hours)	5.22	4.84

*San Diego, CA

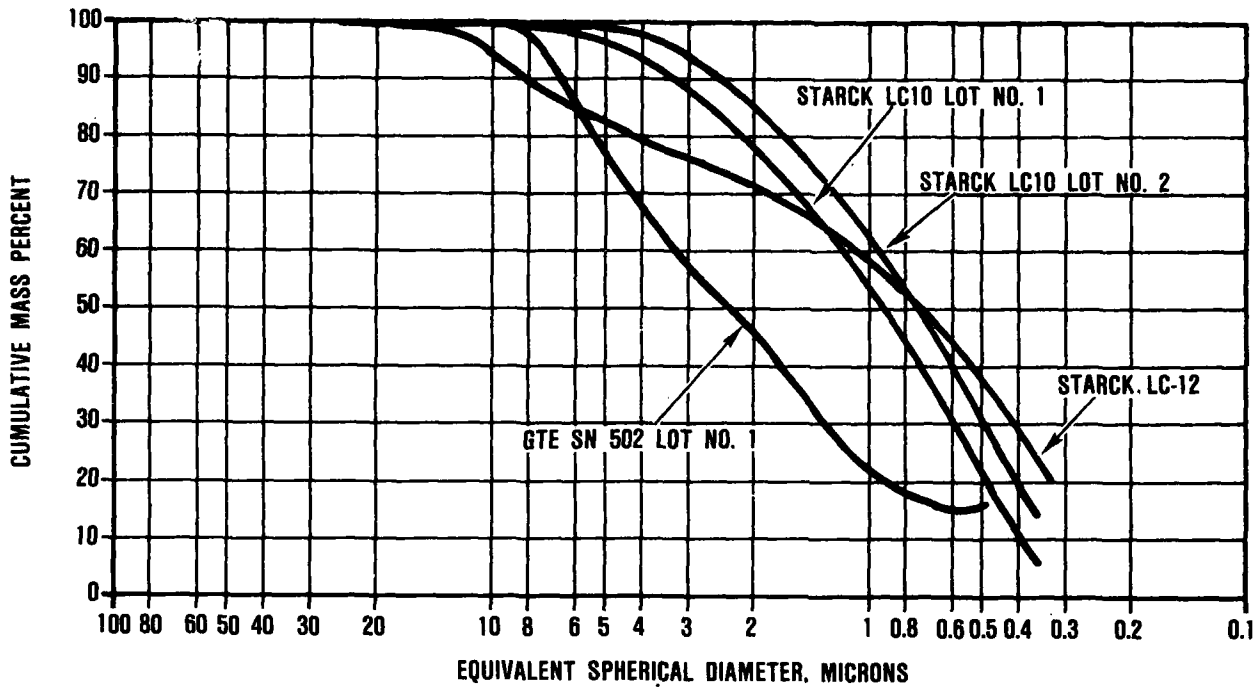

Figure 7. Particle Size Distribution of Si_3N_4 Starting Materials.

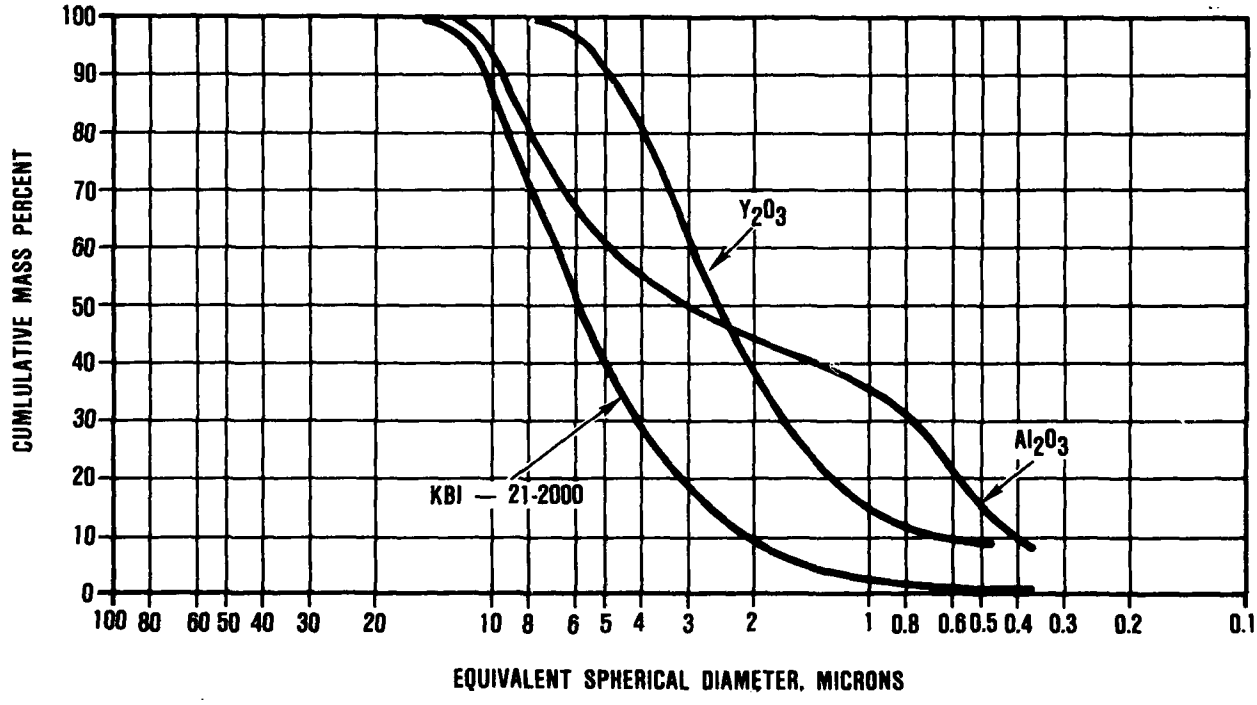

Figure 8. Particle Size Distribution of Si, Al_2O_3, and Y_2O_3 Starting Materials.

The morphology of particles in the starting powders was examined by scanning electron microcopy (SEM). Examples are shown in Figure 9. Large differences in particle shape and the degree of agglomeration are visible for the four powders illustrated (GTE 502, Starck LC-10, Starck LC-12, and Toshiba). The particles in the Starck LC-10, Starck LC-12, and Toshiba powders were essentially equiaxed as compared to the GTE SN 502 powder, which contained both equiaxed and elongated particles. The Toshiba powder was highly agglomerated, while both Starck powders were less agglomerated, and the GTE SN 502 contained relatively few agglomerates.

2.3 Screening of Candidate Compositions

The screening of candidate compositions involved fabricating test bars by procedures based upon prior experience with the Code 1 and Code 6 type compositions. This procedure consisted of blending precise amounts of starting powder and appropriate additives, dry-ball milling the blend in rubber-lined mills for 17 hours using dense Si_3N_4 grinding media and preparing a plastic mixture suitable for injection molding into a test-bar mold.

The plastic mixture was prepared in a heated sigma-blade mixer by adding the milled powder to a given amount of melted binder. Standard practice was to add powder until a 13 percent by weight binder content was reached, a mixture generally too dry to be useful. Small, known amounts of binder were then added until a smooth consistency was achieved. A small addition of a lubricant was added at this point and the batch blended until homogeneous. After cooling, the hardened lumps were pelletized into a form usable in the feed hopper of the screw-type injection-molding machine.

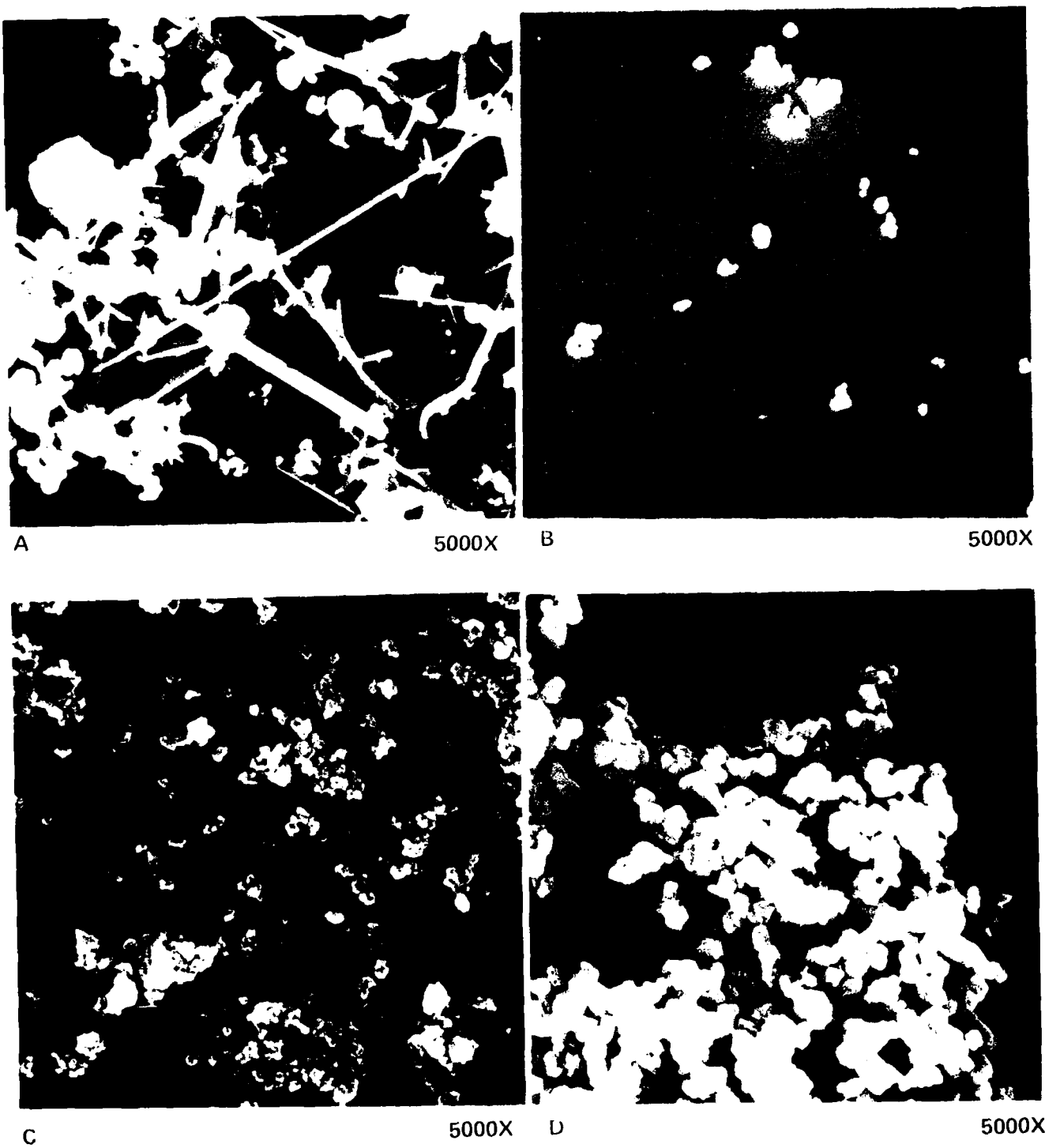

Figure 9. SEM Photomicrographs (5000 X) of Si_3N_4 Powders - (A) GTE 502 (B) Starck LC-10 (C) Starck LC-12 (D) Toshiba.

Molding conditions considered standard on this program were: material temperature, at the injection molder nozzle, of 170F for Si_3N_4 or 150F for silicon-based mixes; die temperature of 90F for Si_3N_4 or 80F for silicon; and injection pressure of 1400 psi. After molding, the binder was removed using a vacuum heat-treating cycle at 400-500F. After binder removal, the bars were nitrided and/or sintered as required. The nitriding was performed using a nitrogen demand cycle at a peak temperature of 2400F in a nitrogen atmosphere, generally requiring about 10 days for complete reaction. The sintering cycle included a 3180F peak temperature and a two-hour hold under a 70 psi nitrogen pressure. In the discussion of the individual compositions, deviations from this standard procedure will be described.

2.3.1 Code 1 - GTE SN 502 with 8-Percent Y_2O_3 and 4-Percent Al_2O_3

This composition responded well to the standard procedure at a binder content of 14.0 percent by weight. An initial 100 test bars were injection molded but were rejected by X-ray radiography due to the presence of metallic inclusions. The source of the inclusions was identified as excessive wear of an improperly heat treated metal star drive in the injection molder. This was repaired, and a replacement set of bars was molded.

Acceptable dewaxed test bars from the replacement lot were used for sintering tests. Several sintering runs on two to four test bars each yielded an acceptable sintering cycle which included a 3180F peak temperature and a two-hour hold under a 70 psi positive nitrogen pressure. This produced a 3.24 g/cc average density and MOR room-temperature strength of over 75 ksi. Selected specimens were strength tested at 2250F and yielded a MOR value of 52.7 ksi.

2.3.2 Code 2 - GTE SN 502 with 6-Percent Y_2O_3 and 2-Percent Al_2O_3

This composition also responded well to the standard procedure probably because of its great similarity to Code 1. It also was fluid at 14.0 weight percent binder and was successfully molded into test bars under the standard Si_3N_4 conditions.

Groups of Code 2 test bars were included in experimental accelerated vacuum dewax runs. A majority of these bars exhibited bloating or blistering during the dewax process. A second group of bars was molded and processed through a slightly positive pressure, rather than vacuum dewax. This process change eliminated the bloating and blistering problem and increased the yield at dewax to 80 percent or better. The positive-pressure dewax was adopted as standard for the remainder of this program.

Sintering to 3180F/2-hour hold under 70 psi nitrogen pressure produced an average density just under 3.1 g/cc and strengths of 68.3 ksi and 55.1 ksi at room temperature and 2250F, respectively. Additional sintering trials showed that an increase to 3272F with a four-hour hold improved the sintered density to 3.19 g/cc with only a slight increase in room temperature strength.

2.3.3 Code 3 - Starck LC-10 with 8-Percent Y_2O_3 and 4-Percent Al_2O_3

This composition required more binder, 16.7 percent by weight, to achieve an acceptable fluidity. Even so, molding of test bars was considered difficult with yields by radiography generally under 50 percent. SEM photographsof the LC-10 powder, as-received, shown in Figure 9 indicated more agglomeration in LC-10 than in SN 502.

Pressure-dewaxed bars sintered at 3180F/two-hour hold yielded a density of 3.21 g/cc, but an unreasonably low strength of 16.0 ksi and 22.5 ksi at room temperature and 2250F, respectively. The fracture surface revealed a series of concentric cores within the specimen along with porous regions near the surface and the core. This indicated poor molding and probably contributed to the low fracture strength. Additional experience with the Starck LC-10 powder on Code 4 (discussed next) and the availability of a newer LC-12 powder from Starck resulted in an early decision to terminate work on Code 3.

2.3.4 Code 4 - Starck LC-10 with 6-Percent Y_2O_3 and 2-Percent Al_2O_3

This composition appeared to respond better to the standard binder amount and molding conditions than did Code 3. However, an evaluation of specimen surfaces and fracture surfaces after sintering revealed surface cracks and interior concentric laminations. On further evaluation, it was found that these defects were present in the molded bars indicating that this composition did not mold well with the standard procedure.

Sintering at the 3180F/two-hour hold cycle yielded a low 2.73 g/cc density and very low strength, similar to the Code 3 results. The test bars did not fracture completely but deformed as cracks progressively extended inwards from the tensile face as the load was increased. This gave the appearance of slow crack growth[1]. However, further examination showed that the test bars contained concentric laminar cracks as well as surface "mudcracks" and reacted much like a composite during strength testing. As the load was increased, a surface crack propagated inwards until it reached the first laminar crack.

The initial crack then turned and followed the laminar crack, allowing lateral slip and permanent, but non-plastic, deformation of the bar. When the local tensile stress became high enough, a crack initiated in, and propagated through the second concentric layer of Si_3N_4 and terminated at the second laminar crack. This sequence repeated itself, resulting in the unusual fracture behavior.

The low fracture strength, molding difficulties, and poor availability of the LC-10 powder resulted in the early elimination of Code 4 from the program and increased efforts on Code 12, which was based on the Starck LC-12 grade Si_3N_4 powder.

2.3.5 Code 5 - Lucas 373 System Complete As-Received

Syalon Grade 373 powder was received at ACC from Lucas Industries under an existing confidentiality agreement. The powder contained proprietary sintering aid additions to a silicon nitride base and was reported to be ready for forming and sintering without additional densification aids. A portion of that shipment was made available for the program at no cost to the Government under the stipulation that only data approved by the supplier (Lucas) would be reported.

The first injection-molding batch prepared indicated an incompatibility of the powder with the standard binder system. Minor variations in a calcining and ball-milling procedure allowed molding of suitable test bars. Sintering was attempted according to the suppliers' recommendations, and densities as high as 3.35 g/cc were achieved. However, a persistent problem of blistering during sintering was encountered. It was concluded that the problem was the inability of the ACC sintering furnace to exactly duplicate the recommended Lucas sintering cycle. Therefore, the decision was made early in Phase I not to continue work on Code 5 in this program.

2.3.6 Code 6 - KBI-21-2000 Silicon with 8-Percent Y_2O_3, 4-Percent Al_2O_3, and 1-Percent Cr_2O_3

This composition was based upon the sintered, reaction-bonded silicon nitride (SRBN) approach in which the oxide sintering aids were added to a metallurgical-grade silicon powder. The blend was molded to shape, then after dewax was nitrided to convert the silicon to Si_3N_4. The material was then sintered to a higher temperature to achieve nearly full density.

The silicon powder chosen was a ball-milled and air-classified fraction of a material that had been under development for some time. In addition to the Y_2O_3 and Al_2O_3 additions, one percent by weight Cr_2O_3 was also added to Code 6. This served as a nitriding aid which appeared necessary only when thick sections, such as the hub region of the rotor, were to be nitrided.

The mixture required more binder than normal to make it moldable, (17.8 w/o) but otherwise responded well to the standard molding procedure. X-ray radiography indicated a high yield of good bars after dewax and nitridation (above 80 percent). The bars nitrided to 2.5 to 2.6 g/cc and had an as-nitrided strength of about 28 ksi. Representative bars were sintered using the 3180F/two-hour cycle to 3.31 g/cc and yielded MOR strengths of 78.0 ksi and 48.1 ksi at room temperature and 2250F, respectively.

2.3.7 Code 7 - KBI-21-2000 Silicon with 6-Percent Y_2O_3, 2-Percent Al_2O_3 and 1-Percent Fe_2O_3

This composition was similar to Code 6 except for the lower sintering aid content and the use of one-percent Fe_2O_3, rather than one-percent Cr_2O_3 as a nitriding aid.

It was found moldable at 16.7 weight percent binder level and behaved similar to Code 6 during the various processing steps. A sintered density of 3.14 g/cc was achieved with a strength of 67.4 ksi at room temperature and 43.5 ksi at 2250F.

2.3.8 Code 8 - KBI-21-2000 Silicon with 8-Percent Y_2O_3 Only

Selection of this composition was an attempt to avoid the addition of a nitridation aid by blending sufficient binder with the silicon - Y_2O_3 powders to maintain a 1.4 g/cc green density, low enough to insure uniform nitridation even in thicker sections. The yttria-only addition would require higher temperatures, and therefore, higher nitrogen pressures for sintering than were available at ACC at the initiation of the program. The potential improvement in high-temperature properties were considered worth the effort to acquire the necessary sintering capability.

This composition mixed and molded quite well producing visually acceptable test bars after molding. After dewax, the specimens exhibited low green density, and handling damage was extensive. Ten specimens were nitrided to a density of only 2.3 g/cc and exhibited poor quality. It was decided not to attempt to process this composition further and to eliminate it from the program.

2.3.9 Code 9 - KBI-21-2000 Silicon with 6-Percent Y_2O_3 and 1-Percent Fe_2O_3

This composition was based upon prior successful HIP work on Garrett IR&D programs. It shared the same silicon starting powder as Codes 6, 7, and 8, and therefore behaved similarly, i.e., required a somewhat above-average binder content (16.5 percent) to produce a good yield of test specimens. The dewaxed bars nitrided well to 2.6 g/cc average density, but

sintered only to 2.81 g/cc at 3272F/four-hour hold at 70 ksi nitrogen pressure.

Based upon higher pressure sintering studies reported by Mangels[2] and Greskovich[3], it appeared likely that the Code 9 composition could be sintered to high density using a higher pressure two-step sintering process. The plan involved the use of the ACC HIP unit for high temperture (>3272F) cladless HIP trials. However, thermocouple and equipment problems were encountered which delayed the high-temperature, high-pressure sintering runs.

As an interim approach to evaluate the potential of this composition, specimens were densified using a cladded HIP approach. Selected nitrided bars were vacuum sealed in Vycor cylinders protected from contact with the Vycor by a layer of BN powder. These were heated at near ambient pressure to 2732F, then the HIP chamber was pressurized to 23 ksi while the temperature was raised to 3180F. A 1- to 1-1/2-hour hold under these conditions increased the density of the Code-9 composition to 3.26 to 3.28 g/cc. The Vycor was removed after cooling by vapor blast using a silica/water/air pressure spray. Strength after HIP processing when measured at 2250F was as high as 94 ksi, in excess of the 70 ksi established as the Phase I goal. Reliability of the Vycor envelopes was poor with many failing during pressurization. Also, in some cases, the Vycor contaminated the specimens. These two conditions resulted in wide scatter of the density and strength data (see Table 9). Fractures typically occurred either at the surface when contamination from the Vycor was present or at subsurface flaws traceable to the as-nitrided material (pores that did not close, inclusions, laminar pores).

TABLE 9. CODE 9 - 2250F FLEXURE STRENGTH

Specimen No.	Density (g/cc)	MOR (ksi)	Remarks
52	2.96	49.8	Low density, fracture origin at internal pores
41	3.26	61.1	Contamination on surface
14	3.27	68.3	Fracture origin at large edge chip
4	3.11	73.0	Fracture origin at internal pre-existing crack
43	3.23	38.7	Contamination on surface
89	3.28	93.9	Fracture origin on large inclusion
68	3.02	27.4	Fracture origin at internal pre-existing crack

.10 Code 10 - DOW S00090 Silicon with 6-Percent Y_2O_3 and 1-Percent Fe_2O_3

This composition was included in order to evaluate a very-h-purity electronic-grade silicon using the same additives in Code 9. The high-purity silicon was received in wafer m and was reduced to a coarse powder by hand crushing in an mina mortar and pestal. No alumina wear was apparent.

The coarse powder was ball-milled with the additives in normal manner to about 3 m^2/g average surface area. A dable mix was achieved at a binder level of 13.6 weight per-t which produced defect-free test bars. These bars were rided to 2.6 g/cc density. Sintering attempts produced only 1 g/cc density at 3272F/6-hour hold at 70 psi nitrogen over-ssure. Attempts at cladded HIP processing resulted in a sity of 3.16 g/cc.

.11 Code 11 - Toshiba with 6-Percent Y_2O_3 and 2-Percent Al_2O_3

The Toshiba powder with the baseline binder content (14 cent) proved difficult to mold. The problem may be related the agglomerates in the as-received powder (see Figure 9). ost half of the molded test bars were rejected for defects ible using radiography. Density after sintering was slight-under 3.00 g/cc and room-temperature strength was 43 ksi.

Using an iterative approach, new molding parameters were ablished that improved the moldability of the material and duced molded test bars with minimal defects. The improved dability is illustrated in Figure 10. The as-sintered sur- e was free of "mud cracks" associated with poor moldability. o, in Figure 10B, there is no evidence of extensive surface nected cracks, laminations, or core effects, all associated h poor molding.

In another molding attempt, the parameters were 130-140F erial temperature, 82F mold temperature, 800 psi molding ssure, and 19 weight percent binder. These bars exhibited a h dewax yield. Subsequent sintering at 3272F produced test s with a density of 2.82 g/cc. The specimens had a uniform e grained microstructure (see Figure 11). The room-tempera- e flexure strength was 62.7 ksi.

.12 Code 12 - Starck LC-12 Powder with 6-Percent Y_2O_3 and 2-Percent Al_2O_3

Starck LC-12 has the highest surface area of all the sili- nitride powders evaluated. It required only slightly more percent) binder than the lowest surface area powder. The ded specimens exhibited knit lines and hairline cracks on surface. These bars readily sintered to densities ap- aching 3.2 g/cc. The defects identified in the molded bars eloped during sintering into extensive surface defects (see ure 12) which contributed to low, 25-35 ksi, room-tempera- e strength.

A second iteration to eliminate the surface cracks by roving the moldability of the material was performed.

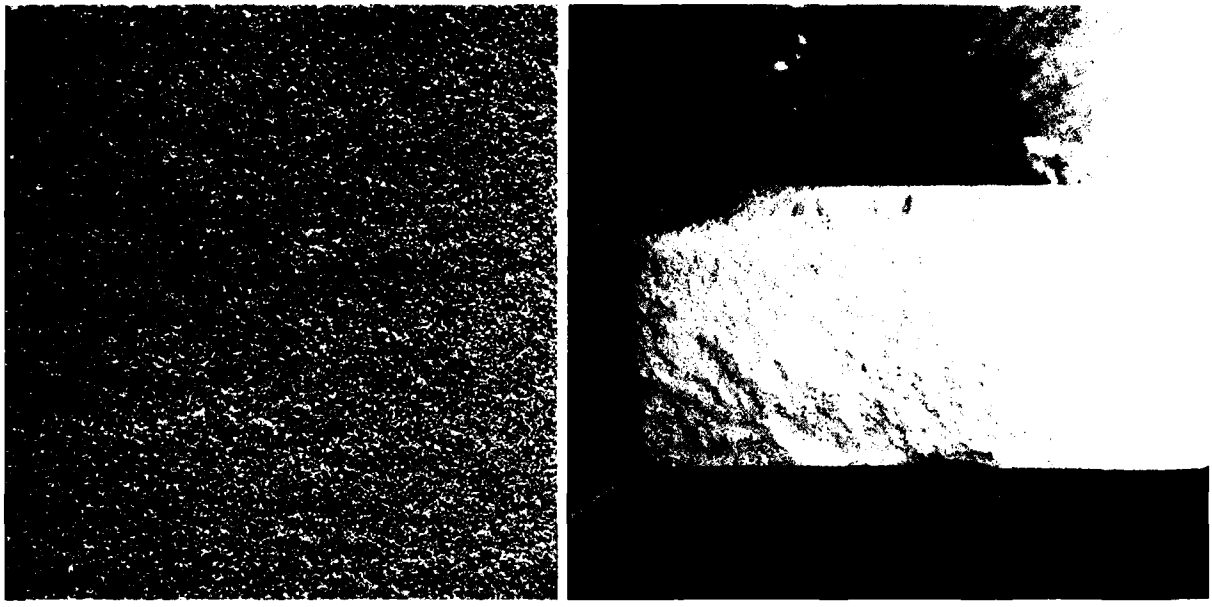

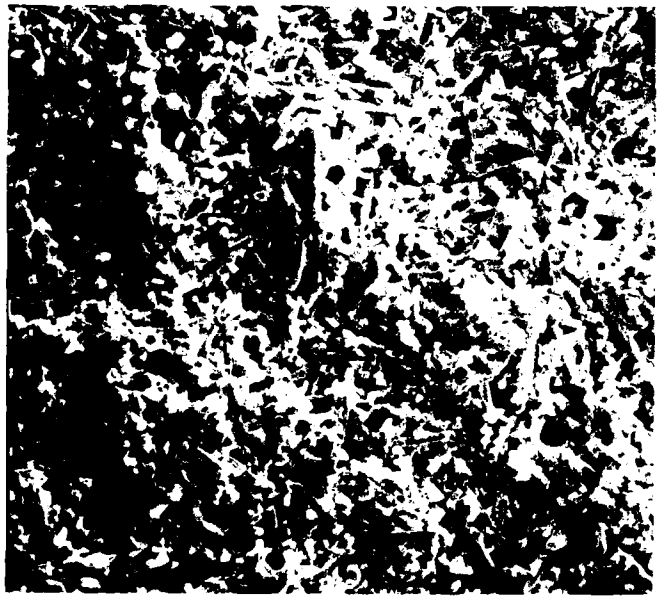

Figure 11. SEM Photomicrograph (1000X) of the Fracture Surface of a Code 11 Specimen.

100X

Figure 12. SEM Photomicrograph (100X) of As-Sintered Surface of a Code 12 Test Bar Molded Under Baseline Conditions.

A series of molding trails were run varying material temperature, mold temperature, molding pressure, and binder content. The baseline conditions were discussed earlier. The surface of a test bar molded under the baseline conditions is shown in Figure 13A. The results of this iterative study produced molded test bars with a significant improvement in moldability and reduction in surface defects (Figure 13B). The improved molding conditions were 180-190F material temperature, 120F mold temperture, 1400 psi molding pressure, and 15.5 weight percent binder. Unfortunately, a large percentage of these test bars contained high-density (metal) inclusions, and subsequent sintering produced test bars with cracks, internal defects, low density, and low room temperature and 2250F strength. The source of the metal inclusions was traced to a damaged auger in the molder.

2.3.13 Code 14 - GTE SN503 with 7-Percent $BeSiN_2$ and 7-Percent SiO_2

This composition was evaluated through the cooperation of the General Electric Company. A 150-gram batch of the additive $BeSiN_2$ was prepared at G.E. and shipped to ACC for processing. Batch size was limited to about 2000 grams, 2/3 the standard batch size; however, mixing was satisfactory, and the standard 14-percent binder produced a good molding mixture. Because of the quantity limitation, only 32 test bars were initially molded, all of which appeared defect-free by X-ray radiography. Six test bars were dewaxed and sintered to the 3772F/four-hour cycle under 70 psi nitrogen pressure. A density on only 2.16 g/cc was achieved.

Several samples, both in the dewaxed condition and sintered to 2.16 g/cc density, were delivered to G.E. for addition of SiO_2, sintering, and testing. Initial sintering resulted in test bars with blisters, and the specimens were not considered suitable for strength testing.

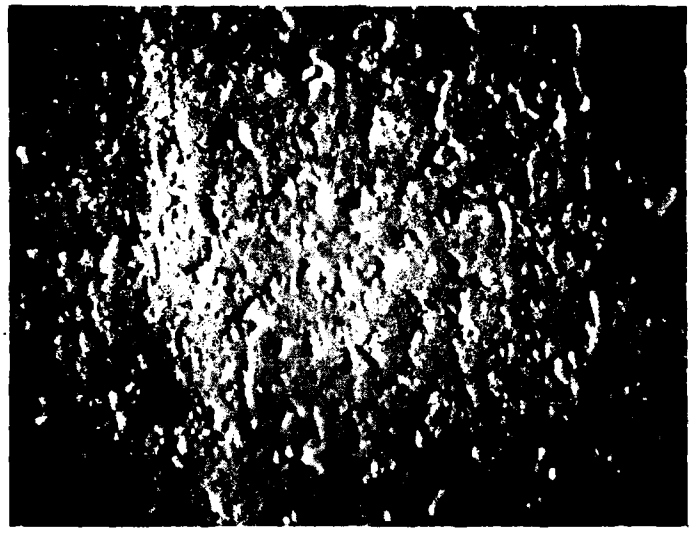

A 94.5X

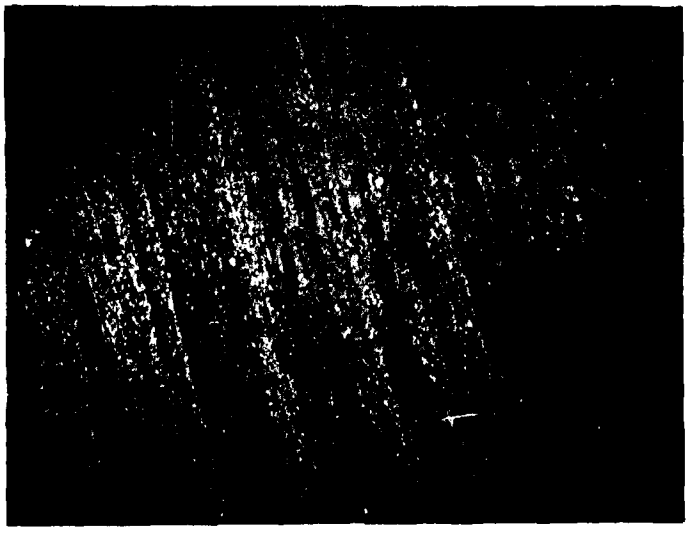

B 94.5X

Figure 13. Photomicrograph Showing Surface of As-Molded Code 12 Test Bars - A) Baseline Molding Condition B) Improved Molding Conditions.

2.3.14 Code 16 - KBI-21-2000 Silicon with 6-Percent Y_2O_3

Preliminary oxidation results from an IR&D program on compositions similar to Code 9 suggested that the one-percent Fe_2O_3 nitriding aid in Code 9 might be detrimental to long-term, high-temperature properties. A new batch of molding mix similar to Code 9, but without the Fe_2O_3, was therefore prepared and designated Code 16. The same 16.5-percent binder was needed to produce a moldable mix in Code 16 as in Code 9. A high yield (over 91 percent) was achieved and dewax bars readily nitrided to 2.6 g/cc density.

2.4 Selection of Compositions for Further Development

Table 10 summarizes the flexural strength results for the best iteration of each composition by the end of Phase I. Both the characteristic strength and Weibull modulus (m) are given in most cases, although it is recognized that the small sample populations (<10) are not adequate for accurate Weibull parameter determination, especially for the Weibull modulus.

Based upon these strength results plus microstructure and processing information, GTEC, ACC, and AMMRC jointly agreed to continue development of seven compositions during Phase II. These are identified in Table 11.

Three of these (Codes 2, 11, and 14) involve the sintering of Si_3N_4 powder preforms while the remainder (Codes 7, 9, 10, and 16) start with a Si preform (plus additives) which is then converted to reaction-bonded silicon nitride (RBSN) prior to final densification by a sintering process. Codes 2 and 7 were to be processed in both rotor and test bar configurations.

TABLE 10. FLEXURE STRENGTH SUMMARY FOR THE BEST ITERATIONS FOR EACH MATERIAL IN PHASE I

Composition	Binder Content[a]	Density (g/cc)	Characteristic Strength, ksi		Weibull Modulus	
			Room Temp	2250F	Room Temp	2250F
1	14.0	3.24	75.8	52.7	10.1	19.0
2	14.0	3.07	68.3	55.1	9.0	8.8
3	16.7	3.21	16.0[b]	22.5[b]	---	---
4	14.0	2.73	15.8[b]	10.8[b]	---	---
6	17.8	3.31	77.8	48.1	9.2	11.5
7	16.7	3.14	70.6	43.5	10.2	21.3
9	16.5	3.27 max	---	94 max	---	---
11	19	2.82	62.7[b]	---	---	---
12	15.5	3.05	32.3[b]	---	---	---

[a]Weight percent

[b]Average strength

Code 14 was to be processed as both rotors and test bars for continued sintering studies in cooperation with the General Electric Company.

Codes 9, 10, and 16 were continued for test bar sintering optimization using HIP processing, with one composition to be selected for potential rotor fabrication.

Code 11 was continued for test bar sintering studies as a potential substitute for Codes 2 and 7.

TABLE 11. COMPOSITIONS FOR CONTINUED DEVELOPMENT

Code	Powder	Additives[a]
2	GTE SN 502 Si_3N_4	6% Y_2O_3, 2% Al_2O_3
7	KBI-21-2000 Si	6% Y_2O_3, 2% Al_2O_3, 1% Fe_2O_3
9	KBI-21-2000 Si	6% Y_2O_3, 1% Fe_2O_3
10	DOW 500090 Si	6% Y_2O_3, 1% Fe_2O_3
11	Toshiba Si_3N_4	6% Y_2O_3, 2% Al_2O_3
14	GTE SN 502 Si_3N_4	7% $BeSiN_2$, 7% SiO_2
16	KBI-21-200	6% Y_2O_3

[a]Percent by weight (in case of additions to Silicon, the percentage is based on the final Si_3N_4 weight)

2.5 Results of Test Bar Processing Iterations

During Phase II several lots of test bars were used in iterative sintering studies to increase density and achieve improved strength. Hot isostatic pressing (HIP) of test bars was also accomplished. The following paragraphs present a summary report on each composition studied.

2.5.1 Code 2 - GTE SN502 Si_3N_4 With 6-Percent Y_2O_3 and 2-Percent Al_2O_3

At the conclusion of Phase I, the best results for this composition were 3.07 g/cc density, 68.3 ksi and 55.1 ksi characteristic strength at room temperature and 2250F, respectively, with a Weibull slope of 9 at both temperatures. These results were obtained on test bars sintered at 3182F for two hours. A series of sintering experiments was conducted in which both temperature and nitrogen pressure were the variables studied. Although the lot of test bars used in this study exhibited large flaws attributed to the molding/dewax process, some encouraging results, presented in Table 12, were obtained. As can be seen, there appears to be significant improvement in strength as a result of increased temperature and pressure. The lot sintered at 3362F (1850C)/90 psi exhibited a characteristic strength of 88.4 ksi with a Weibull slope of 5.1 (see Figure 14).

Several additional lots of test bars were sintered to verify these results. One lot (number 11229-11241), sintered at 3317F/90 psi N_2, exhibited an average density of 3.22 g/cc and an average weight change of -2.5 percent. The specimens had excessive surface pitting, which was attributed to dissociation. The specimens were machined to remove the surface defects, and the room-temperature flexure strength was measured. The fracture strength and fracture origin for each

TABLE 12. CODE 2 SINTERING RESULTS

Temp. F	Nitrogen Pressure (psi)	Sintered Density (g/cc)	Weight Change (%)	Room Temp. Flexural Strength[a] (ksi)
3272	70	3.10	+1.18	37
3272	90	3.10	+0.6	34
3326	70	3.17	+0.13	50.4 ±11.1
3326	90	3.16	--	54.7 ±18
3362	70	3.21	+0.15	67.0 ±8.2
3362	90	3.22	+0.4	81.2 ±16

[a]All flexural strength data reported was obtained from specimens approximately 0.125" x 0.025" x 2" in size; 4-point bend testing was performed with an outer span of 1.5" and an inner span of 0.75".

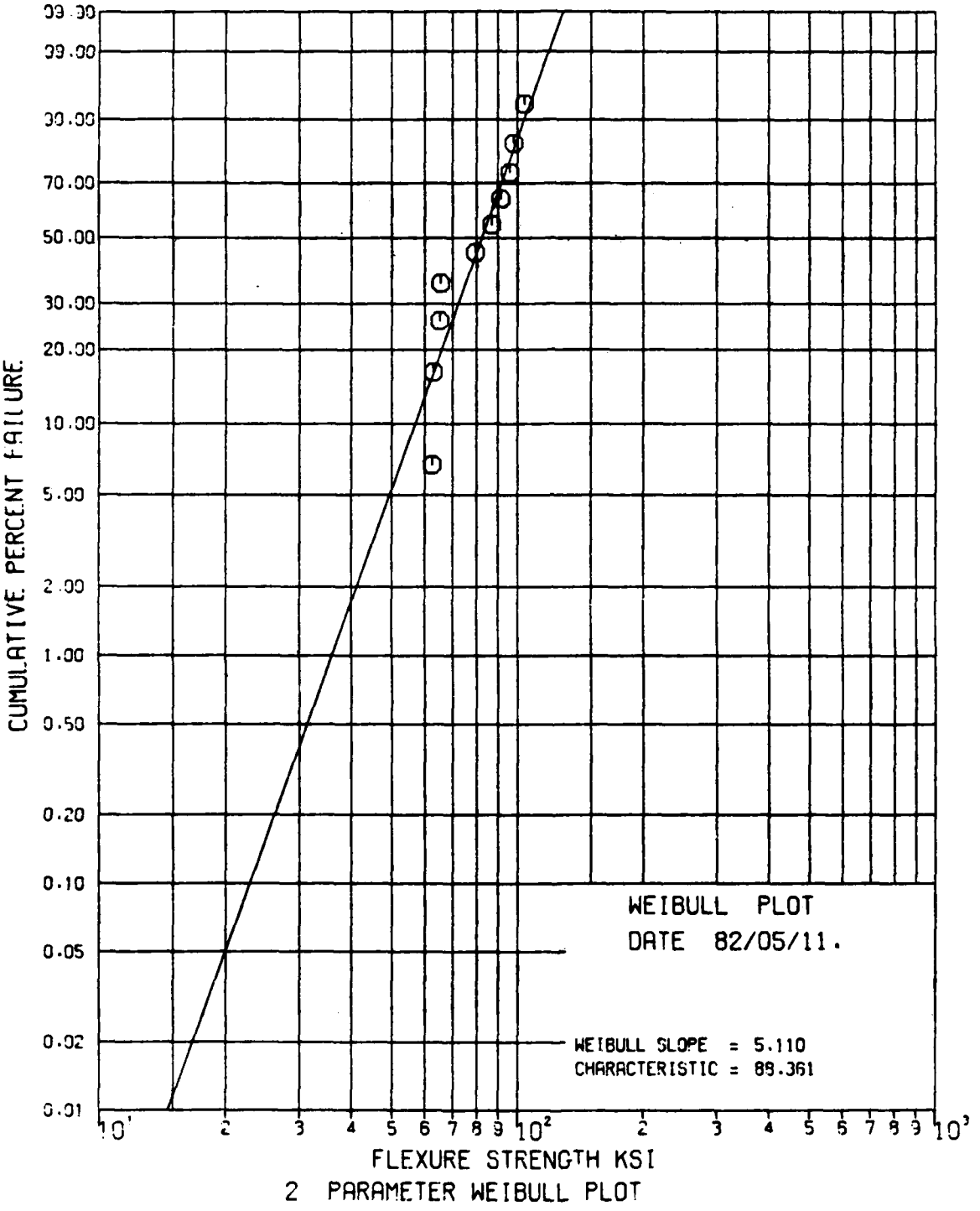

Figure 14. Room Temperature Flexure Strength of Code 2 Test Bars Sintered at 3362F, 90 psi N_2.

specimen is presented in Table 13. The low strength (<70 ksi) failures were caused by large molding flaws, not removed by machining, in the chamfer area. The high-strength (>85 ksi) failures, attributed to microstructural flaws, are more indicative of the potential strength of this composition.

A second lot of test bars (numbers 11159-11181), also sintered at 3317F/90 psi N_2, had an average density of 3.21 g/cc, an average weight change of -1.8 percent, and excessive surface pitting. The test bars were machined prior to strength testing to remove the surface defects and the molding flaws in the chamfer area. The results at room temperature and at 2250F (1232C) for this lot are presented in Table 14 and in Figures 15 and 16. All fracture origins (at 40X) were associated with microstructural features.

The weight loss measured for the two lots discussed above was different than the weight gain previously reported for similar sintering conditions. It was determined that test bars and rotors exhibited a weight gain when sintered with powder of a similar slip-cast composition. The slip-cast compositions contained some air-calcined powder and, therefore, probably some SiO_2 which retarded the decomposition of the Si_3N_4 and caused the weight gain. Since decomposition (weight loss) led to excessive surface pitting, all subsequent sintering runs of Code 2 test bars and rotors contained some slip-cast material. These procedures appeared to produce components with good as-sintered surfaces and as-sintered test bars with strengths similar to machined test bars.

To date, the best sintering procedure for Code 2 test bars involves holding them for four hours at 3362F under 90 psi N_2 with slip-cast powder in the sintering crucible. This procedure produces test bars with 97-percent theoretical

TABLE 13. FLEXURE STRENGTH OF CODE 2 TEST BARS (NUMBERS 11229-11241)

Specimen	Room Temperature Strength (ksi)	Fracture Origin
11229	103.7	Small internal flaw
11230	68.5	Molding flaw in chamfer
11231	64.8	Molding flaw in chamfer
11232	51.8	Molding flaw in chamfer
11233	111.0	Small internal flaw
11234	103.7	Silicon inclusion below tensile face
11235	63.5	Molding flaw in chamfer
11236	102.0	Internal void
11237	38.9	Molding flaw in chamfer
11238	40.7	Molding flaw in chamfer
11239	105.5	Small pre-existing crack
11240	103.6	Tensile face
11241	86.6	Subsurface void

TABLE 14. FLEXURE STRENGTH RESULTS FOR CODE 2 TEST BARS (NUMBERS 11159-11181)

	Room Temperature	2250F
Average Strength (ksi)	93.05 ±9.23	64.0 ±6.5
Weibull Slope	11.3	10.3
Characteristic Strength (ksi)	97.2	67.0

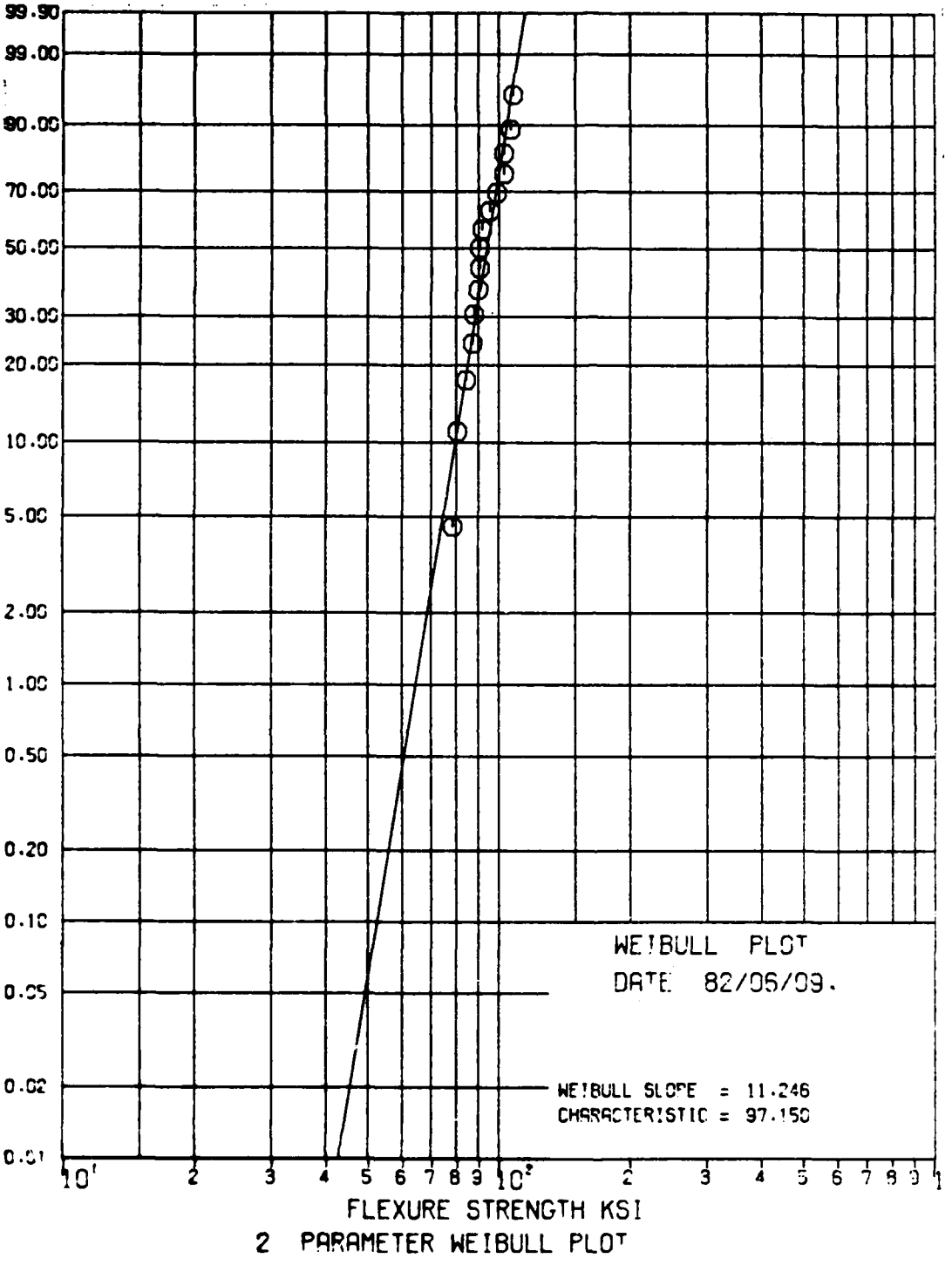

Figure 15. Room Temperature Flexure Strength of Code 2 Test Bars Sintered at 3317F, 90 psi N_2.

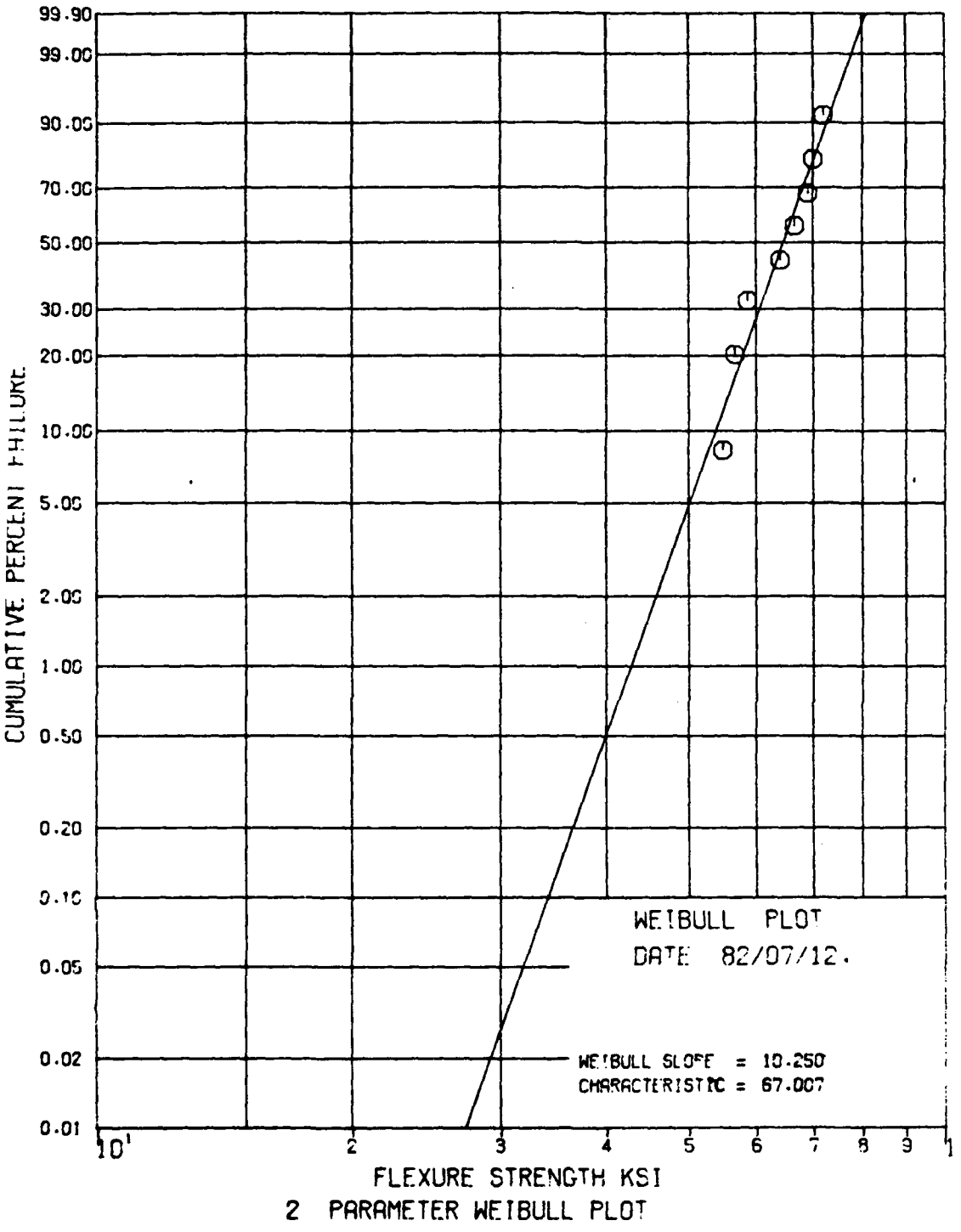

Figure 16. 2250F Flexure Strength of Code 2 Test Bar Sintered at 3317F, 90 psi N_2.

density, good as-sintered surfaces, and the highest room-temperature and 2250F strengths measured on this composition.

2.5.2 Code 7 - KBI-21-2000 Silicon With 6-Percent Y_2O_3, 2-Percent Al_2O_3, and 1-Percent Fe_2O_3

A lot of Code 7 test bars sintered at 3272F for four hours, exhibited a density of 3.21 g/cc and an average room-temperature flexure strength of 73 ksi. The characteristic strength and Weibull slope were determined to be 76.5 ksi and 10, respectively (see Figure 17). The 2250F strength was determined to be 53.7 ksi.

Two lots of 10 specimens each were sintered at 3326F and 3362F for four hours, respectively, at the standard N_2 pressure of 70 psi. Average densities of 3.25 g/cc and 3.28 g/cc, respectively, were obtained, but the room-temperature strengths were only about 55 ksi in each case. The low stength was attributed to surface pits caused by dissociation. Five specimens from each lot were machined to remove the surface pits and the measured strength was found to be about 75 ksi in each case. These results suggested that if the surface pitting could be eliminated, the strength of the composition could be improved.

Two additional lots of Code 7 were sintered at 3317F, 90 psi N_2, and 3407F, 90 psi N_2, respectively. The lot sintered at 3317F had an average density of 3.15 g/cc and an average weight change of -0.16 percent. Since surfaces of the test bars were pitted, they were machined before strength testing. The room-temperature strength was 58.9 ±18.7 ksi, with individual test bar strengths up to 90 ksi. The lot sintered at 3407F had a higher average density (3.21 g/cc) but also exhibited a weight loss (0.9 percent) and surface pitting and were,

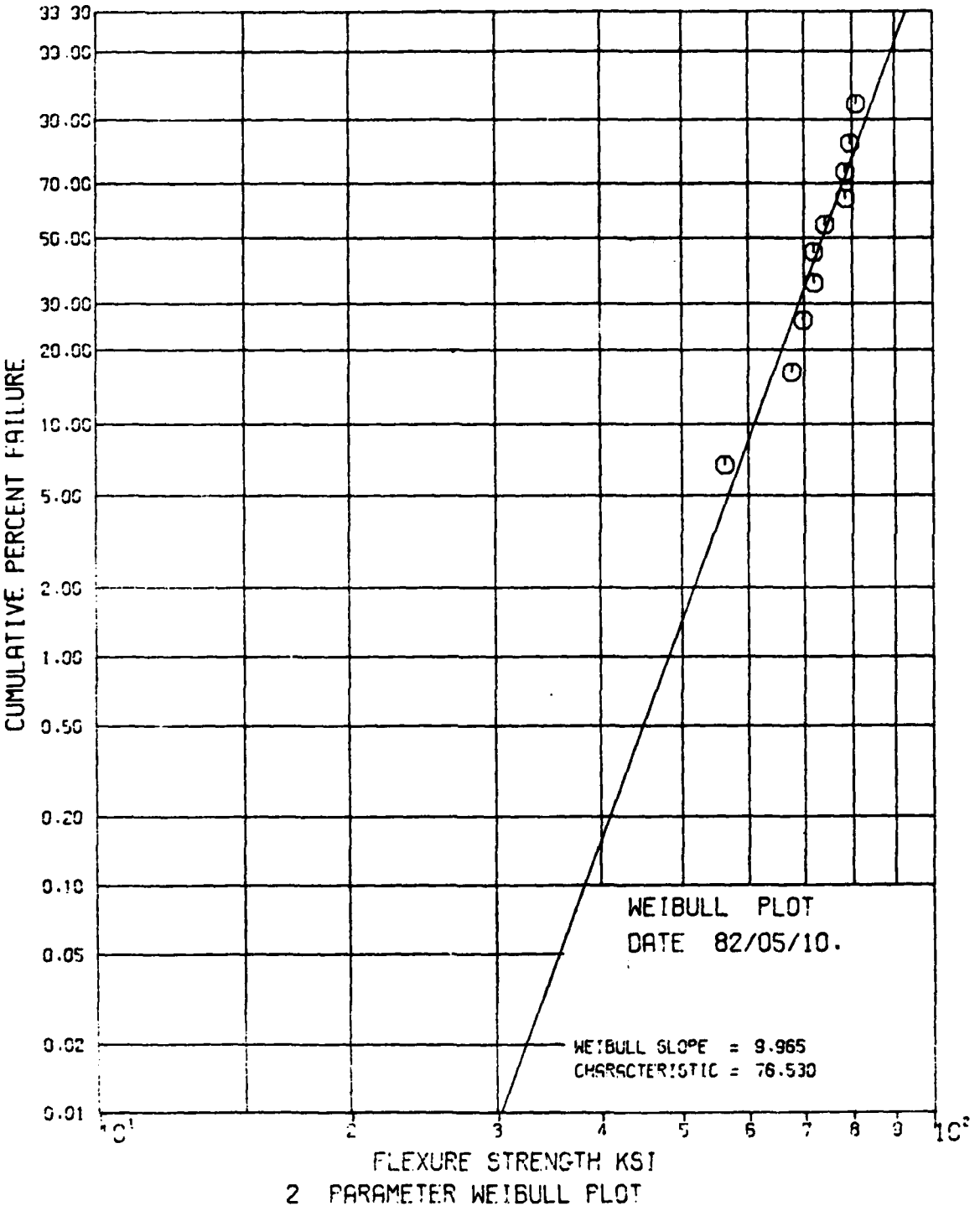

Figure 17. Room Temperature Flexure Strength of Code 7 Test Bars Sintered at 3272F, 70 psi N_2.

therefore, machined. The average room temperature strength of machined bars was 80.8 ±22.3 ksi, with high values measured on individual test bars of 92.6, 100.5, and 106.9 ksi. The low strengths of other individual test bars in these lots were attributed to large flaws developed during the dewax cycle.

To date, the best sintering procedure for Code 7 test bars is a 4-hour hold at 3362 to 3407F with 90 psi N_2.

2.5.3 Codes 9, 10, and 16 - Silicon With 6-Percent Y_2O_3

ACC has densified Codes 9, 10, and 16 test bars using HIP of specimens vacuum sealed in Vycor cylinders and protected from contact with the Vycor by a layer of BN powder. Unless stated to the contrary, all HIP runs were at 3182F and 23 ksi with a 90-minute hold. Table 15 summarizes the HIP results. The results suggest that both Codes 9 and 16 can consistently be HIP processed at 3182F and 23 ksi pressure to produce specimens with densities greater than 3.23 g/cc (98 percent theoretical) and 2250F strengths greater than 80 ksi (the Phase II goal).

Both G.E. and Ford have previously demonstrated[2,3] that improved densification with less weight loss can be achieved by sintering at higher temperature and higher nitrogen pressure than can currently be achieved in the ACC sintering furnace. Ford Motor Company, Scientific Research Laboratory, Dearborn, Michigan agreed to conduct limited sintering runs of selected compositions in their respective high-temperature/high-pressure furnaces.

Two lots each of Codes 9 and 16 test bars were sintered by the Ford Motor Company in their high-pressure furnace. The

TABLE 15. HIP RESULTS FOR VYCOR ENCAPSULATED TEST BARS

Code	Specimen No.	Density (g/cc)	Flexure Strength @ 2250F, (ksi)	Remarks
9	3	3.26	68.2	
9	5	3.29	61.3	White inclusion prenitrided pore.
9	1027104B	3.27	--	Too short to test
9	83	3.16	50.9	BN spray used. Glass contamination on surface
9	2	3.28	93.1	
9	1	3.30	79.7	
9	6	3.26	84.3	
10	65	3.06	--	RT MOR 54.8 ksi
10	--	3.16	--	Too short to test
10	61	3.13	--	Too short to test
10	--	3.16	--	Too short to test
16	100601	3.23	80.4	
16	100603	3.23	95.1	
16	100604	3.25	82.5	
16	100606	3.26	--	HIP @ 3146F Too short to test
16	100602	3.28	85.1	HIP @ 3146F

TABLE 16. SINTERING RESULTS FOR TEST BARS SINTERED AT FORD

Specimen Code	Density (Percent Theoretical)[a]	Shrinkage (Percent)	Weight Change (Percent)
Code 9, Lot 1	99.5	7.8	-0.2
Code 9, Lot 2	100	8.5	-1.0
Code 16, Lot 1	100	7.5	+0.005
Code 16, Lot 2	100	8.4	-0.42

[a]Theoretical Density 3.3 g/cc

density, shrinkage, and weight change results are presented in Table 16. The room-temperature and 2250F flexure strength results are presented in Table 17. The results were very encouraging and indicated that the flexural strength goals of the program (90 ksi at room temperature and 80 ksi at 2250F) were obtainable.

2.5.4 Code 11 - Toshiba Si_3N_4 With 6-Percent Y_2O_3

Table 18 presents the results of the sintering studies conducted on Code 11 specimens. This composition exhibited good room-temperature strength considering the low density. The data indicated that a higher density could not be obtained using the standard sintering process, which used an overpressure of 70 psi N_2. Increased temperatures resulted in weight loss and lower strength.

The best results were obtained with specimens sintered at 1830C for 6 hours at 70 psi N_2 pressure. The characteristic strength and Weibull slope for this lot of 11 test bars was 84.4 ksi and 8.3, respectively (see Figure 18). The average density of these specimens was 2.86 g/cc.

Five specimens were sintered by ACC at 3452F and 100 psi nitrogen overpressure. The specimens had a density of 3.06 g/cc (92-percent theoretical) and a weight loss of 2.5 percent. The 2250F average flexural strength on machined specimens was determined to be 76.8 ±2.9 ksi.

TABLE 17. ROOM TEMPERATURE AND 2250°F FLEXURE STRENGTH OF TEST BARS SINTERED AT FORD.

Specimen Code	Room Temperature				2250F			
	Sintered		Machined[a]		Sintered		Machined[a]	
	Flexure Strength (ksi)	Fracture[b] Origin	Flexure Strength (ksi)	Fracture[a] Origin	Flexure Strength (ksi)	Fracture[b] Origin	Flexure Strength (ksi)	Fracture[b] Origin
Code 9, Lot 1					59.0	3	68.1	4
					63.8	1	72.5	2
					61.5 (avg)		84.6	1
							83.0	6
							77.1 (avg)	
Code 16, Lot 1					74.9	1	82.1	2
					70.8	2	66.6	7
					72.9 (avg)		71.9	1
							84.4	1
							76.3 (avg)	
Code 9, Lot 2			109.3	1	73.6	3	71.3	5
			98.7	1	75.7	1	66.3	5
			96.5	1	74.2	1	76.1	8
			101.5 (avg)		72.9	3	71.7	1
					74.1 (avg)		71.4 (avg)	
Code 16, Lot 2			107.9	1	79.3	4	83.9	2
			111.8	2	57.2	2	87.8	1
			113.8	2	67.3	4	81.7	4
			111.2 (avg)		70.8	2	81.0	4
					68.7 (avg)		83.6 (avg)	

[a]Longitudinal grind using 320 grit compound.

[b]Fracture Origin Key

1. Tensile face
2. Chamfer
3. Tensile face at surface roughness
4. Tensile face at chamfer
5. Internal inclusion
6. Tensile face at machining groove
7. Linear flaw
8. Inclusion at tension face

TABLE 18. CODE 11 SINTERING STUDY RESULTS

Lot	Sintering Temperature F	Hold Time (hrs)	Density, g/cc	Room-Temperature Flexure Strength[a] (ksi) (Sample Size)	Sintering Weight Change, %
1	3272	--	2.73	51.2 (3)	-0.3
2	3272	4	2.81	62.7 (4)	+0.9
3	3326	6	2.86	79.8 (11)	-1.5
4	3326	8	2.88	73.7 (12)	-4.0
5	3362	4	2.78	63.0 (9)	-5.4

[a]Average value

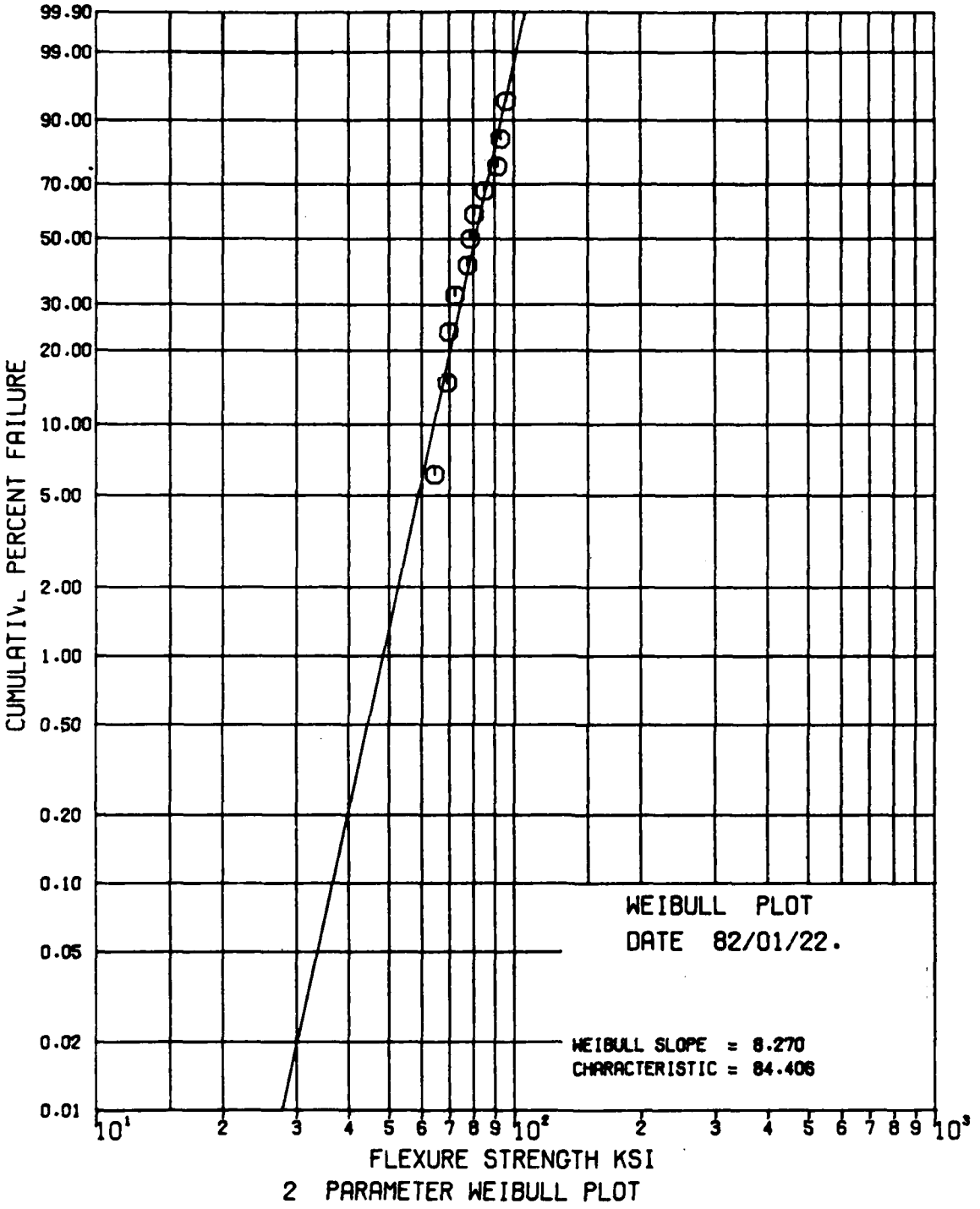

Figure 18. Room Temperature Flexure Strength of Code 11 Test Bars Sintered at 3326F for Six Hours, 70 psi N_2.

2.5.5 Code 14 - GTE SN 502 Si_3N_4 With 7-Percent $BeSiN_2$ and 7-Percent SiO_2

G.E. sintered ACC molded test bars to 99.99-percent theoretical density. The average room-temperature strength of three specimens, as measured at GTEC, was 31 ksi. The low strength was attributed to surface pores.

Because of the problems experienced by G.E., no more Code 14 test bars were sintered.

2.5.6 Summary of Test Bar Results

Table 19 summarizes the best test bar results for each composition evaluated during Phase II.

2.5.7 High-Pressure Sintering

To improve the flexure strengths of Codes 2, 7, and 11 specimens, it was necessary to increase the density and reduce the weight loss. The weight loss was attributed to dissociation of the Si_3N_4 which caused surface defects. The densities of Codes 2, 7, and 11 specimens were increased by increasing the sintering temperature; however, the limit of the current ACC furnace was reached--3452F. Furthermore, at these temperatures, the weight loss was excessive, even at the maximum N_2 pressure (100 psig) capability of the ACC furnace.

The results obtained at Ford on Codes 9 and 16 specimens sintered above 3452F with high N_2 pressure, indicated that increased density (100-percent theoretical) and low weight loss (<1.0 percent) could be achieved. Also, there seemed to be a qualitative improvement in surface smoothness of the specimens sintered at high pressures. Therefore, high-temperature/high-pressure sintering studies of Codes 2, 7, 9, and

TABLE 19. SUMMARY OF TEST BAR RESULTS

Composition	Sintering Conditions		Density, % Theoretical	Weight Change %	Strength (ksi)[a]	
	Temperature (F)	Pressure (psi)			Room Temperature	2250F
2	3362	90	97	±1	93	64
7	3362-3407	90	97	±1	93	64
9	b	b	99.5	-1	102	74
11	3452	100	92	-2.5	--	77
16	b	b	99.5	-0.5	111	80

[a]Average strength
[b]Ford Motor Co. Proprietary

11 specimens were initiated. Garrett worked with several independent laboratories that had high-temperature/high-pressure sintering facilities to accomplish this task.

Codes 2, 7, 9, and 11 specimens were supplied to both NASA-Lewis and AMMRC. NASA-Lewis ran seven sintering experiments using Codes 2, 7, 9, and 11 test bars. The experiments were carried out at 400 psi nitrogen overpressure over a temperature range of 3407 to 3880F. Although the densities and flexural strength were below that exhibited by specimens sintered at ACC and Ford, the results were informative and provided direction for the next series of experiments.

AMMRC sintered a limited number of test bars of Codes 2, 7, 9, and 11 compositions at 3407 to 3452F and 400 to 1200 psi in a nitrogen atmosphere. Densities in excess of 3.20 g/cc were obtained for Code 2, 7 and 9 test bars. Code 11 test bars proved difficult to sinter.

Four-point flexure strengths were measured on as-sintered specimens. Code 2 test bars exhibited strengths of 81.4, 88.7, and 81.0 ksi. Code 7 test bars exhibit very low strengths that were attributed to large internal cracks. X-ray radiography revealed that this particular lot of Code 7 test bars exhibited cracks in the as-dewaced condition and subsequently wer discarded.

Further studies were conducted at AMMRC to develop a sintering procedure to densify Code 9 Si_3N_4 test bars. The best results were obtained under two sintering conditions: a) 3595F/300 psi N_2 then decrease to 3460F/800-1200 psi N_2; and b) 3490F/300 psi N_2 then increased to 3595-3460F/800-1200 psi N_2. Under these conditions, the test bars obtained densities in excess of 98 percent theoretical and exhibited as-sintered room temperature strengths of 85 to 97 ksi. Four test bars were

evaluated for stress rupture behavior. These results are presented in Section 2.6.2.

2.6 Miscellaneous Test Bar Evaluations

2.6.1 Oxidation Study

Some of the first silicon nitride ceramics to contain yttria exhibited oxidation-related strength reduction for exposures in the 1500 to 2000F range. Since the compositions being evaluated as part of this program all contain Y_2O_3, then oxidation stability is of interest. During Phase I, the oxidation behavior of the Code 1 composition (Si_2N_4 + $4Al_2O_3$ + $8Y_2O_3$) was assessed. The weight change was negligible at temperatures up to 2300F after 240 hours and only 0.6 percent at 2552F after 170 hours. No evidence of an oxidation-degradation problem was observed. These initial studies indicated that the Code 1 composition was relatively stable to oxidation in this temperature range.

As a continuation of the oxidation study, Code 1, along with Code 7 (silicon with 2 percent Al_2O_3, 6 percent Y_2O_3 and 1 percent Fe_2O_3), Code 9 (silicon with 6 percent Y_2O_3 and 1 percent Fe_2O_3) and Code 16 (silicon with 6 percent Y_2O_3) were evaluated for oxidation (weight gain) and room temperature strength reduction after exposure in the 1350 to 2200F range for 340 hours. Code 1 and 7 specimens were sintered by ACC under conditions similar to those described in Paragraphs 2.5.1 and 2.5.2. Codes 9 and 16 specimens were HIP processed by ACC as described in Paragraph 2.5.3. Again, no evidence of oxidation degradation was observed in either case. The results in terms of weight change are presented in Table 20. The weight changes for Codes 1, 7, 9, and 16 are negligible. This study

ABLE 20. OXIDATION WEIGHT CHANGE AFTER 340-HOURS EXPOSURE AT INDICATED TEMPERATURE

Code	Specimen	Temperature (F)	Weight Change (%)
1	10750	1350	-0.03
	10741	1640	0
	10742	1910	+0.04
	10743	2060	0
	10747	2200	0
7	10963	1350	+0.03
	10961	1640	+0.08
	10956	1910	+0.05
	10957	2060	0
	10959	2200	+0.05
9	3	1350	-0.03
	6	1640	0
	1	1910	0
	2	2060	-0.05
	5	2200	+0.04
16	100603	1350	-0.14
	100604	1640	-0.05
	100601	1910	-0.01
	100602	2060	-0.03
	100606	2200	0

indicates that Codes 1, 7, 9, and 16 are relatively stable with respect to oxidation in the 1350-2200F range.

The specimens used in this study were halves of test bars used for room temperature strength measurements. When the geometry of the exposed specimen permitted, the room temperature strength was measured and compared with the strength in the unexposed conditions. For this limited sample, there was no evidence of change in strength caused by the oxidation exposure. The surfaces of the specimens after exposure for 340 hours are shown in Figure 19.

Thus, Codes 1, 7, 9, and 16 appear to be relatively stable to oxidation and do not exhibit strength reduction related to the exposure in the 1350 to 2200F range. These conclusions are based on individual specimens at each test condition and, therefore, cannot be evaluated statistically.

2.6.2 Stress Rupture Behavior

Codes 2, 9, 11, and 16 test bars were evaluated by AMMRC for step-temperature stress-rupture (STSR) behavior. Codes 2 and 11 were sintered by ACC and Codes 9 and 16 were sintered by Ford Motor Company. The experiments covered the temperature range of 1472F to 2240F with stresses ranging from 29 ksi to 87 ksi. The experimental procedure consisted of heating the specimen to 1472F and applying a specified stress for 24 hours. If the specimen survived, it was heated under stress to the next temperature level (i.e., 1652F) and held for 24 hours. This procedure was repeated at 1832F, 2012F, and 2240F. The results of the STSR testing are presented in Figure 20. The failures in the case of Code 2 are consistent with the reduction in fast fracture strength from 93 ksi at room temperature to 64 ksi at 2250F. Code 11 specimens were not sintered to

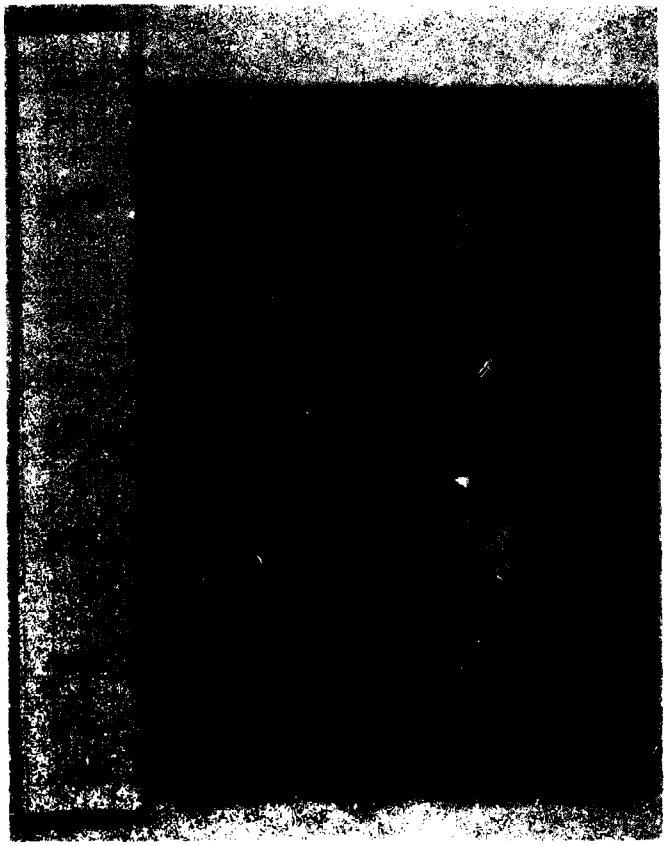

Figure 19. Specimens Exposed in a Gradient Furnace for 340 Hours. Codes 7, 16, 9, 1, Respectively Left to Right. Temperature Scale (F) on Left.

MP-83132

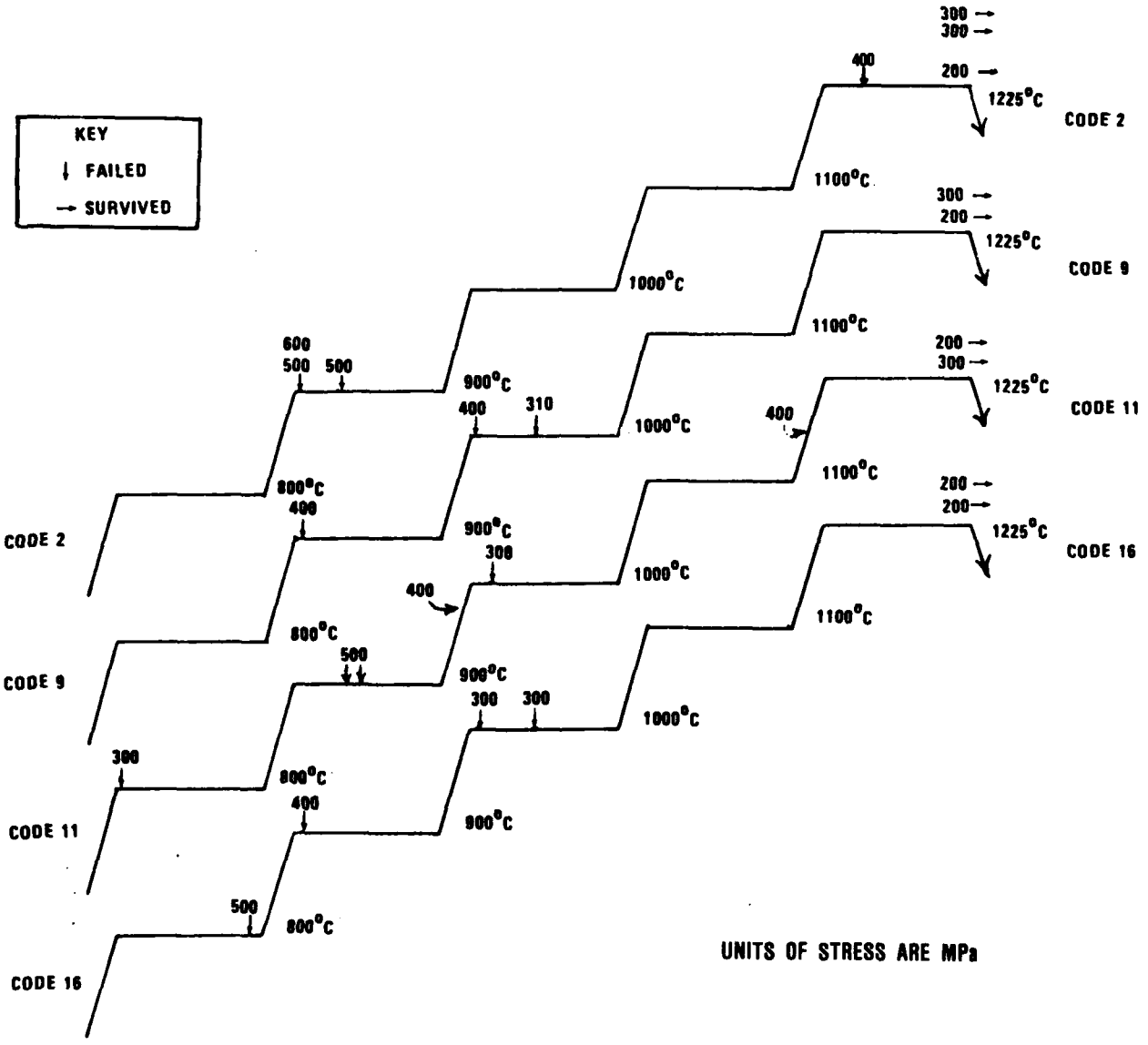

Figure 20. Step-Temperature Stress-Rupture Results.

full density, and the results may be a combination of porosity and processing defects.

All STSR test survivors were analyzed for creep deformation. For Codes 9 and 16, there was negligible creep (0.1 percent) deformation while Codes 2 and 11 exhibited noticeable permanent deformation. At 43.5 ksi Code 2 specimens had 0.77 to 1.03 percent creep deformation and Code 11 specimens had 0.68 percent creep deformation.

A more detailed discussion of the STSR test procedure and the above results is provided in a report by George Quinn of AMMRC included here was Appendix A.

Four Code 9 test bars sintered at AMMRC to 98 percent theoretical density (see section 2.5.7) were evaluated for stress-rupture behavior at 43.5 ksi, 2192F for 1000 hours. After unloading, the permanent strain (curvature) was approximately 0.15 to 0.20 percent. The stress-rupture tested bars were then fractured at room temperature under four point loading at a crosshead speed of 0.002 in/min. The room temperature strengths were calculated as 74.3, 96.6, 84.0, and 70.0 ksi respectively. The fracture origin of the four test bars were related to internal processing defects. No sign of oxidation degradation was evident.

2.6.3 Microstructure Evaluation

Scanning electron microscopy was used to evaluate the sintered microstructures of the various compositions under study. Figure 21 shows photomicrographs of the 6-percent Y_2O_3 compositions (Codes 9 and 16). For comparison, Ford's RM-2 sintered

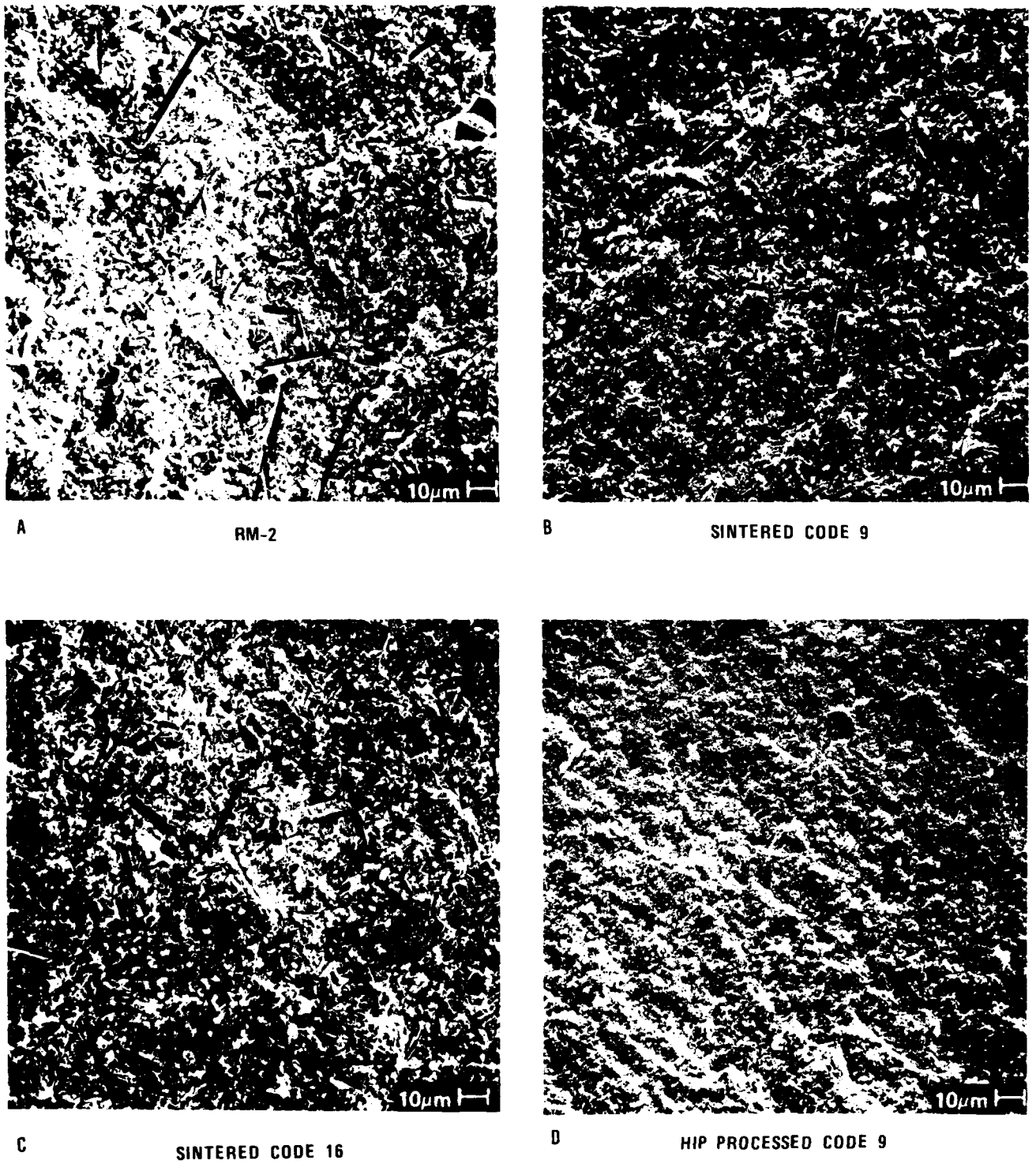

A RM-2

B SINTERED CODE 9

C SINTERED CODE 16

D HIP PROCESSED CODE 9

Figure 21. Scanning Electron Photomicrographs of 6-Percent Y_2O_3 Compositions (Codes 9 and 16).

Si_3N_4 is also included. Sintered specimens of Codes 9 and 16 compositions have similar microstructures consisting of a fine-grain matrix with elongated grains throughout the specimen. The Codes 9 and 16 microstructures are very similar to the RM-2, with the exception that the RM-2 elongated grains appear to be more highly developed. Figure 21 shows a Code 9 microstructure for a specimen HIP processed at 3132F. The microstructure is very fine and has fewer elongated grains.

Figure 22 shows photomicrographs of the 2-percent Al_2O_3 and 6-percent Y_2O_3 compositions (Codes 2, 7, and 11). Code 2 consists of a fine grain matrix with some evidence of grain elongation. Code 7 also has a fine grain matrix with more development of the elongated grains. Neither Code 2 or 7 have the elongated grain development to the extent observed in the 6-percent Y_2O_3 compositions. This is probably related to the lower sintering temperature of the compositions containing 2-percent Al_2O_3 as compared to the compositions having no Al_2O_3. Figure 22C shows a Code 11 composition sintered to a density of 93 percent of theoretical. Again, the microstructure is a fine-grain matrix with some evidence of grain elongation similar to Codes 2 and 7.

2.6.3 Heat Treatment Studies

The reduction in strength of sintered Si_3N_4 materials at high temperature has generally been attributed to softening of a glass composition at the grain boundaries.[4,5] The strength reduction can potentially be minimized by decreasing the glass at the grain boundaries or by making the glass more refractory. Composition variations[6], such as those being evaluated in Codes 1-16, represent one approach. An alternate approach is post-sintering heat treatment to either crystallize [7] the glass or modify its composition.[8,9]

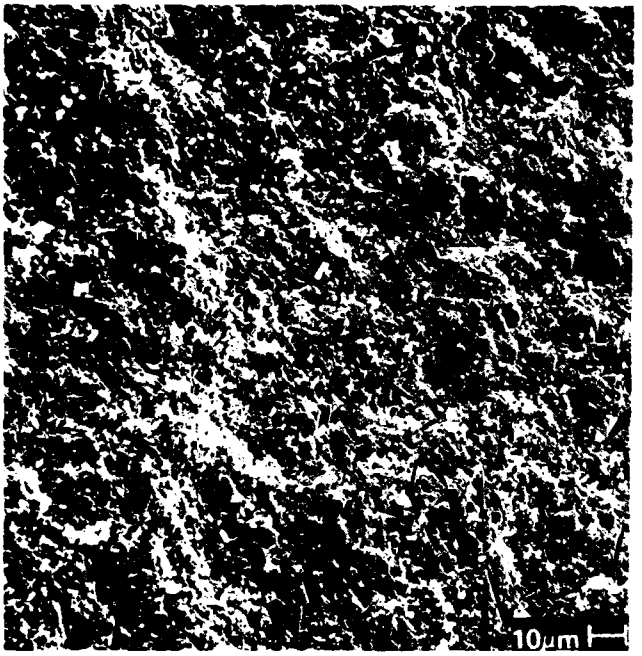

SINTERED CODE 2

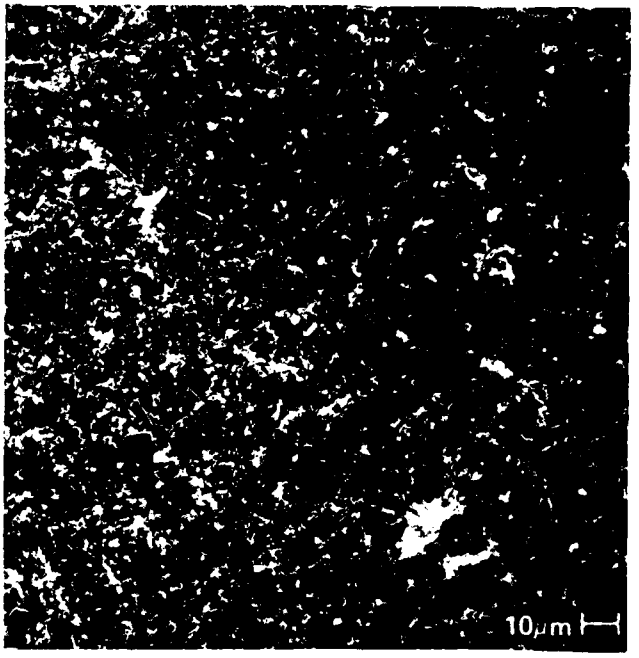

B

SINTERED CODE 7

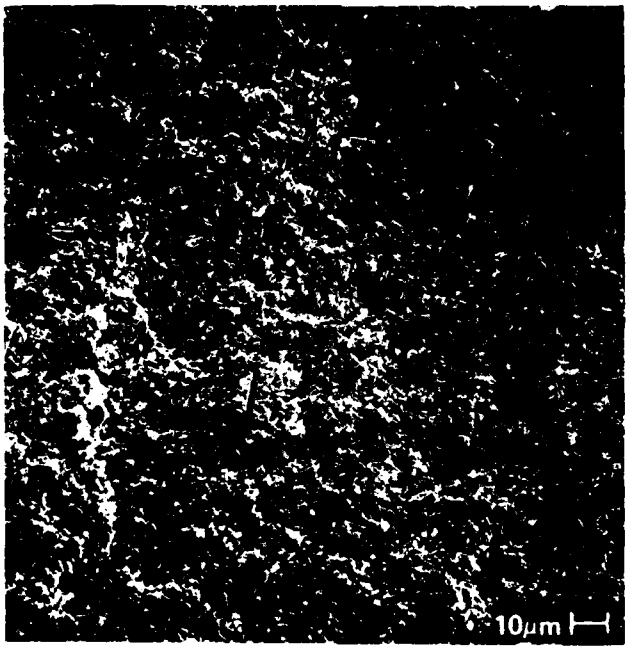

C

SINTERED CODE 11

Figure 22. Scanning Electron Photomicrographs of 2-Percent Al_2O_3 and 6-Percent Y_2O_3 Compositions.

This section describes efforts during Phase I to improve the high-temperature strength of the Code 1 composition by post-sintering heat treatments over the temperature range 1832-2732F. Initially, 48- to 60-hour exposures were conducted in static air.

The test-bar surface and cross sections were examined visually to assess the oxidation characteristics. No oxidation or discoloration was visible after exposure at 1832F and 1292F. A thin glassy layer having a slight brownish or golden discoloration was present after 2372F exposure. A similar, but thicker and slightly darker, glassy layer resulted from the 2552F exposure. Exposure at 2732F resulted in pitting of the Si_3N_4 and a very thick glassy layer containing gas evolution bubbles. This temperature was clearly above the use capability of the Code 1 material. Use at 2552F would also be questionable based upon the thickness of the glassy layer.

The heat-treated specimens were analyzed by X-ray diffraction (XRD) to determine the crystalline phases present after each exposure. The results are summarized in Table 21. The as-received material is nearly pure beta Si_3N_4 with only a few minor XRD peaks which have not been identified. Phases reported in the literature such as the H, J, and K phases are not present at detectable levels. The β Si_3N_4 peaks show little variation after heat treatment. The other peaks progressively disappear at increasing heat treatment temperature. After 2372F exposure, only β Si_3N_4 plus a weak pattern for $Y_2Si_2O_7$ are present for the bulk material. After 2552F exposure, the $Y_2Si_2O_7$ is replaced by an even weaker (and possibly questionable) pattern for Y_2SiO_5. After 2732F exposure, only β Si_3N_4 is detectable in the specimen interior and α cristobalite in the oxide layer.

TABLE 21. X-RAY DIFFRACTION ANALYSIS OF HEAT-TREATED CODE 1 COMPOSITION

Heat Treatment	X RD Phases
As-Received	βSi_3N_4 + Unidentified Peaks At 28.4, 32.6, and 46 degrees
1830F/48 Hours	βSi_3N_4 + Peak at 32.6 degrees and Doublet at 45.3 degrees
2200F/48 Hours	βSi_3N_4 + Peak at 32.6 degrees and Hump at 45.3 degrees
2370F/48 Hours	βSi_3N_4 + $Y_2Si_2O_7$
2550F/48 Hours	βSi_3N_4 + Y_2SiO_5
2730F/60 Hours	Only Si_3N_4 in Interior; α Cristobalite in Oxide Layer

These initial studies indicated that the Code 1 material was relatively pure and free of unstable secondary phases that might cause catastrophic oxidation or strength-degradation effects. The studies also indicated that the oxidation rate was very low in the intended use temperature range of 2192F. Finally, these exposures indicated by the discoloration of the glassy surface layer at higher temperature that impurities were possibly diffusing from the grain boundaries and concentrating in the surface layer. Lange[9] and Clarke[10] have shown that thermal extraction of grain boundary impurities can substantially increase the high temperature strength by changing the grain-boundary glass to a more refractory composition. Thus, it was decided that longer-term, heat treatment exposures directed towards impurity extraction should be conducted.

The thermal extraction studies by Lange and Clarke were conducted at 2732F. However, the prior thermal-exposure tests under this program for Code 1 material determined that severe oxidation and pitting occurred at 2732F. Therefore, longer term heat treatments were only conducted up to 2552F, specifically at 2192F and 2552F in static air and at 2373F packed in submicron size silicon dioxide powder. An adequate supply of injection-molded Code 1 test bars was not available for this study, so the supply was supplemented by prior lots of slip cast and injection-molded bars of the same composition fabricated under an IR&D program. These had a lower baseline strength, primarily due to the presence of pores resulting from air entrapment during processing.

The weight-gain data for the three heat treatment temperatures is summarized in Figure 23. After static oxidation exposure at 2192F for 242 hours, the weight change was barely measureable. No discoloration or sign of an oxide scale was visible. After 286 hours packed in SiO_2 powder at 2372F, the

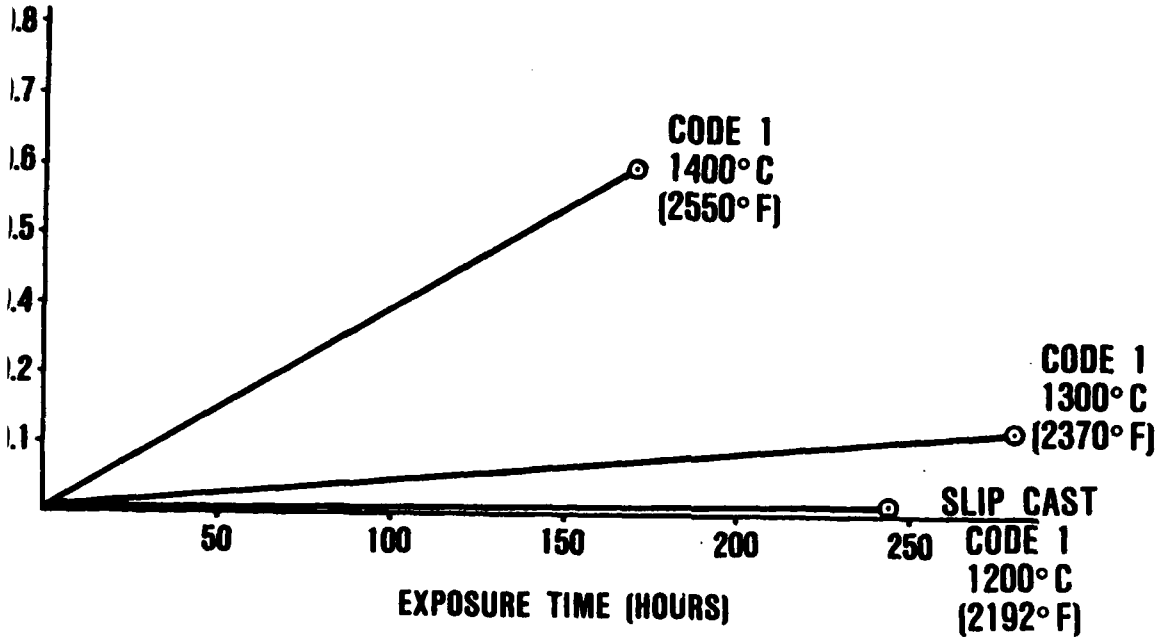

Figure 23. Weight Gain of Code 1 Composition After Static Air Exposure.

weight gain was less than 0.15 percent. The test bars were not discolored, but the SiO_2 powder was sintered and had a slight brownish discoloration where it was in contact with the test bars. The test bar in this contact region had an unglazed roughened appearance. In other regions where the SiO_2 had shrunk away from the Si_3N_4 and was not in contact, the test bar was glazed.

After static oxidation exposure at 2552F for 170 hours, approximately 0.6-percent weight gain had occurred, and a glassy layer with a slight brownish or golden discoloration coated the surface of the test bars. Some of the test bars were sandblasted to remove the glassy layer. The bars were then placed back in the furnace and the treatment at 2552F continued for an additional 116 hours (286 hours total). Both sandblasted and unsandblasted bars continued to gain weight. The sandblasted bars again picked up a slightly discolored glassy oxide layer.

A few slip-cast bars of the Code 13 composition from an IR&D program were included in the heat treatment studies. The Code 13 material developed a heavy brown oxide scale at 2552F with a 1.4-percent weight gain after 170 hours. After exposure at 2192F for 242-hours, weight changes were barely measurable.

The strengths of the Code 1 and Code 13 test bars were measured at 2250F in four-point flexure. The data for the Code 1 and 13 compositions are compared in Figure 24 with baseline data. Although the number of data points was limited, it appeared that the Code 1 composition had good strength retention after exposures at 2192F and 2552F. The Code 13 composition had good strength retention for 2192F exposure but a significant strength drop for 2552F exposure. Neither Code 1 nor Code 13 showed any indication of strengthening due to the heat treatments.

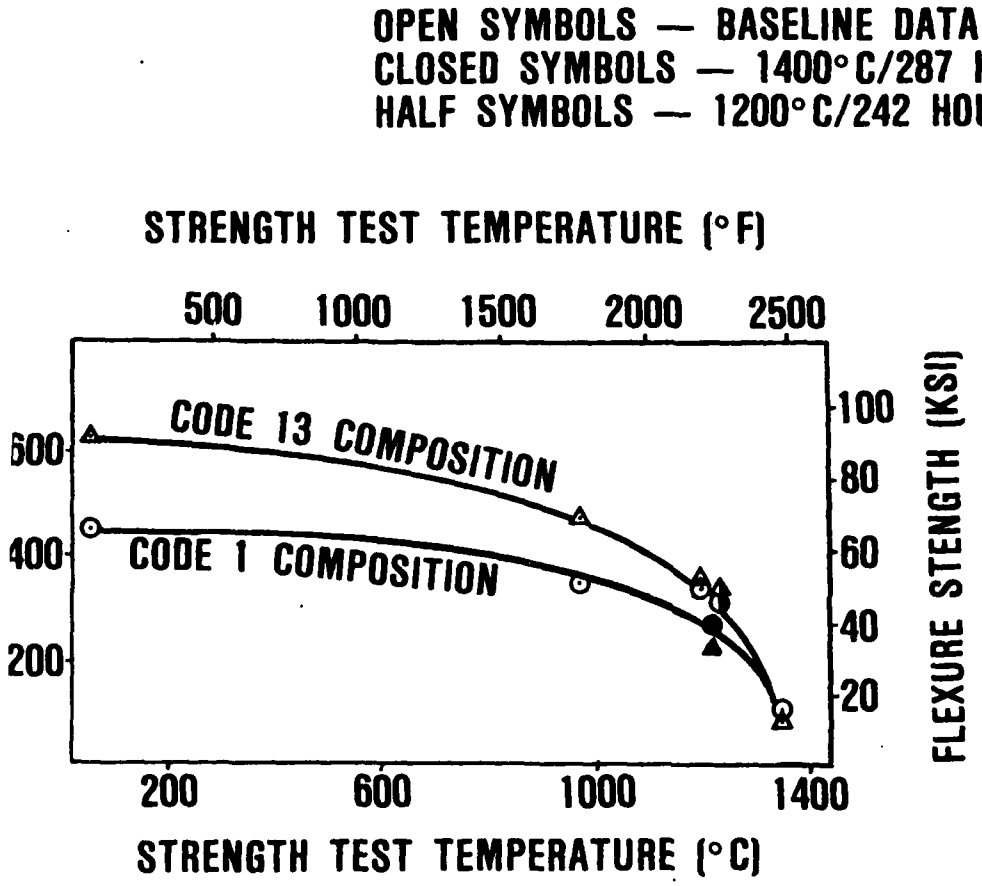

igure 24. Strength Comparison of Heat Treated and aseline Specimens.

Selected Code 1 and Code 13 composition test bars were evaluated by energy dispersive X-ray analysis (EDX) to determine if impurities and grain boundary constituents were migrating to the surface during oxidation heat treatments. The EDX plots for the oxide layers and base materials are shown in Figures 25 and 26.*

In both cases, the concentration of iron, aluminum, yttrium, and calcium is much higher in the oxide layer and indicates that these elements have diffused to the surface during the thermal treatment. This suggests that extraction strengthening is possible. However, SEM analysis of the fracture surface showed that fractures initiated at oxidation pits at the interface of the oxide layer and the Si_3N_4. The severity of the pits was great enough to preclude assessment of any change in high-temperature strength due to composition change at the grain boundaries. Additional study outside the scope of this program is required to evaluate the competing mechanisms of strengthening due to composition change and weakening due to formation of surface defects.

*The gold (Au) peaks in Figure 25 are due to the gold coating sputtered on to prevent charging during the SEM and EDX analyses. To avoid the overlap between the gold and yttruim peaks, the Code 13 specimen shown in Figure 26 was sputtered with carbon instead of gold.

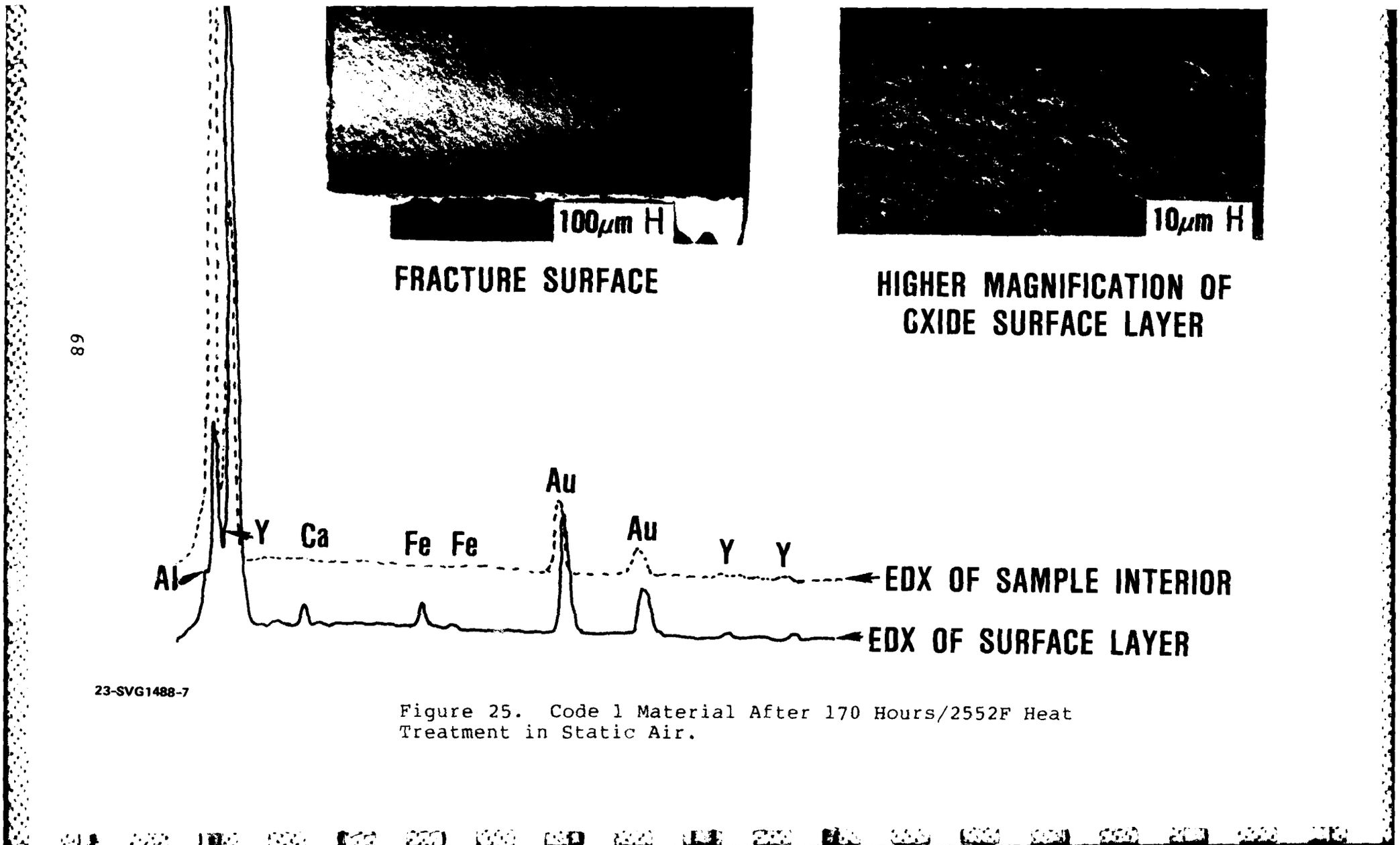

Figure 25. Code 1 Material After 170 Hours/2552F Heat Treatment in Static Air.

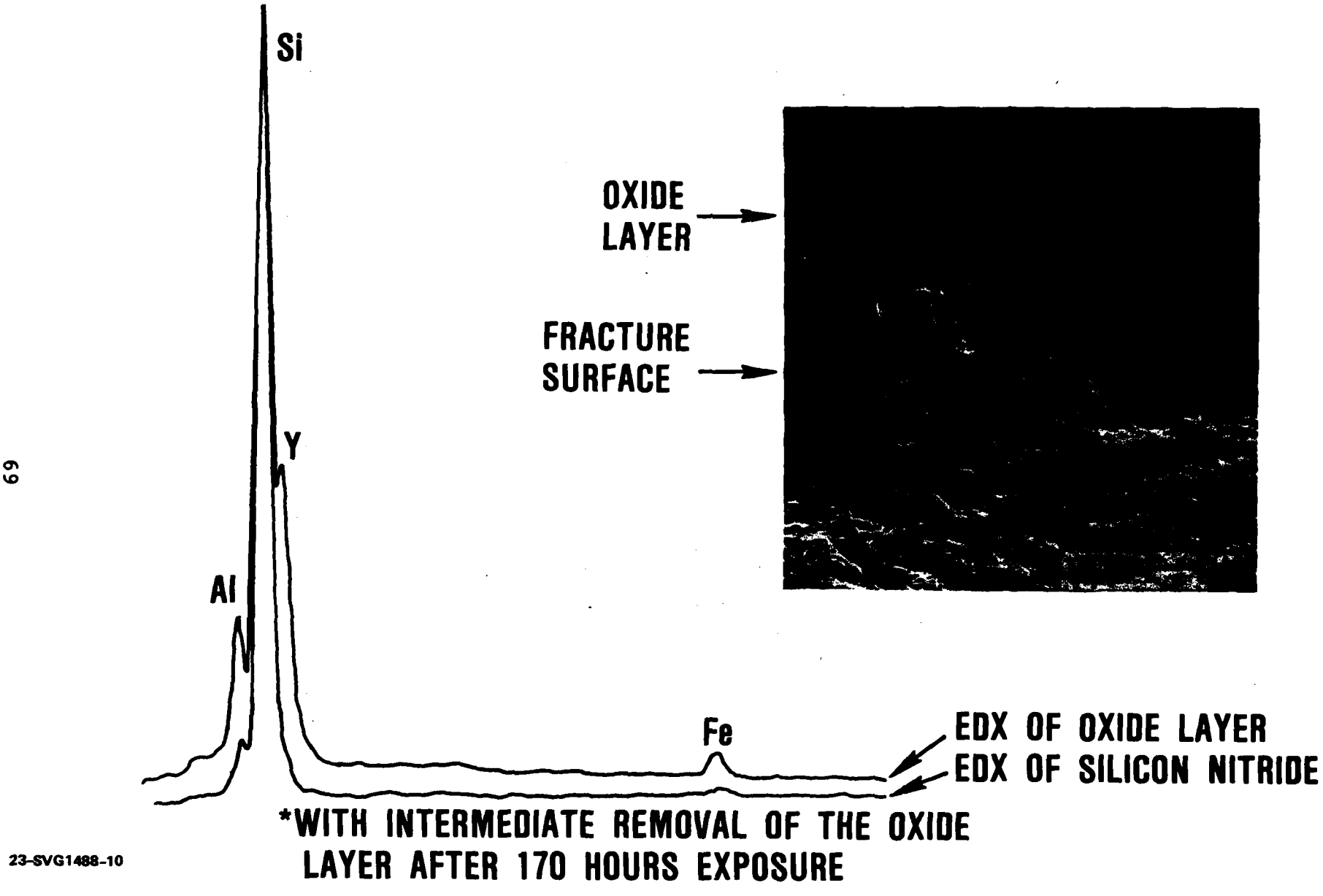

Figure 26. Evaluation of Code 13 Composition Sintered RBSN Specimen 8680 After Oxidation at 2552F for 287 Hours with Intermediate Removal of the Oxide Layer After 170 Hours Exposure.

3. RADIAL ROTOR FABRICATION

The initial program plan called for molding radial rotors using an existing aluminum T04 tool that was designed to make wax patterns for casting of metal T04 turbocharger rotors. The tool was modified in the area of the shaft, but all radii were left unchanged and were smaller than normally would be incorporated in a tool designed specifically for ceramic components. Many difficulties were encountered in fabricating rotors using the T04 injection molding tool. These problems manifested themselves as cracks and shrink voids in the rotor.

Although rotors of adequate quality could not be processed using the T04 tooling, the exercise provided some valuable information. Molding parameters (material temperature, mold temperature, molding pressure, etc.) were identified along with binder content and mixing procedures. The inspection procedures for evaluating molded rotors were also determined. This inspection consisted of visual (10 to 40X) examination for surface defects (cracks, pits, flow lines, etc.) and X-ray radiography examination for internal defects (void, cracks, inclusions, etc.). A dewax/presintering cycle was also developed to increase the green strength of the rotors. This cycle consisted of a normal dewaxing procedure up to 800F followed by a presintering treatment at 1200F for Code 2, and 950F for Codes 7 and 9. The dewaxing cycle was also identified as an area that needed further improvement.

As indicated above, difficulties were encountered in attempts to fabricate rotors of the T04 turbocharger size. These problems were attributed to a combination of the molding tool, molding equipment, and the component size. The T04 rotor mold is a modified aluminum wax molding tool and was not designed to injection mold ceramics compositions. In addition, the injection molder required for this size tool did not provide close control of the molding parameters. As a result, it

was decided to change to a smaller turbocharger rotor size (T02) for the program.

The steel T02 rotor tooling, made available through company funding, was specifically designed for ceramics. It was a smaller tool, and could be used in ACC's Arburg injection molder where a closer control of molding parameters is possible. In addition, the smaller size resulted in more moldings per batch and more rotors per dewax cycle and sintering run.

Changing to the T02 rotor took advantage of the concurrent effort being expended by ACC and GAPCO to develop ceramic T02 turbocharger rotors. This included GAPCO's experience in rotor machining, balancing, shaft attachment, and hot spin testing.

The initial rotors molded with the T02 die exhibited internal shrinkage cracks after sintering similar to those observed in T04 rotors. These cracks were attributed to poor flow of material and incomplete fill during molding. As a result, several modifications of the gate and sprue in the molding tool were undertaken. By increasing the gate area and providing a sprue system that allowed the ceramic material to remain more moldable, rotors were produced without shrink cracks. The molding parameters (i.e., material, die temperatures, pressure, etc.) were also modified to improve the flow of the material. The overall results were a molded rotor free of internal defects (by X-ray radiography) and minimization of surface defects or cracks (by 40X visual examination).

All rotors molded with the initial T02 tool had varying degrees of surface defects. These defects were of two types: (1) flow lines (cracks) in the hub and shaft area, and (2) cracks at the blade/hub transition at the exducer end of the rotor. In general, the Codes 7 and 9 rotors exhibit only

slight flow lines and fewer cracks at the blade/hub transition as compared to Code 2. The cracks at the blade/hub transition were attributed to the tool design (small radii), and the tooling was modified to improve this situation. Examples of Codes 2 and 7 molded T02 rotors are shown in Figure 27.

The dewax cycle was a major problem since molded rotors consistantly developed cracks of varying degrees during the dewax operation. Experiments revealed that a slower heating rate in the initial part of the cycle reduced the extent of cracking.

In addition to experimental observation, thermo-gravimetric analysis and a knowledge of the physical properties of the binder (viscosity, melting point, evaporation point, etc.) were used to modify the dewax cycle. The goal was to develop a cycle with the proper heating rate to allow the binder to become sufficiently fluid to maintain a uniform distribution throughout the part as the binder is removed from the surface of the rotor.

Although dewaxed rotors completely free of surface defects were not achieved, the best rotors were still processed through densification. At this point, ACC's standard nitriding cycle appeared adequate for Codes 7 and 9 rotors. Upon completion of the nitriding, Code 7 rotors were sintered at the best conditions developed for test bars. Code 9 rotors were to be sintered when an appropriate high-temperature/high-pressure cycle (see subsection 2.5.7) was identified.

Fifteen Code 2 rotors were sintered at 3362F/90psi N_2 with a powder bed. These rotors exhibited densities of 3.20 to 3.22 (97-percent theoretical) and a weight loss of 0.06 to 1.6 percent. Fourteen rotors were free of internal defects as indicated by X-ray radiography but all exhibited some degree of

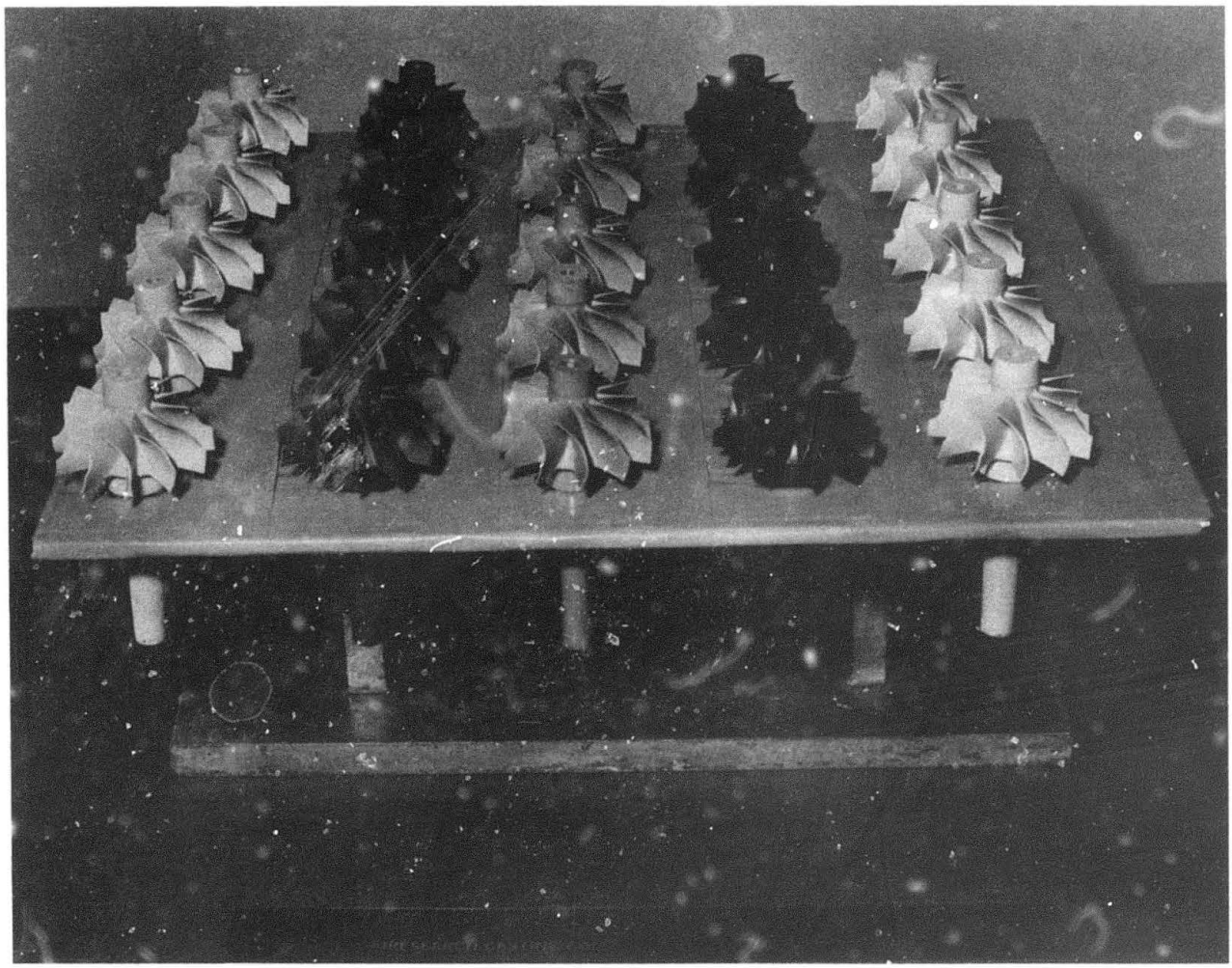

Figure 27. Codes 2 and 7 Molded and Dewaxed T02 Rotors (Row 1-Code 2 Dewaxed, Row 2-Code 7 Dewaxed, Row 3-Code 2 Molded, Row 4-Code 7 Molded, Row-5 Code 2 Dewaxed).

MP-86605

flow lines or cracks in the hub/shaft area and cracks at the blade/hub transition. Figure 28 shows a comparision between molded and sintered Code 2 T02 rotors.

Efforts continued on the fabrication of rotors from Codes 2, 7, and 9 compositions. Rotors fabricated from the Code 2 composition have demonstrated the potential of exceeding 200,000 rpm in spin testing. The Code 2 T02 rotors with known surface cracks were room temperature spin tested to 183,000 rpm and survived intact (see Section 5.2). Similarly processed rotors with known surface cracks were spin tested at 1750C and exceeded 190,000 rpm before failing (see Section 5.3).

In order to eliminate the surface cracks that led to rotor failure during spin testing, the T02 injection molding die was modified to increase the radius at the blade root. Code 2 rotors were molded using the modified die and then dewaxed. Although the die modification appeared to eliminate the cracks at the blade root, large axial cracks were encountered in the shaft and hub region. These axial cracks did not appear to be related to the molding die.

The dewax cycle was modified to incorporate a slower heating rate up to peak temperature and a slow cool down from the peak temperature. This procedure alleviated the large axial cracking problem. Eighteen Code 2 rotors that were visually acceptable after dewax were sintered. Three groups of five to seven rotors each were sintered at 3362F/90 psi N_2/4 hours. The rotors exhibited densities of 3.22-3.25 g/cc and a weight loss of 2 percent. Unfortunately, all the rotors exhibited surface (40X visual) and internal (X-ray radiography) cracks. These defects were attributed to the mixing and injection molding steps. They were identified as flow or knit lines that did not completely bond during molding and developed into cracks during subsequent heat treatment.

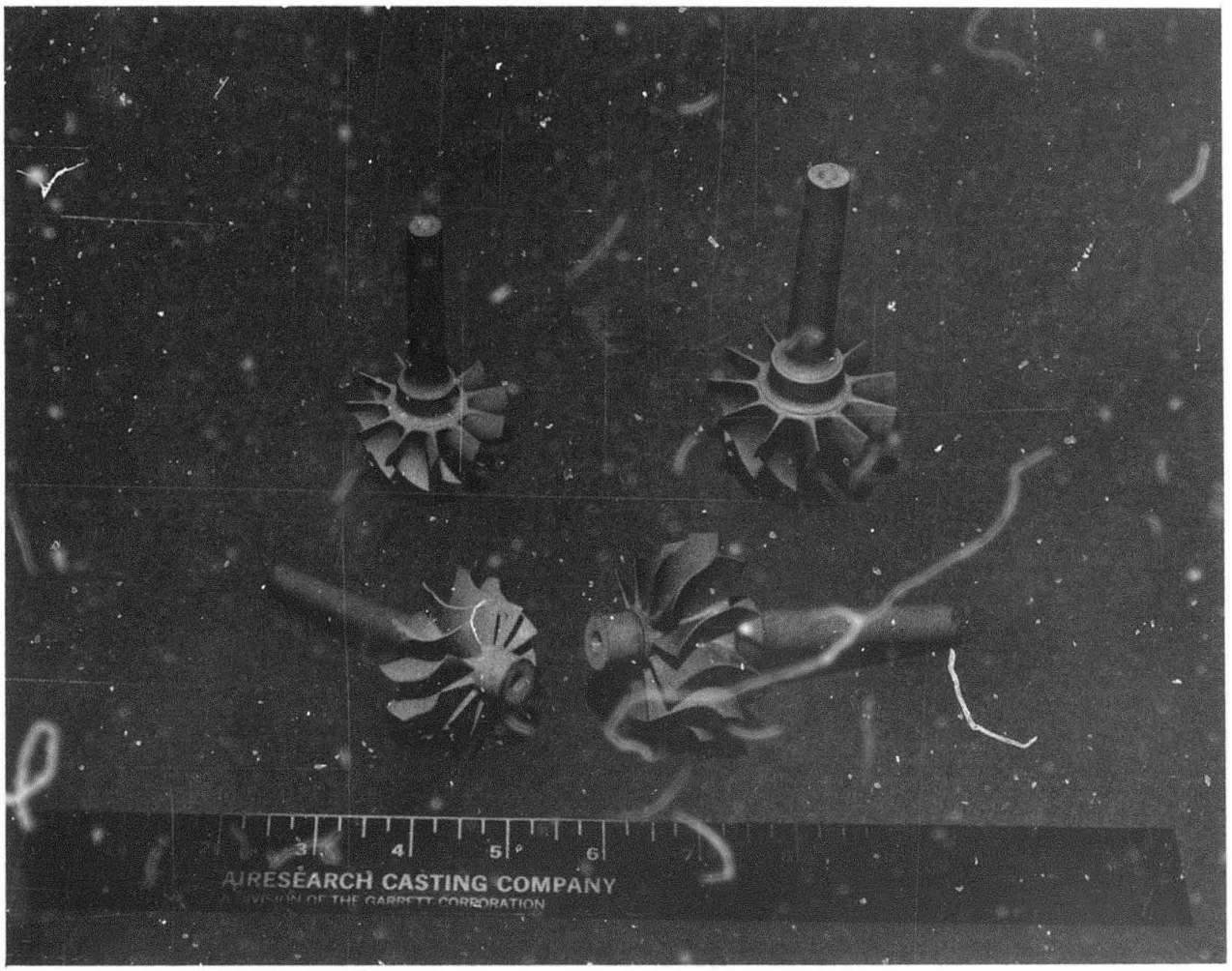

Figure 28. Comparison Between Molded and Sintered T02 Rotors (Sintered on Left, Molded on Right).

Initial efforts with rotors molded from the Code 7 composition suggested that they were less susceptible to cracking during dewaxing than Code 2 rotors. This difference was probably related to the larger particles of silicon used in producing Code 7 compared to the fine-particle Si_3N_4 used for the Code 2 material. The larger particle size in Code 7 provided larger pore channels and increased permeability of the binder from the interior of the component.

Based on the improved results from the Code 7 dewax cycle and the similarity in flexure strengths of the Codes 2 and 7 compositions (93 ksi at room temperature and 64 ksi at 2250F), the effort was increased to produce rotors of spin quality from the Code 7 composition. A group of Code 7 rotors were processed through molding, dewaxing, nitriding, and sintering. The rotors exhibited sintered densities in the range of 3.21 to 3.23 g/cc (96 to 97 percent theoretical). The rotors were evaluated as follows:

- Three fully processed rotors were visually (10-40X) and X-ray radiographically inspected and were spin tested at elevated temperature. The spin test results are reported in Section 5.3.

- Three fully processed rotors were machined into test bars from which room-temperature and 2250F flexure strengths, and fracture origins were determined.

- One rotor in the nitrided condition was evaluated by X-ray diffraction (XRD) and metallography.

The flexural strength results are presented in Table 22.

For the most part, the measured strengths shown in Table 22 were significantly lower than previously reported for

TABLE 22. ROOM-TEMPERATURE AND 2250F FLEXURAL STRENGTHS OF TEST BARS MACHINED FROM FULLY PROCESSED CODE 7 ROTORS

Specimen No.	Flexure Strength[a] (ksi)	Fracture Origin[b]
	Room Temperature	
04053-8A	48.8	Internal Flow Line
04053-9A	84.4	Tensile Face
04053-11A	88.1	Tensile Face
04063-2A	79.5	Internal Flow Line
04063-3A	64.5	Pore
04083-2A	80.3	Inclusion at Tensile Face
	2250F	
04053-8B	54.0	Internal Flow Line
04053-9B	59.6	Internal Flow Line
04053-11B	52.3	Internal Flow Line
04063-2B	63.0	Internal Flow Line
04063-3B	57.9	Internal Flow Line
04083-2B	59.1	Internal Flow Line

[a] 4-point bend
[b] 10-40X

injection-molded test bars of the same composition. The low-strength fractures originated at internal flow lines. These results suggested that the defects originated during rotor molding due to poor flow of the molding mix and incomplete knitting of flow lines.

A nitrided Code 7 rotor (specimen no. 04083-1) was evaluated metallographically and by XRD. Figure 29 presents photomicrographs of a polished section. The nitrided hub had a core (Figure 29, Part A) that was rich in silicon. The high-magnification photomicrographs (Figure 29, Parts B to D) indicate that the hub interior contained a large amount of unreacted silicon (white phase), whereas the hub exterior was almost free of silicon.

The XRD results are presented in Figure 30. The blades contained primarily alpha and beta Si_3N_4 with very little silicon. The hub interior contained substantial silicon, as witnessed by the high intensity of the silicon XRD peak at 28.4° 2θ, which agrees with the photomicrograph results.

A second nitrided rotor (Specimen No. 08253-4) was evaluated by XRD. In this case, sections of the blade, hub exterior, and hub interior were analyzed. The results, shown in Figure 31, verify the photomicrographs in Figure 29, and suggest that complete nitriding only took place in the blades and exterior portion of the hub, leaving the hub interior rich in silicon. In addition to the flow lines previously discussed, the residual silicon could be another factor in the low measured strengths of these rotors.

Sintered Code 7 rotors representing several molding lots were evaluated metallographically and by XRD. Figures 32 and 33 present photomicrographs of polished sections of two rotors fabricated in April 1983. In both cases the hub has a core

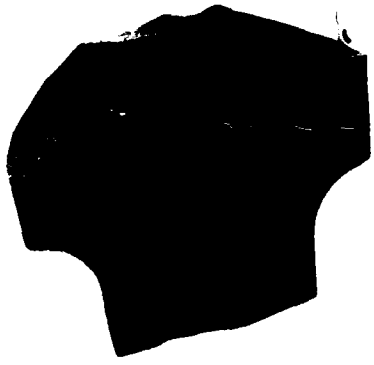

(A) HUB CROSS SECTION 3x

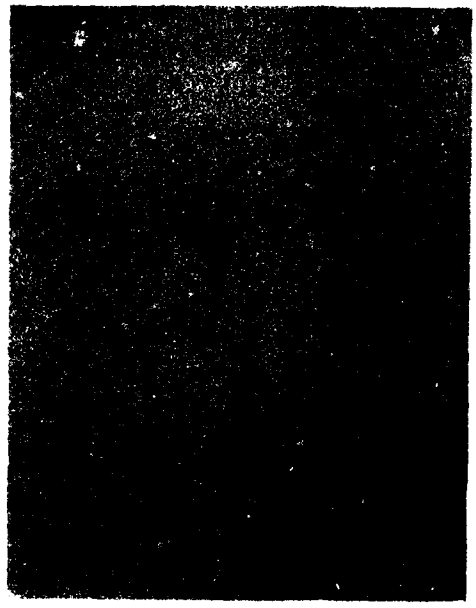

(B) HUB EXTERIOR 100x
(LIGHT AREA)

(C) TRANSITION LIGHT TO
DARK AREA 50x

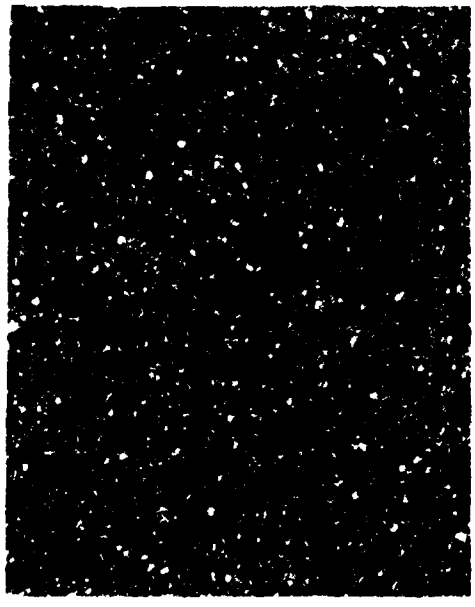

(D) HUB INTERIOR 100x
(DARK AREA)

Figure 29. Photomicrographs of Hub Section of Nitrided Code 7 Rotor, No. 04083-1.

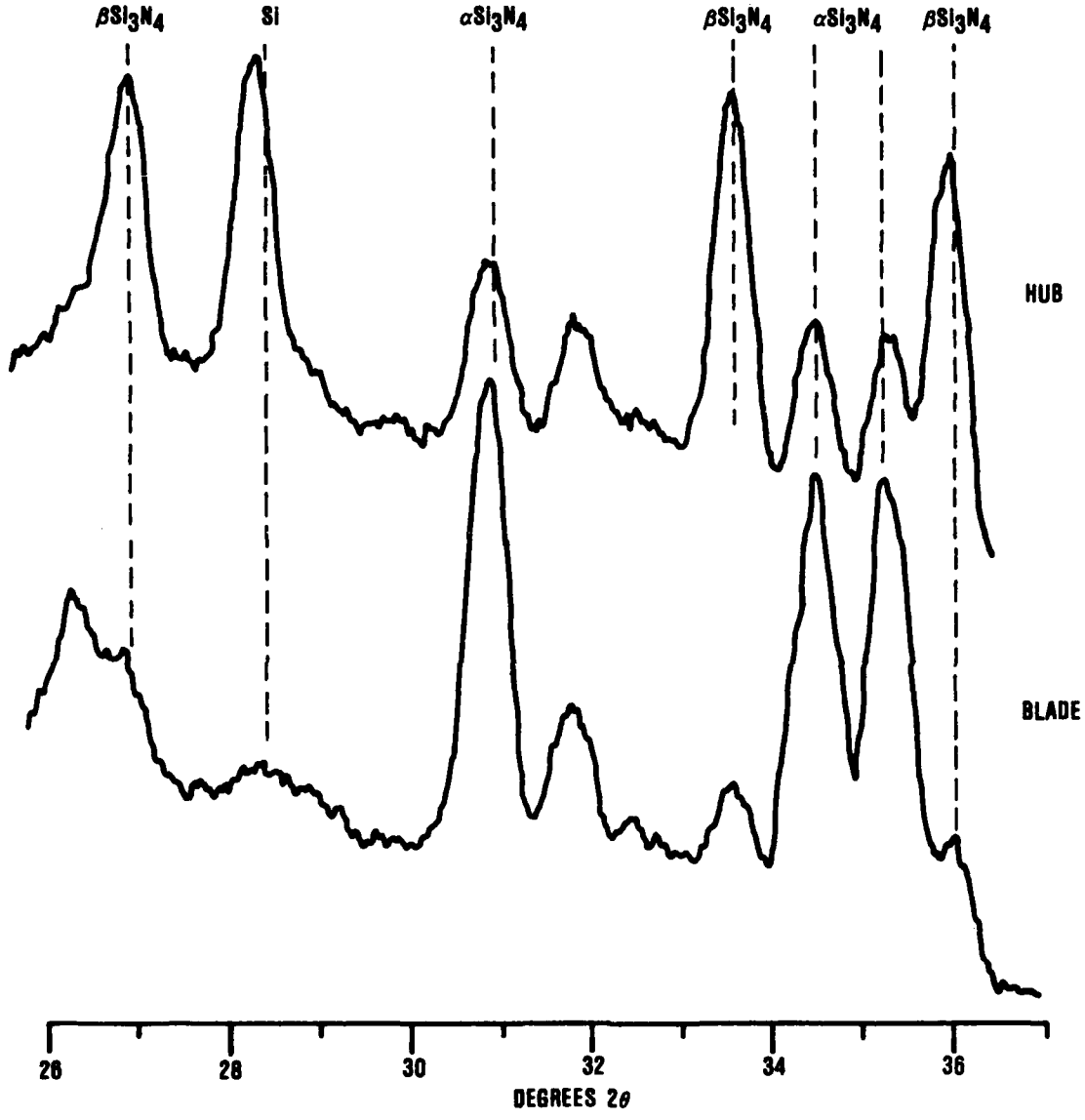

Figure 30. X-Ray Diffraction Patterns, Rotor No. 04083-1 as Nitrided.

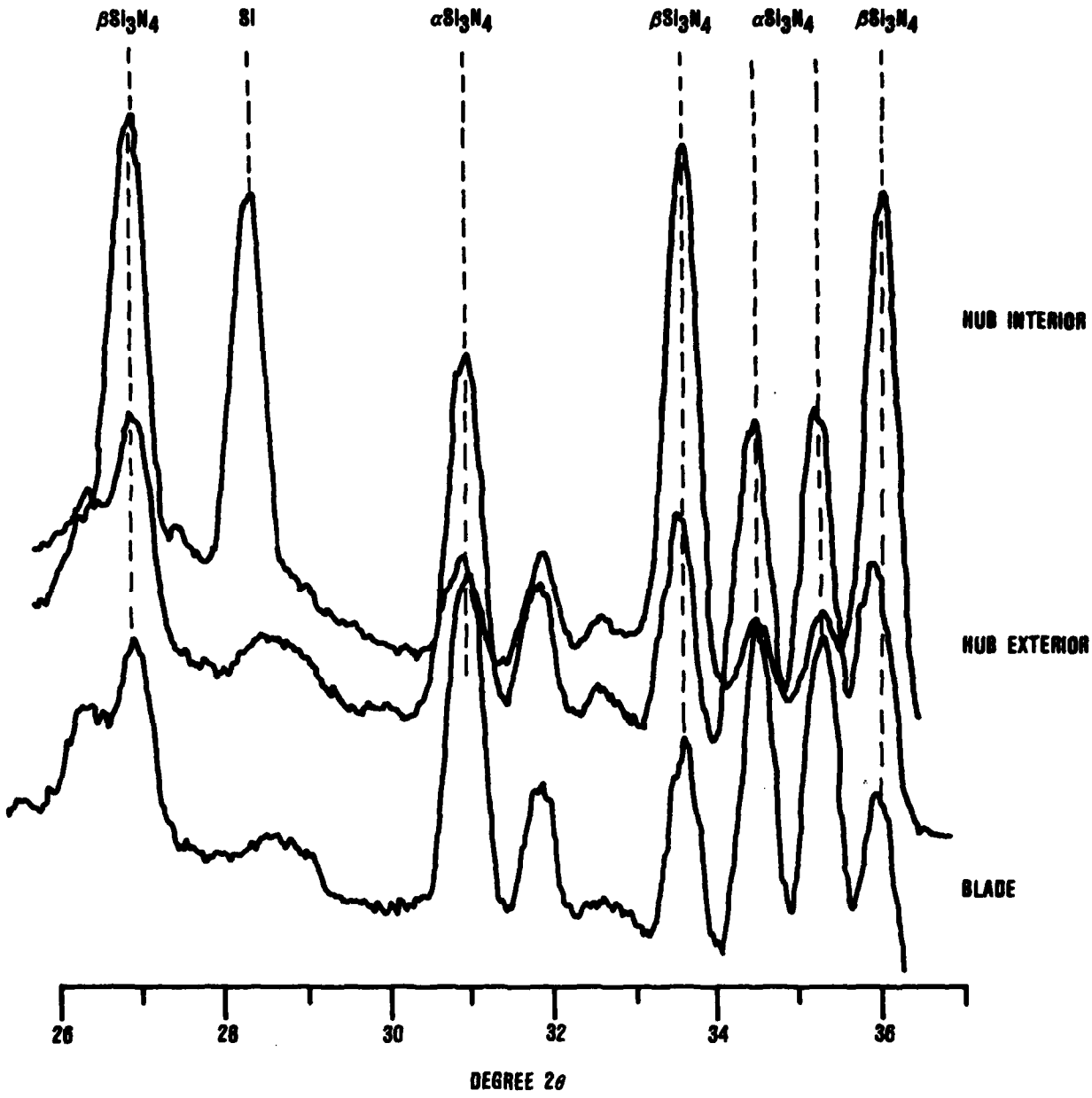

Figure 31. X-Ray Diffraction Patterns, Rotor No. 08253-4 as Nitrided.

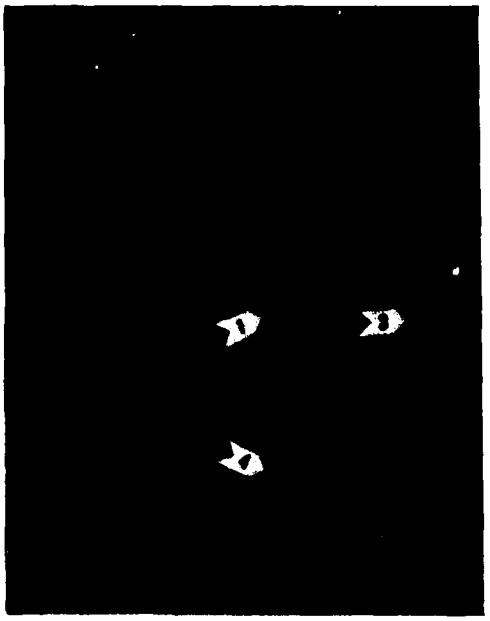

A) ROTOR SECTION 2x

B) AREA 1 200x

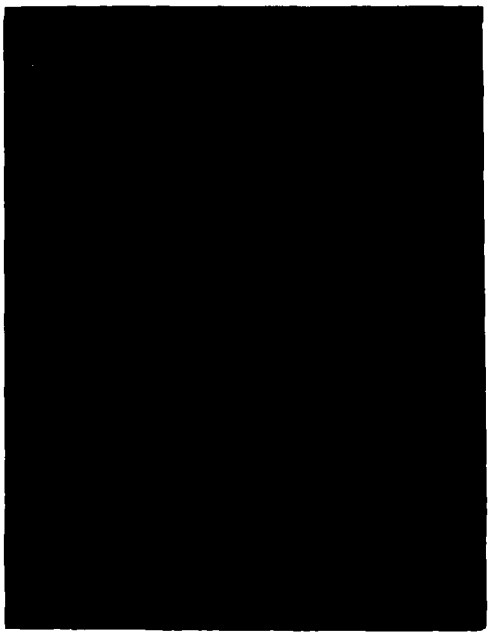

C) AREA 3 200x

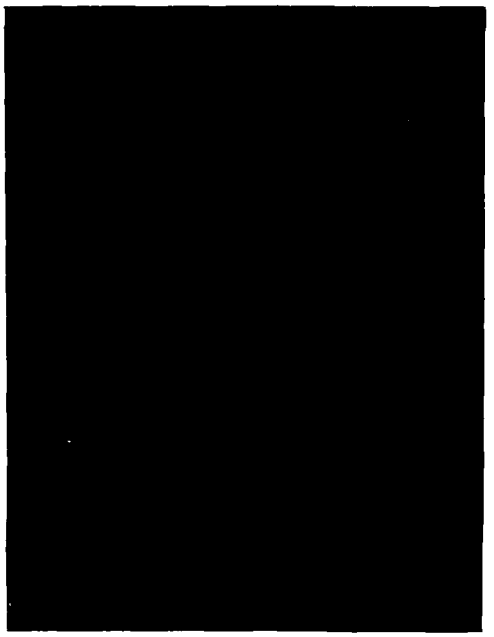

D) AREA 4 200x

Figure 32. Photomicrographs of Sintered Code 7 Rotor No. 04083-2

A) ROTOR SECTION 2x

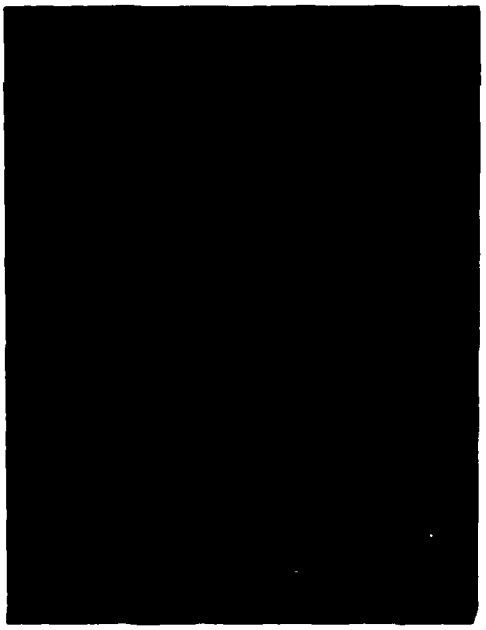

B) AREA 1 200x

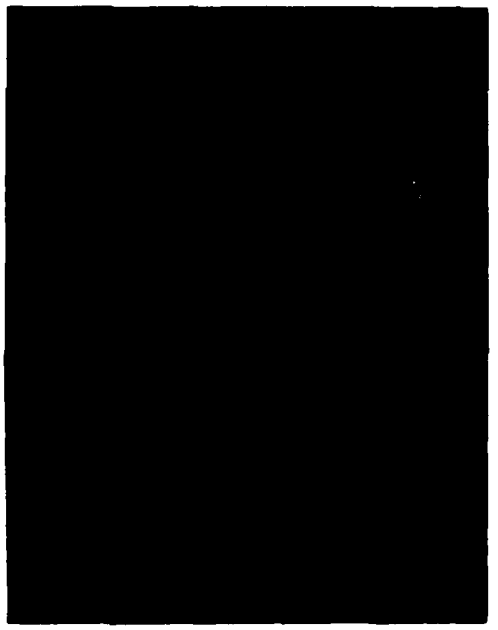

C) AREA 2 200x

Figure 33. Photomicrographs of Sintered Code 7 Rotor, Specimen 04073-8

MP-92954

(Figures 32 and 33, Part A). The high-magnification photomicrographs (Figures 32 and 33, Parts B to D) indicate that the hub interior contains a large amount of unreacted silicon, whereas the hub exterior and blades are almost free of silicon. These results agree with those in the nitrided condition (see Figure 29). A sintered Code 7 rotor (No. 04053-9) from the April 1983 time period was evaluated by XRD. These results are presented in Figure 34. The hub exterior contains primarily beta Si_3N_4 and negligible silicon. The hub interior contains silicon which agrees with the photomicrograph results and agrees with the results in the nitrided condition (see Figure 30).

Figures 35 and 36 present photomicrographs of polished sections of two rotors fabricated in August 1983. Rotor 08253-5 exhibits the silicon rich core (Figure 35, Parts A and B) similar to rotors 04083-2 and 04073-8. In Area 2, a small amount of silicon is detected, while Area 3, which also appears dark like the core (Area 1), exhibits negligible silicon.

The macro structure of rotor 08253-35 is very different from those previously reported. There is no evidence of excess silicon (see Figure 36, Parts B to D) in the microstructure. Also, the XRD results (Figure 37) confirm the absence of silicon. The low peak at 28.65 degrees is probably $Y_{20}N_4Si_{12}O_{18}$. Although rotors in this lot did not exhibit residual silicon, they did exhibit a different problem. As can be seen in Figure 38, Parts A and B, the microstructure does contain defects in the form of porous areas. As reported in Section 5.3, a rotor from this lot did achieve the highest burst speed for a Code 7, but failed at a speed of only 126,000 rpm.

Figure 38 presents photomicrographs of a polished section of a rotor (No. 10033-5) fabricated in October 1983. The rotor exhibits an interior with distinct light and dark regions.

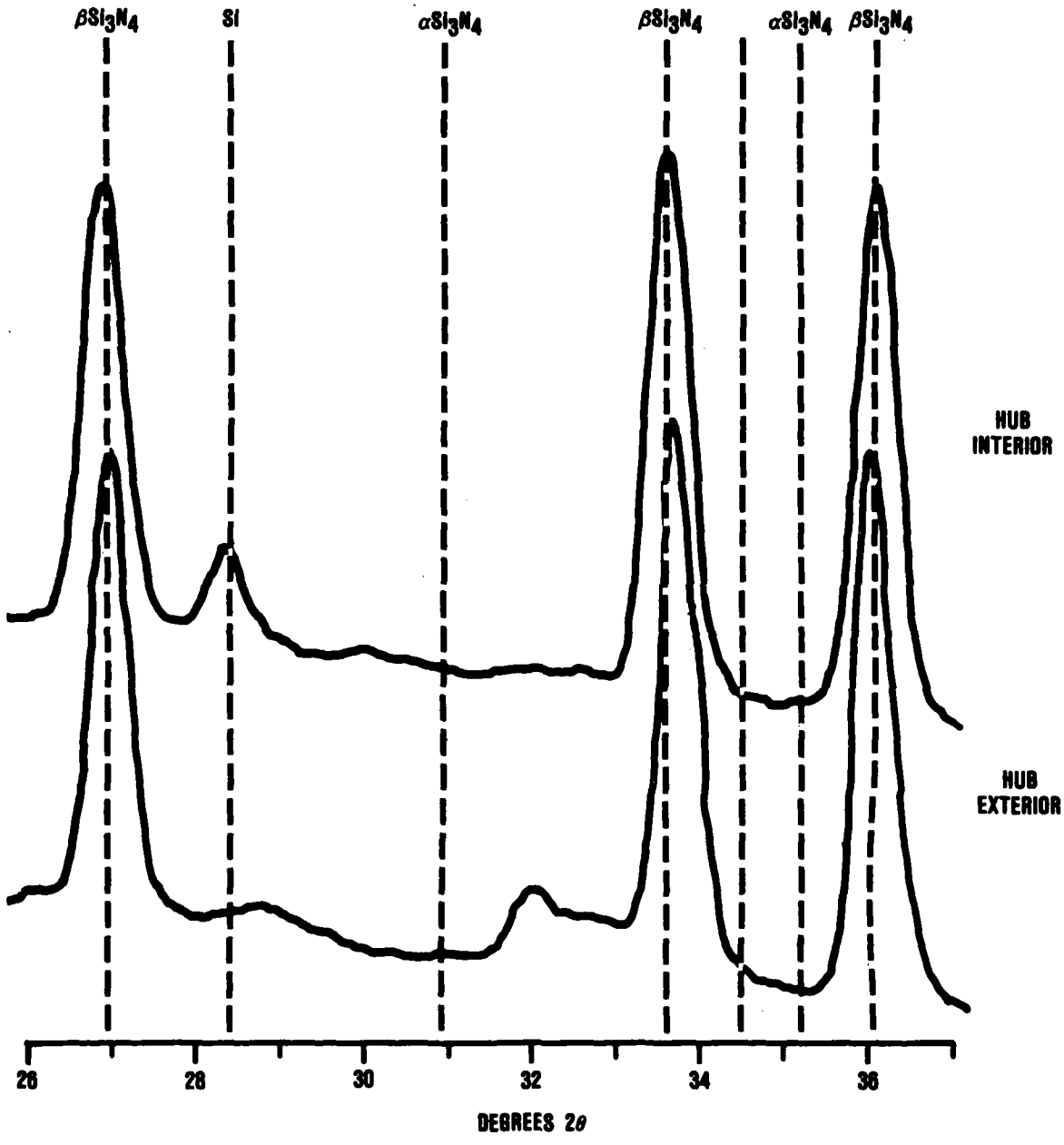

Figure 34. X-Ray Diffraction Patterns, Rotor No. 04053-9 as Sintered.

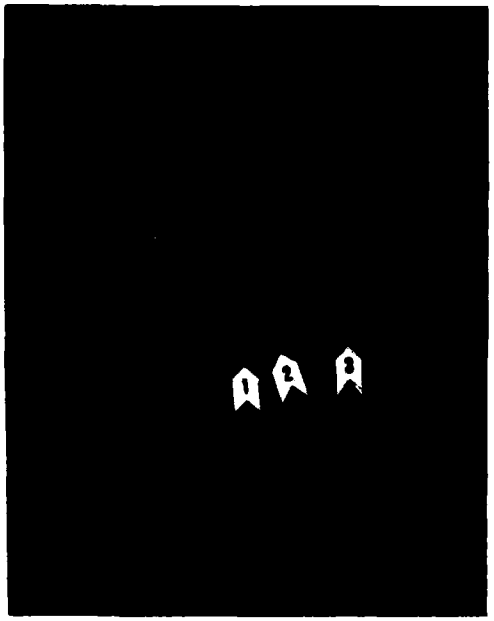

A) HUB SECTION 2x

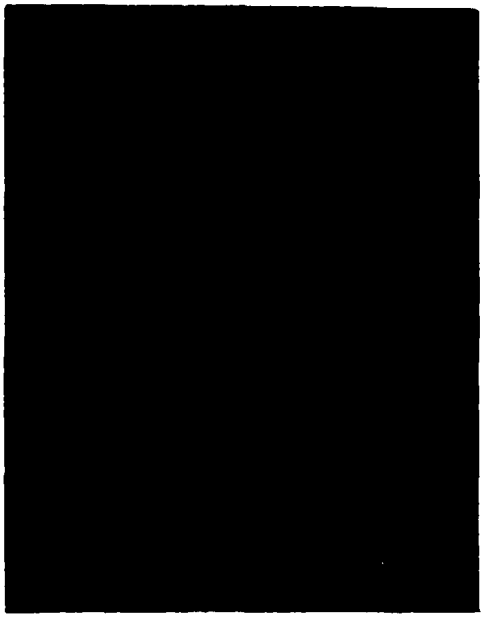

B) AREA 1 200x

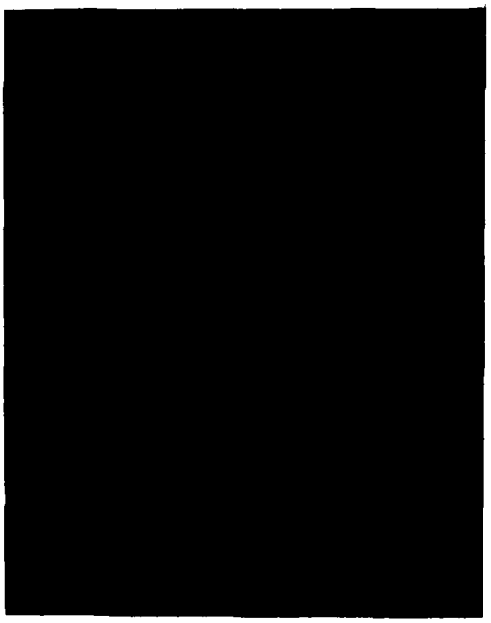

C) AREA 2 200x

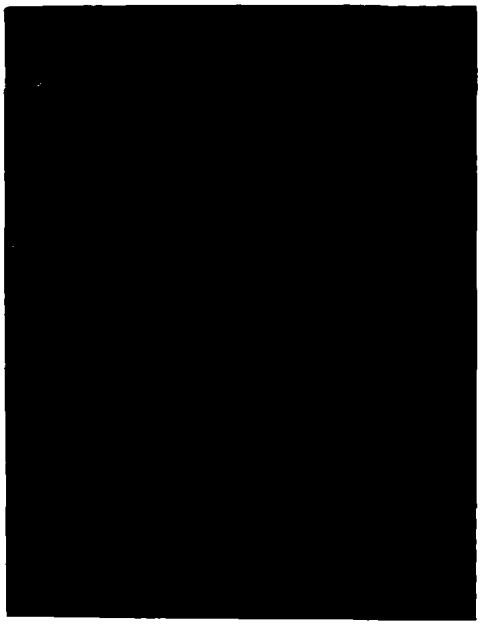

D) AREA 3 200x

Figure 35. Photomicrographs of Sintered Code 7 Rotor No. 08253-5.

MP-92953

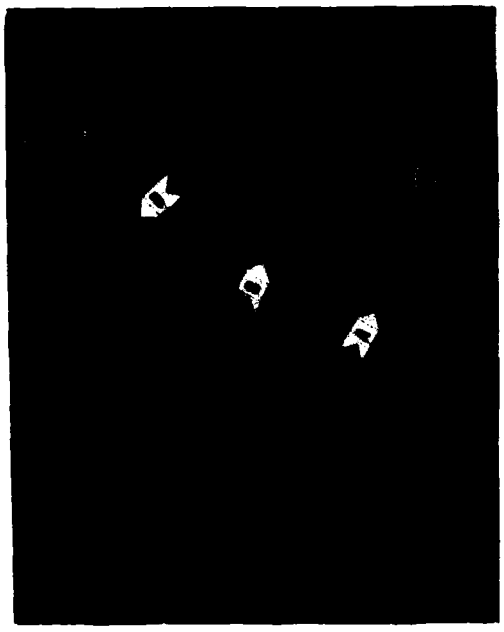

A) SECTION OF ROTOR 6x

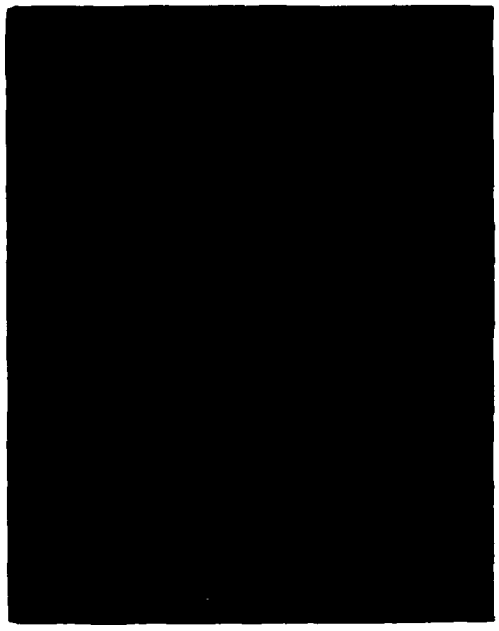

B) AREA D 200x

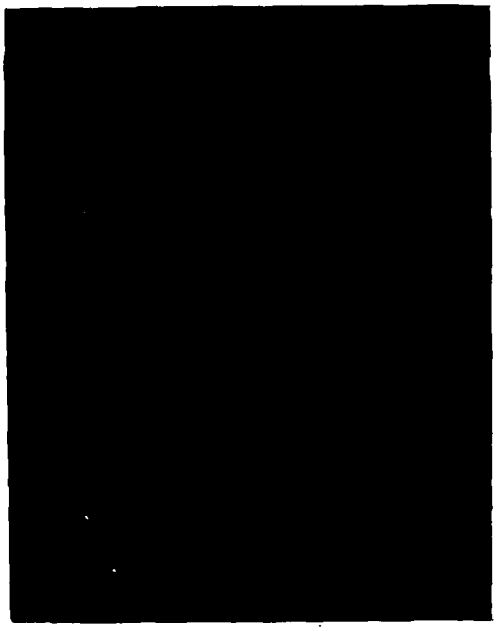

C) AREA B 200x

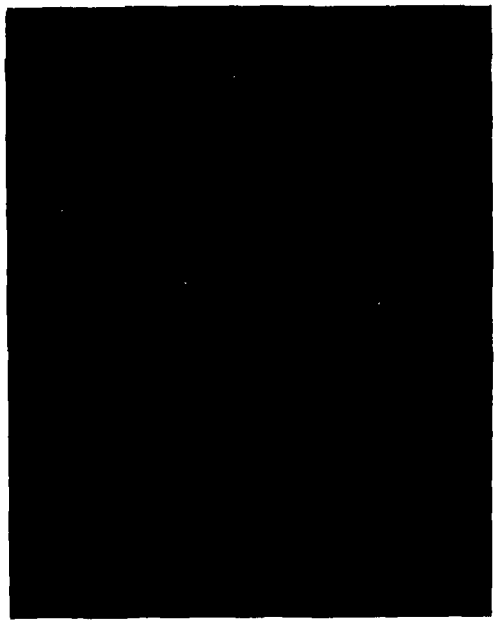

D) AREA A 200x

Figure 36. Photomicrographs of Sintered Code 7 Rotor No. 08253-35.

MP-92950

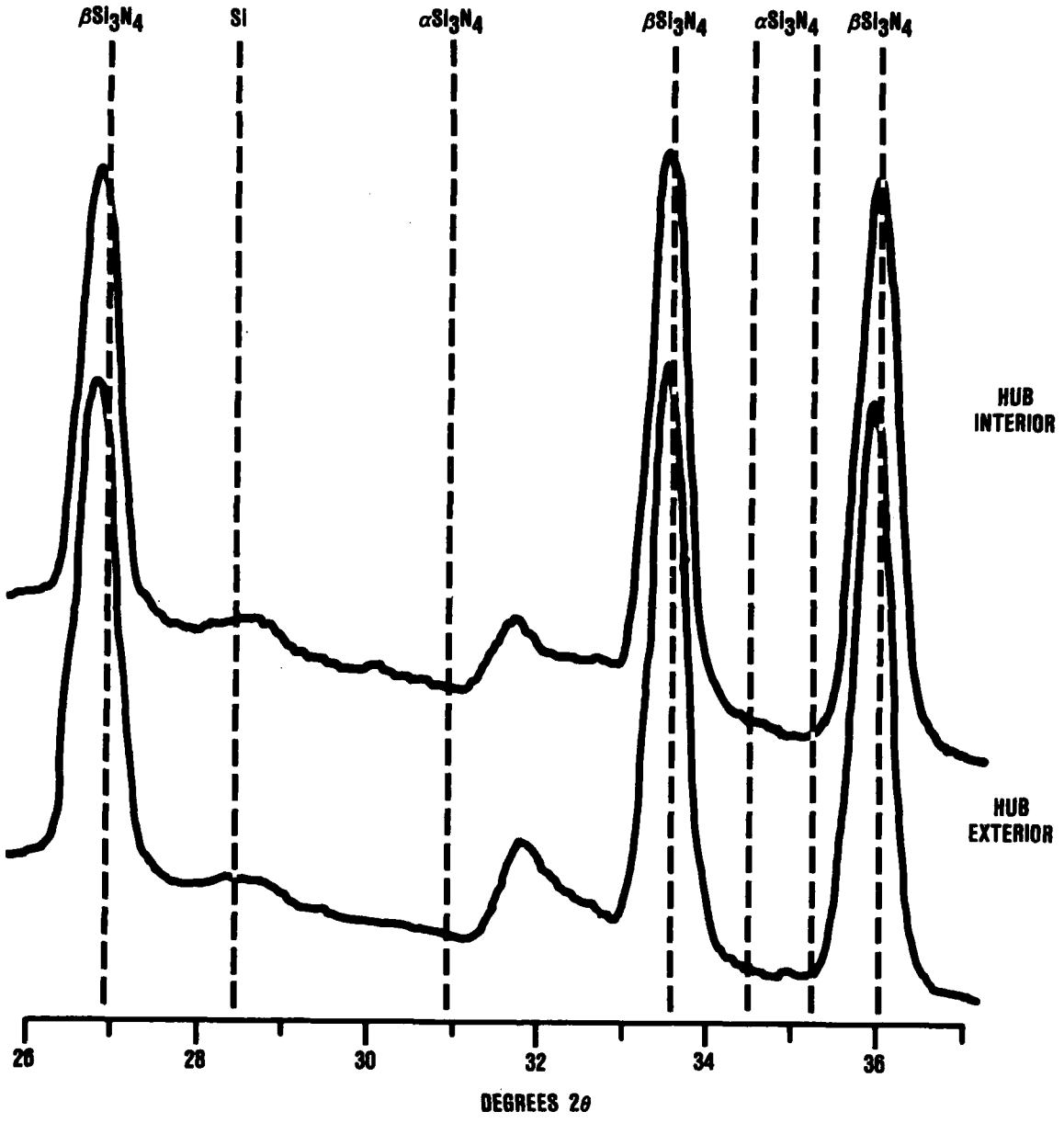

Figure 37. X-Ray Diffraction Patterns, Rotor No. 08253-35.

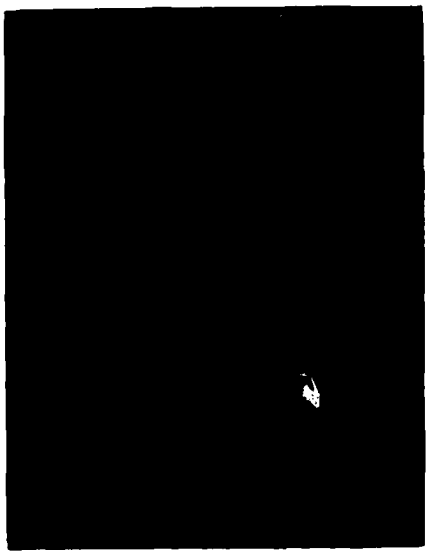

B) AREA 1 200x

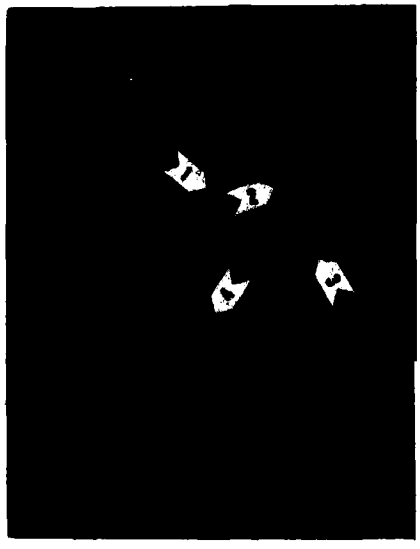

A) ROTOR SECTION 2x

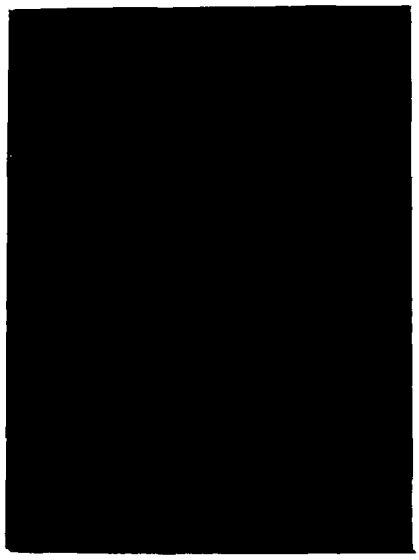

C) AREA 2 200x

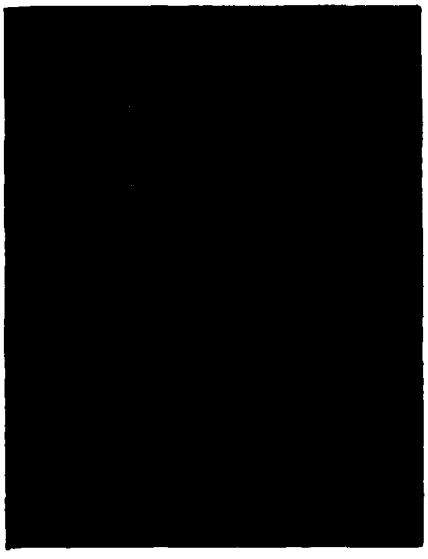

D) AREA 4 200x

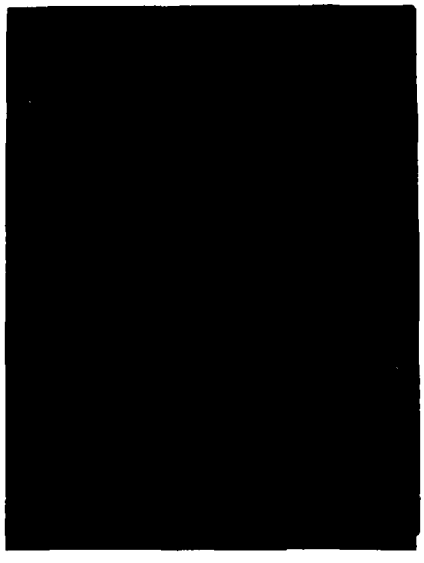

E) AREA 3 200x

Figure 38. Photomicrographs of Sintered Code 7 Rotor No. 10033-5.

There appears to be no residual silicon throughout the microstructure. The near surface regions (2 and 3) appear more dense than the interior regions (1 and 4). See Figure 38, Parts B through D. The interior appears to have excessive porosity which could cause low stress (low rpm) failure.

Fully-processed Codes 2 and 7 rotors representing the latest iterations were machined into test bars from which room-temperature and 2250F flexure strength and fracture origins were determined. These results are presented in Table 23.

Two other materials are being evaluated by GAPCO as part of a Company-funded effort to develop a T02 turbocharger with a ceramic rotor. Fully-processed rotors of Kyocera's SN220 sintered silicon nitride and NGK Insulator's SN50 sintered silicon nitride were machined into test bars from which room- and elevated-temperature flexure strength were determined. These results are presented in Table 24 for a comparison with the results obtained on materials developed under this program.

TABLE 23. FLEXURE STRENGTH OF TEST BARS MACHINED FROM FULLY-PROCESSED CODES 2 AND 7 ROTORS

Specimen No.	Flexure Strength[a] (ksi)	Fracture Origin[b]
	Room Temperature	
Code 2		
12063-5	104.1	---
12063-6	83.8	---
12063-9	83.8	---
12063-11	97.9	---
12063-18	45.6	Flow line
12063-21	30.9	Large low density area
Code 7		
09143-5	80.1	---
09143-6	70.3	---
10033-4	87.2	---
10033-14	54.0	Large internal void
10033-16	57.4	Internal flow line
10033-17	68.6	Subsurface porous area
	2250F	
Code 7		
09143-3	46.1	Subsurface flow line
09143-5	45.0	Tensile face
09143-6	49.5	Subsurface low density area
10033-4	48.9	Subsurface low density area
10033-14	43.3	Large internal pore
10033-16	38.3	Tensile face
10033-17	42.8	Tensile face

[a] 4-point bond
[b] 10-40X

TABLE 24. FLEXURE STRENGTH OF TEST BARS MACHINED FROM FULLY-PROCESSED KYOCERA SN220 AND NGK SN50 ROTORS

Specimen No.	Flexure Strength (ksi)	Fracture Origin
	Room Temperature	
NGK SN50		
N 116A	68.7	Large Grain or Agglomerate
N 133A	52.1	Large Grain or Agglomerate
N 133B	63.5	Large Grain or Agglomerate
N 136A	54.2	Large Grain or Agglomerate
N 136B	62.5	Large Grain or Agglomerate
N 141A	54.2	Large Grain or Agglomerate
N 141B	46.9	Large Grain or Agglomerate
N 141A	53.6	Large Grain or Agglomerate
N 141B	58.3	Large Grain or Agglomerate
N 150A	46.9	Large Grain or Agglomerate
Kyocera SN220		
14767	124.4	Tensile Face
14768	100.8	Inclusion
14769	112.3	Tensile Face
14770	91.6	Tensile Face
	1830F	
NGK SN50		
N 116B	37.0	Large Grain or Agglomerate
N 150B	30.2	with Associated Slow Crack Growth
Kyocera SN220		
14771	95.0	Tensile Face
14772	74.9	Tensile Face
14773	98.0	Tensile Face
14774	92.2	Tensile Face

TABLE 24. FLEXURE STRENGTH OF TEST BARS MACHINED FROM FULLY-PROCESSED KYOCERA SN220 AND NGK SN50 ROTORS (Contd)

Specimen No.	Flexure Strength (ksi)	Fracture Origin
	2200F	
Kyocera SN220		
14995	53.3	--
14996	49.5	--
14997	40.3	--
14998	42.6	--
14999	44.6	--

4. ROTOR MODELING AND ANALYSIS

4.1 T04 Rotor

The initial rotor modeling effort was directed toward the T04 rotor size. The dimensions of the blade and hub sections of the green, injection-molded rotor were established from a combination of metal rotor print dimensions and measurements made directly on molded rotors. Based on measurements made on test bars, two shrinkage levels were established: 7 percent for the sintered RBSN (Codes 7 and 9) and 13 percent for the sintered Si_3N_4 powder (Code 2). Two finite-element stress-analysis models were constructed, one for each shrinkage level. Independent of the shrinkage, the shaft diameter and length were established as 0.5 inches and 2.5 inches, respectively, for all rotors fabricated.

The 2-D finite-element model for a Code 2 rotor is shown in Figure 39. A stress analysis was completed at room temperature using material properties shown in Table 25. The radial stress distributions are shown in Figure 40. The peak hub stress is only about half the maximum value at the root of the blade in the saddle region.

TABLE 25. SINTERED Si_3N_4 PROPERTIES

Temperature (F)	Elastic Modulus (10^6 psi)	Coefficient of Thermal Expansion (10^{-6}/F)	Poisson Ratio
70	45.0	1.00	0.268
400	44.6	1.28	0.261
800	44.0	1.35	0.256
1200	43.6	1.51	0.250
1600	41.4	1.85	0.234
2000	38.2	2.00	0.200
Density = 0.117 lb/in^3			

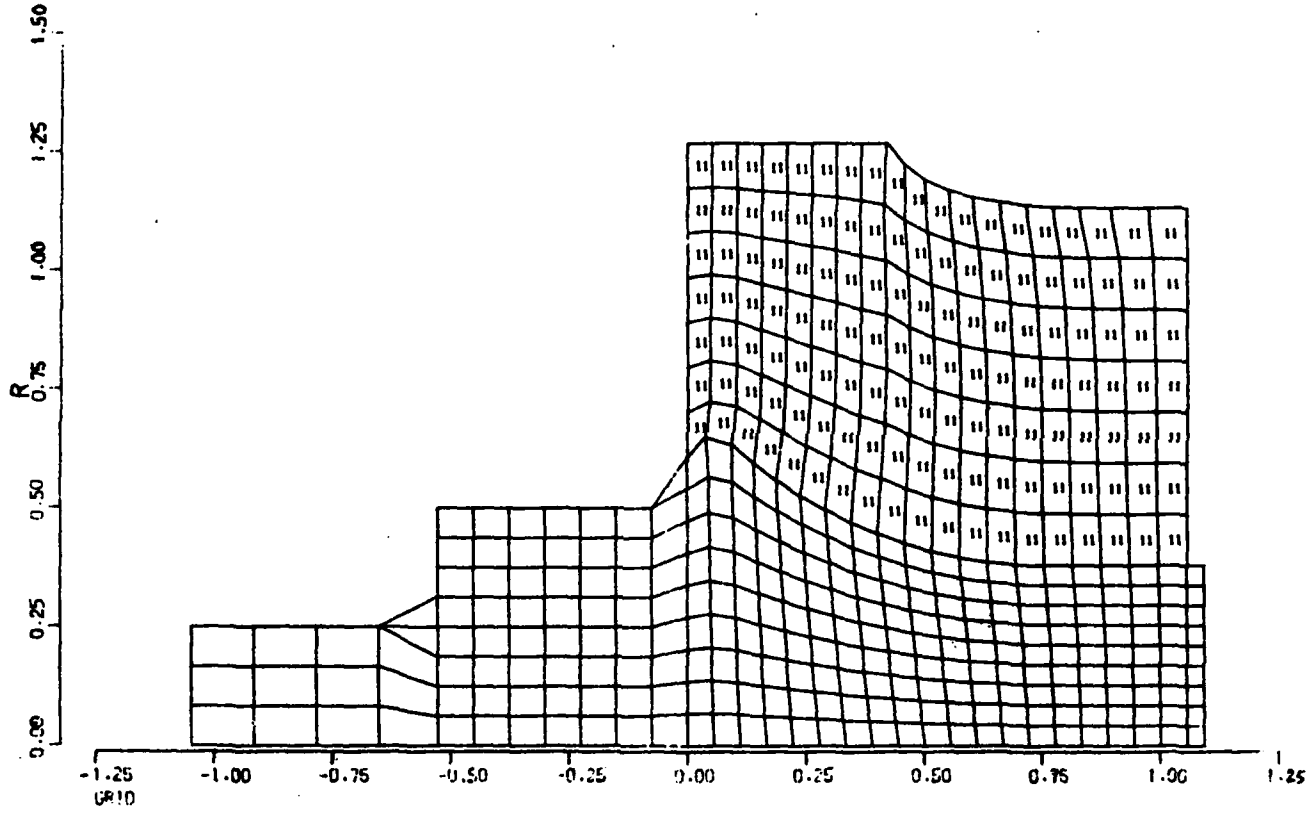

Figure 39. Finite Element Model for T04 Turbocharger with 13-Percent Shrinkage (Dimensions in Inches).

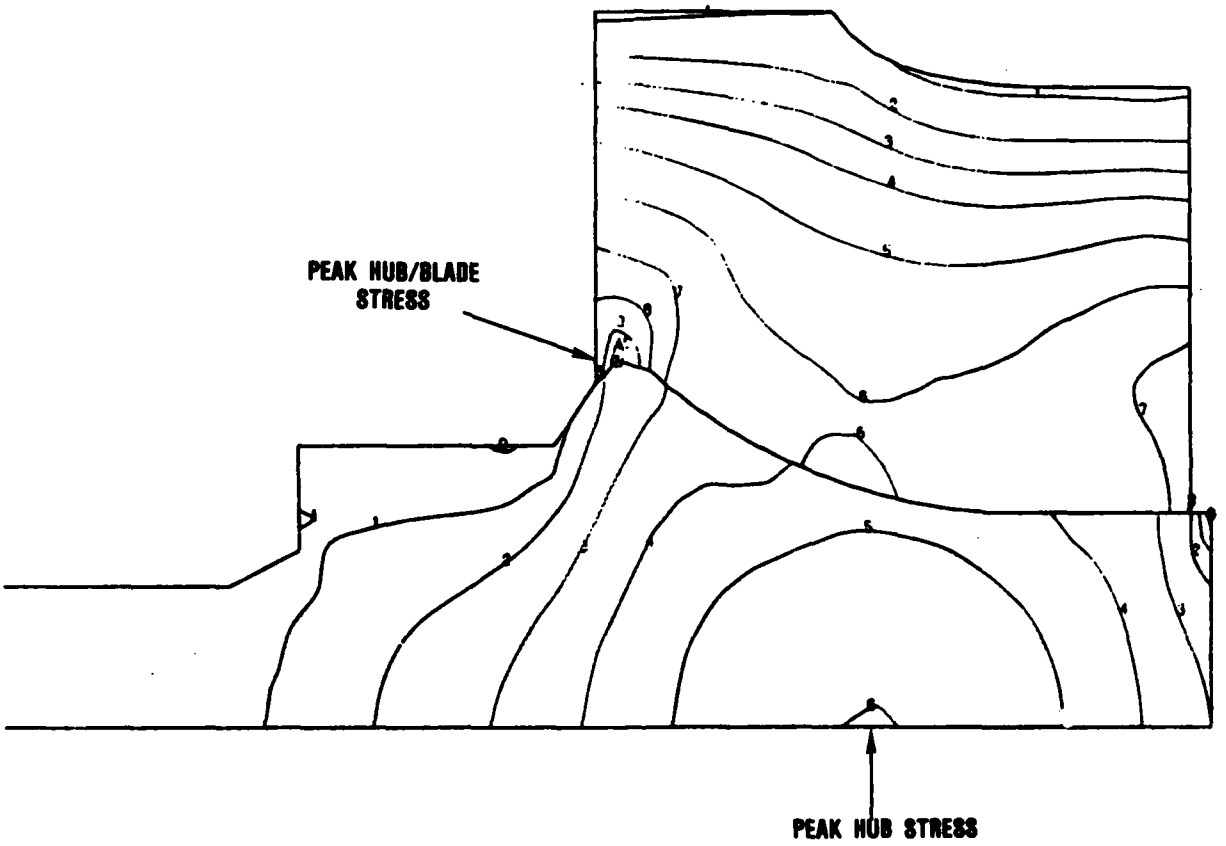

Figure 40. Radial Stress Distribution at 80 krpm for T04 Turbocharger Rotor with 13-Percent Shrinkage (Stress in ksi).

A Weibull statistical analysis was performed to determine the probability of failure of the T04 rotor as a function of speed. Although Phase II goals were 90 ksi room temperature characteristic strength with a Weibull slope of 10, analyses were run for characteristic strengths of 70 ksi and 90 ksi and Weibull slopes of 8 and 10. The following equation was used to convert from bend strength values to tensile strengths. This assumes that the same flaw population controls both bending and tensile strength.

$$\sigma \text{ Tensile} = \sigma_{4\text{-pt}} \left(\frac{V_F}{V_T} \left(\frac{m+2}{4(m+1)^2} \right)^{1/m} \right)$$

Where σ Tensile is the predicted tensile strength, $\sigma_{4\text{-pt}}$ is the measured 4-pt flexural strength, V_F is the volume under stress in the 4-pt flexural test, V_T is the volume under stress in a tensile test, and m is the Weibull slope.

The four cases are tabulated in Table 26, and the Weibull plots for the 7 percent shrinkage model are shown in Figures 41 and 42. The 7 percent shrinkage model represents the predicted size of the T04 rotor fabricated by the RBSN route (i.e., Codes 7 and 9).

TABLE 26. TENSILE STRENGTHS[a] CALCULATED FROM FLEXURAL STRENGTHS[a]

$\sigma_{4\text{-pt}}$(ksi)	σ_{Tensile}(ksi)	
	m = 8	m = 10
70	45.3 ①	48.4 ③
90	55.8 ②	62.1 ④

[a]Characteristic strength

①-④ case number

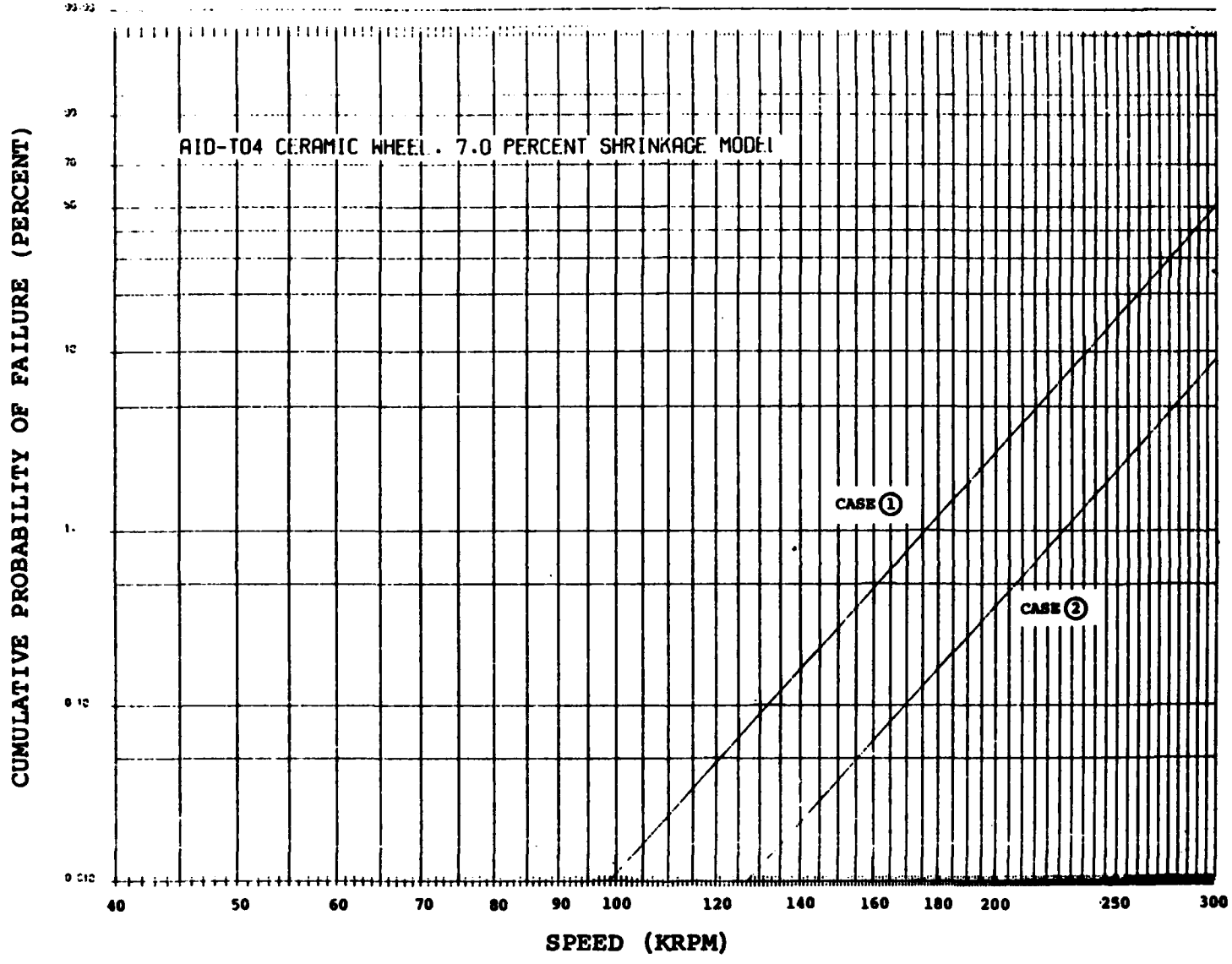

Figure 41. CPF Versus Speed for Weibull Modulus of 8 and Characteristic Flexural Strengths of 70 ksi ① and 90 ksi ② .

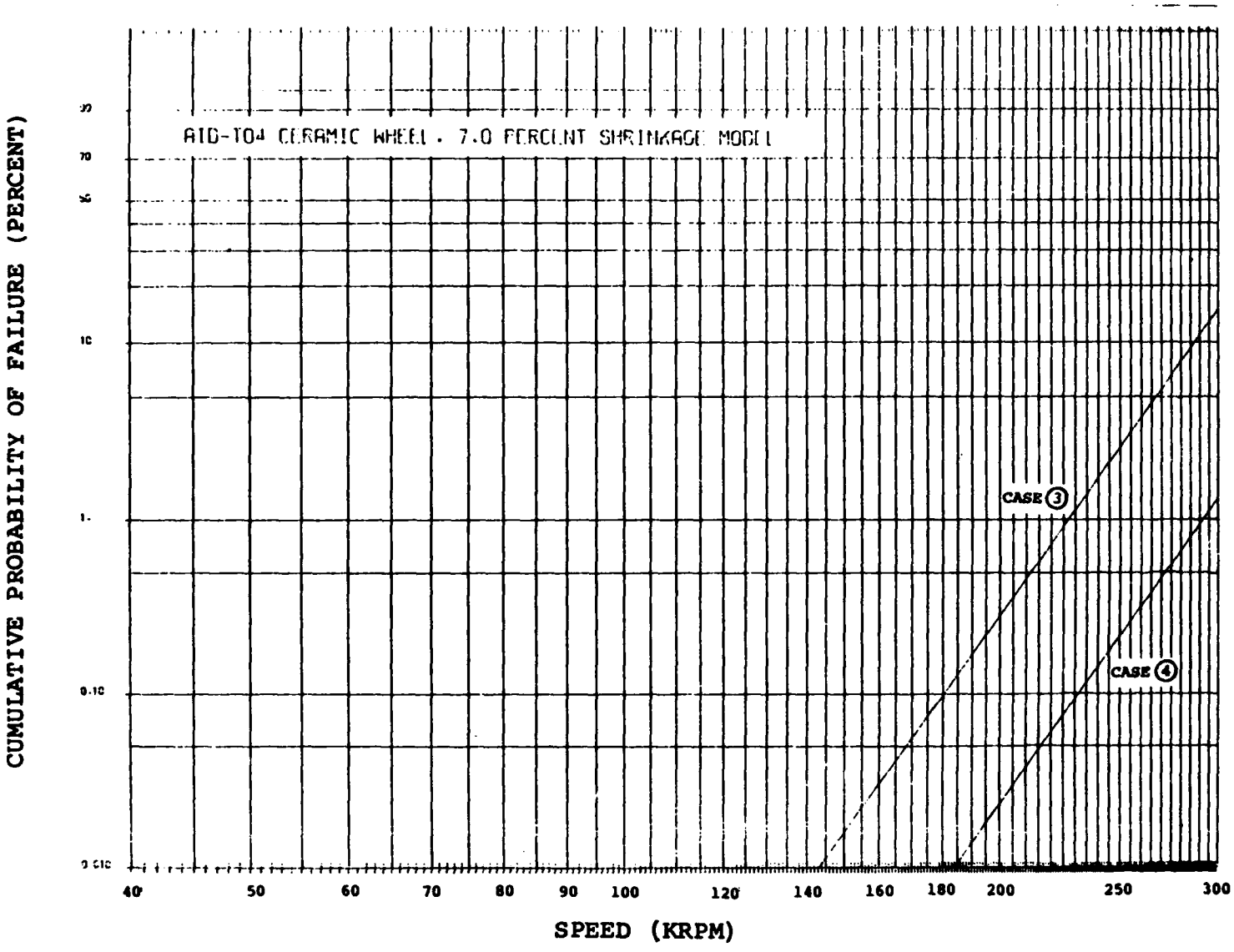

Figure 42. CPF Versus Speed for Weibull Modulus of 10 and Characteristic Flexural Strengths of 70 ksi (3) and 90 ksi (4) .

As indicated, the relatively small size of the T04 turbocharger rotor combined with high strength material properties results in very high predicted rotor failure speeds.

4.2 T02 Rotor

Concurrent with the change to the T02 size rotor, the modeling and analysis were redirected toward the T02 size. A 3-D finite-element model was created for a portion of the rotor--a single blade and a wedge portion of the disk. A stress analysis was then performed using the model shown in Figure 43.

Using the material data from Table 25, the stress levels were determined. Figure 44 presents the distribution of the maximum principle stresses. In this case, the peak hub stress is comparable to the peak blade and blade/hub line stresses.

A Weibull statistical analysis was performed on the above model to determine the probability of failure of the T02 rotor as a function of speed. The analysis used actual Weibull data measured on Code 2 test bars. The results of this analysis are presented in Figure 45, which shows that to exceed a 0.1-percent probability of failure, the rotor speed must be greater that 380,000 rpm. Also plotted in Figure 45 are curves that represent materials with 70 and 80 ksi characteristic strengths and Weibull slopes of 11.25. The relation between the material strength and the probability of failure can readily be determined from this data. Also, the effect of varying the Weibull slope was evaluated and the results are presented in Figure 46.

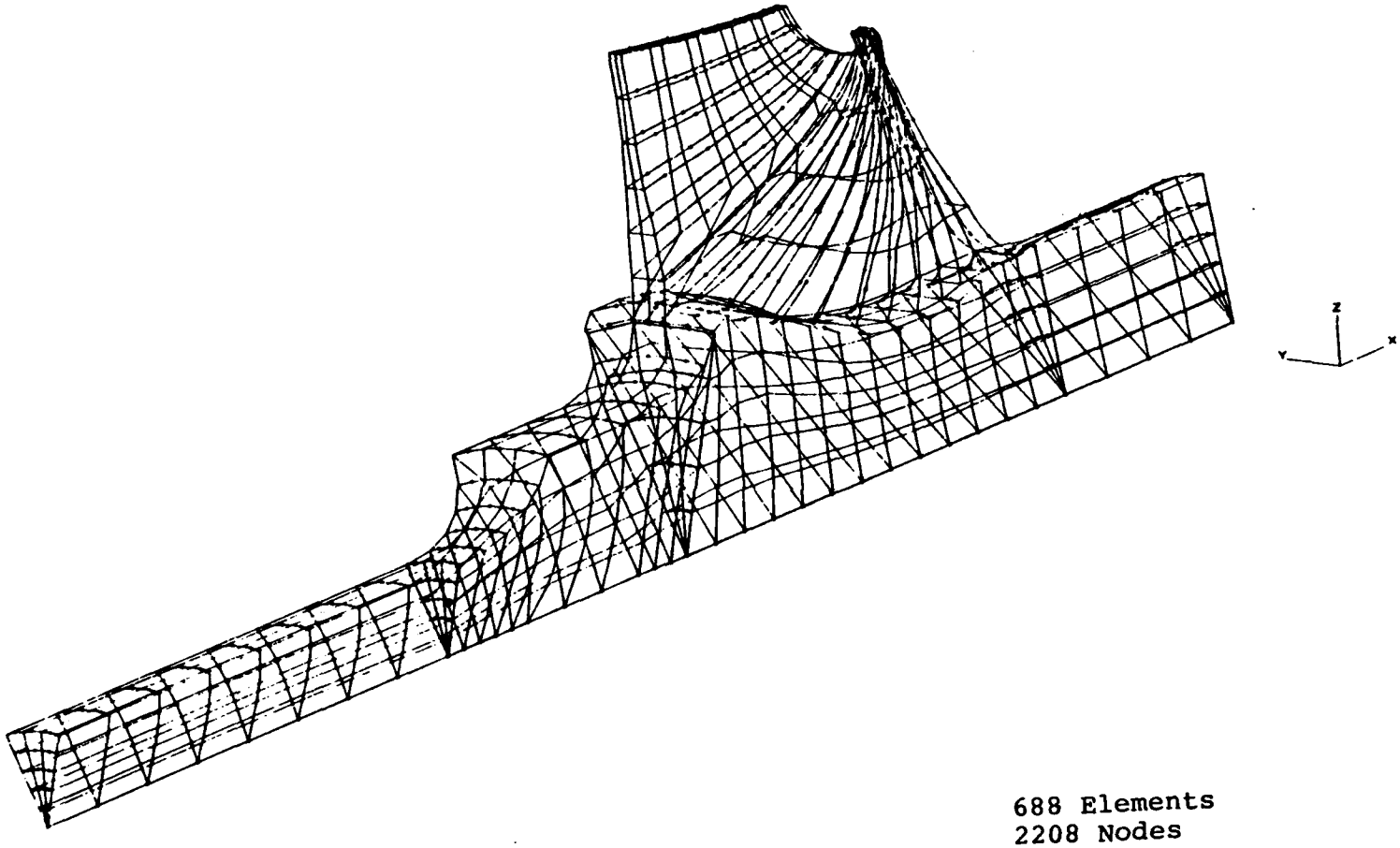

Figure 43. 3-D Finite Element Model for T02 Rotor Stress Analysis.

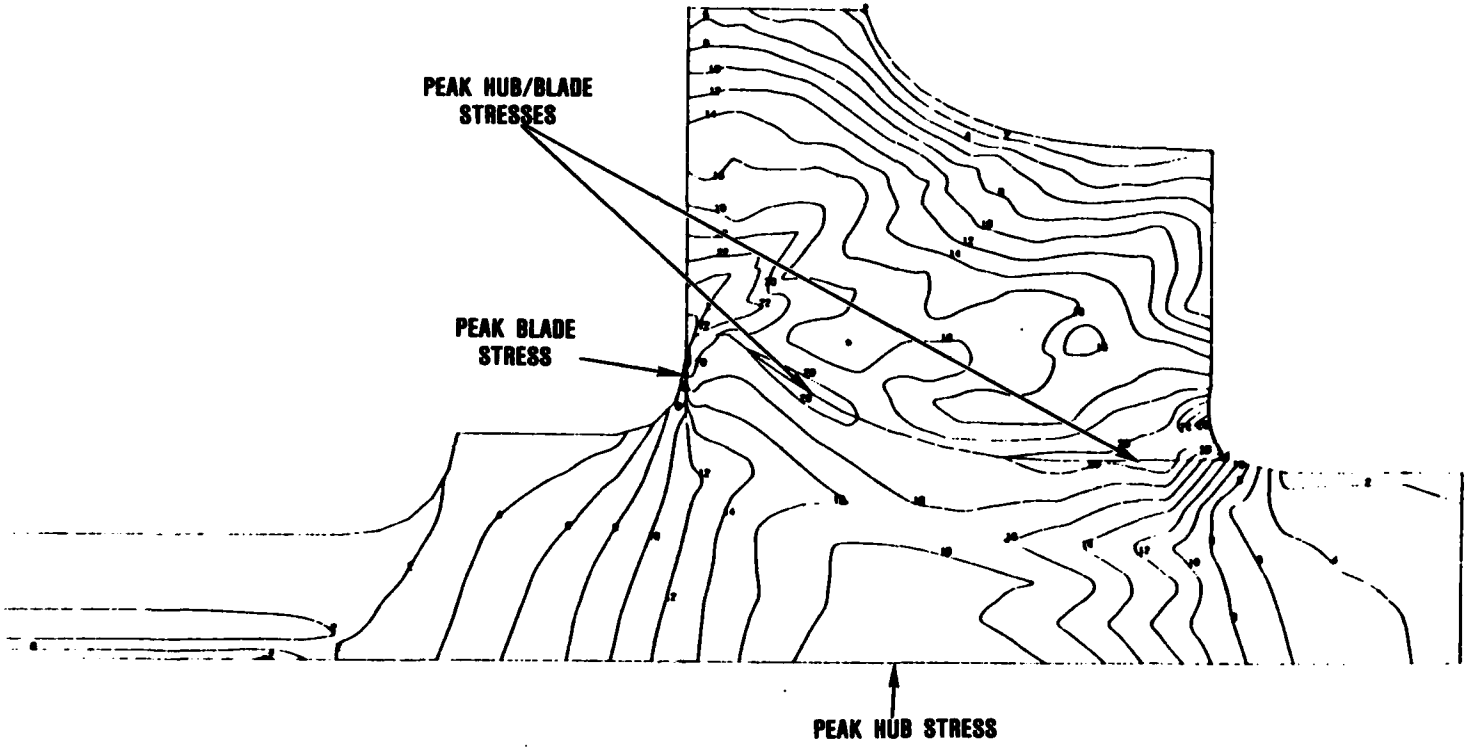

Figure 44. Distribution of the Maximum Principle Stresses for T02 Rotor at 200,000 rpm.

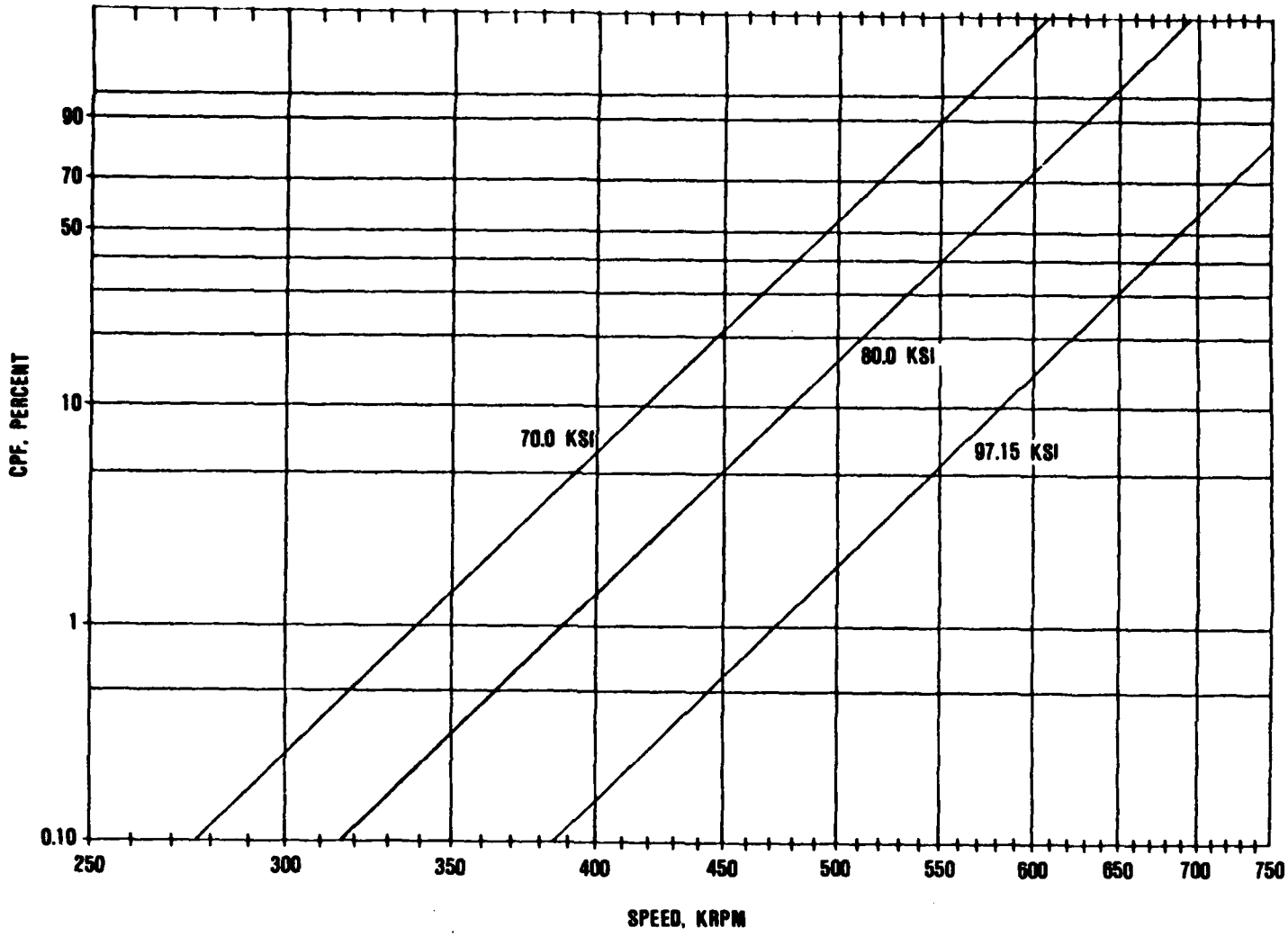

Figure 45. Probability of Failure for T02 Turbocharger Ceramic Turbine Rotor.

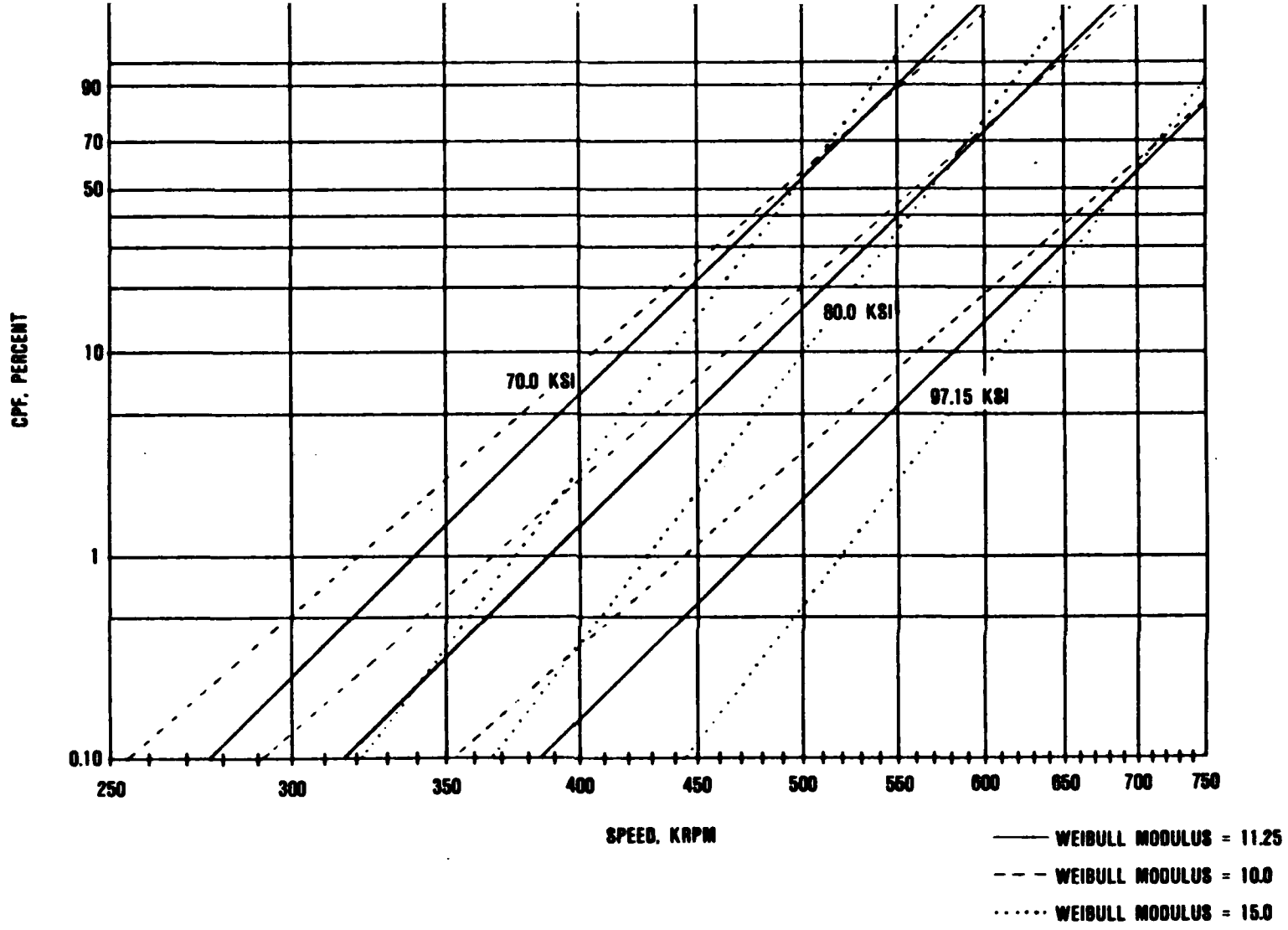

Figure 46. Effect of Weibull Modules on Probability of Failure for T02 Turbocharger Ceramic Turbine Wheel.

5. ROTOR SPIN TESTING

5.1 Machining and Shaft Attachment

Rotors of acceptable quality for spin testing were machined into two different shaft configurations, one for cold spin testing and a second for hot spin testing. Rotor machining for the shaft attachment and balancing was performed at GAPCO.

A shrink-fit attachment was used for cold spin testing. The ceramic rotor shaft was machined to a 0.3686/0.3690 inch diameter, to which a 4340 steel sleeve (Figure 47) was attached. For elevated temperature spin testing, two methods of shaft attachment were utilized: 1) a Garrett proprietary joint that used a high temperature adhesive, and 2) shrink-fit INCO 907 shafts.

5.2 Room-Temperature Spin Testing

Cold-spin shaft attachment and final balancing were completed on four Code 2 T02 rotors. Visual (10-40x) and fluorescent penetrant inspections identified surface cracks in the hub (oiler) area and at the blade/hub transition. Despite these known flaws, the rotors were spin tested to develop baseline data, evaluate the test procedure, and evaluate fractographic techniques on failed rotors.

The room-temperature testing was to be accomplished in the GTEC evacuated spin pit using an air turbine motor with a reported 200,000 rpm capability. Several attempts to run the spin test resulted in failure of the spin motor. Several design modifications were incorporated into the motor, and it was rebuilt. A Code 2 rotor was attached to the motor, the

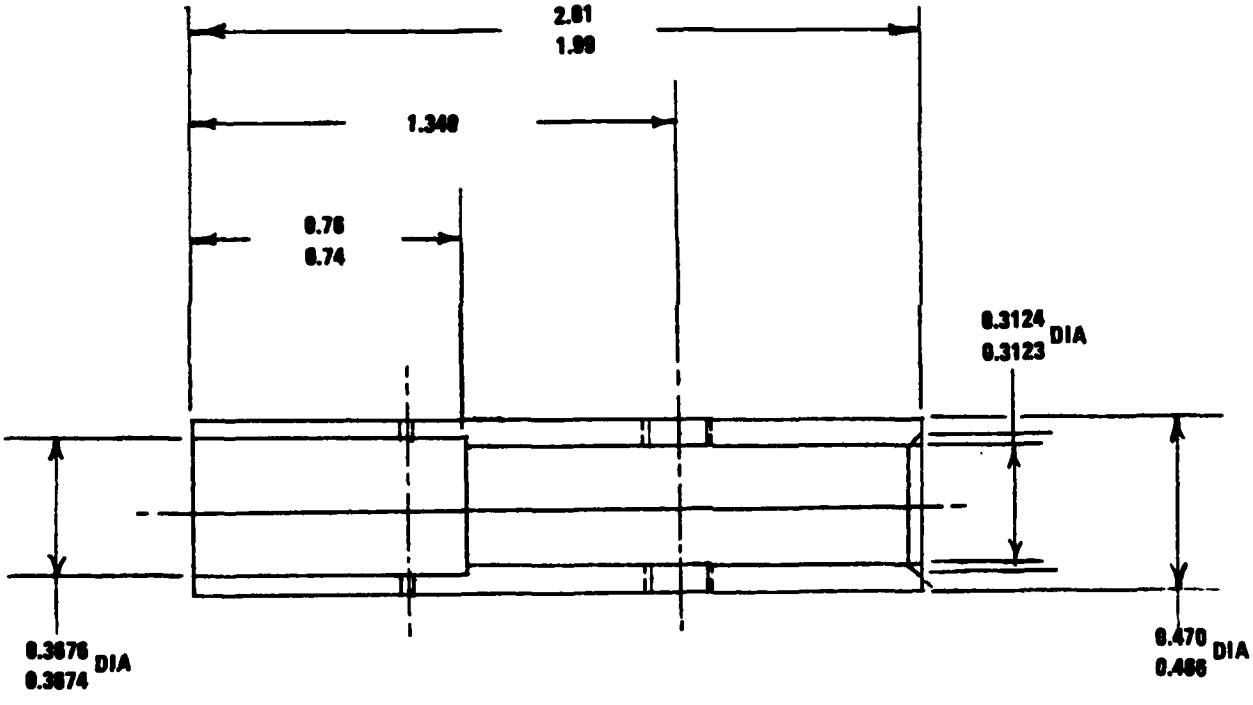

Figure 47. Sleeve for Cold Spin Testing (Dimensions in Inches).

speed was increased to 183,000 rpm at which time the spin motor failed again. Subsequent examination of the ceramic rotor and teardown of the motor revealed the following:

- The ceramic rotor survived the 183,000 rpm test intact.
- The spin motor failure was due to the fracture of the metal shaft on the air turbine.

Figure 48 is a photograph of the ceramic rotor and the spin motor's metal rotor after the 183,000 rpm spin test.

Because of the continual problems with the room-temperature spin test equipment, it was decided to delete the cold-spin testing and increase the number of planned elevated-temperature spin tests which had already been successfully demonstrated at GAPCO.

5.3 Elevated Temperature Spin Testing

The elevated temperature spin testing was conducted at GAPCO using an actual turbocharger housing (see Figure 49). During the test, the speed and inlet temperatures were increased to approximately 120,000 rpm and 1700-1750F, respectively. After a 10-minute dwell at these conditions, the rotor was accelerated rapidly to burst. During the test time, inlet temperature, rotor speed, and g levels were recorded.

Six Code 2 rotors were machined to the elevated temperature spin configuration, attached to metal shafts, and balanced. The rotor/shaft assemblies were installed in turbocharger housings and spin tested. Figure 50 is an example of the data trace from such a test (rotor No. 01273-2, which had a burst speed of 154,000 rpm). The burst speed for the six

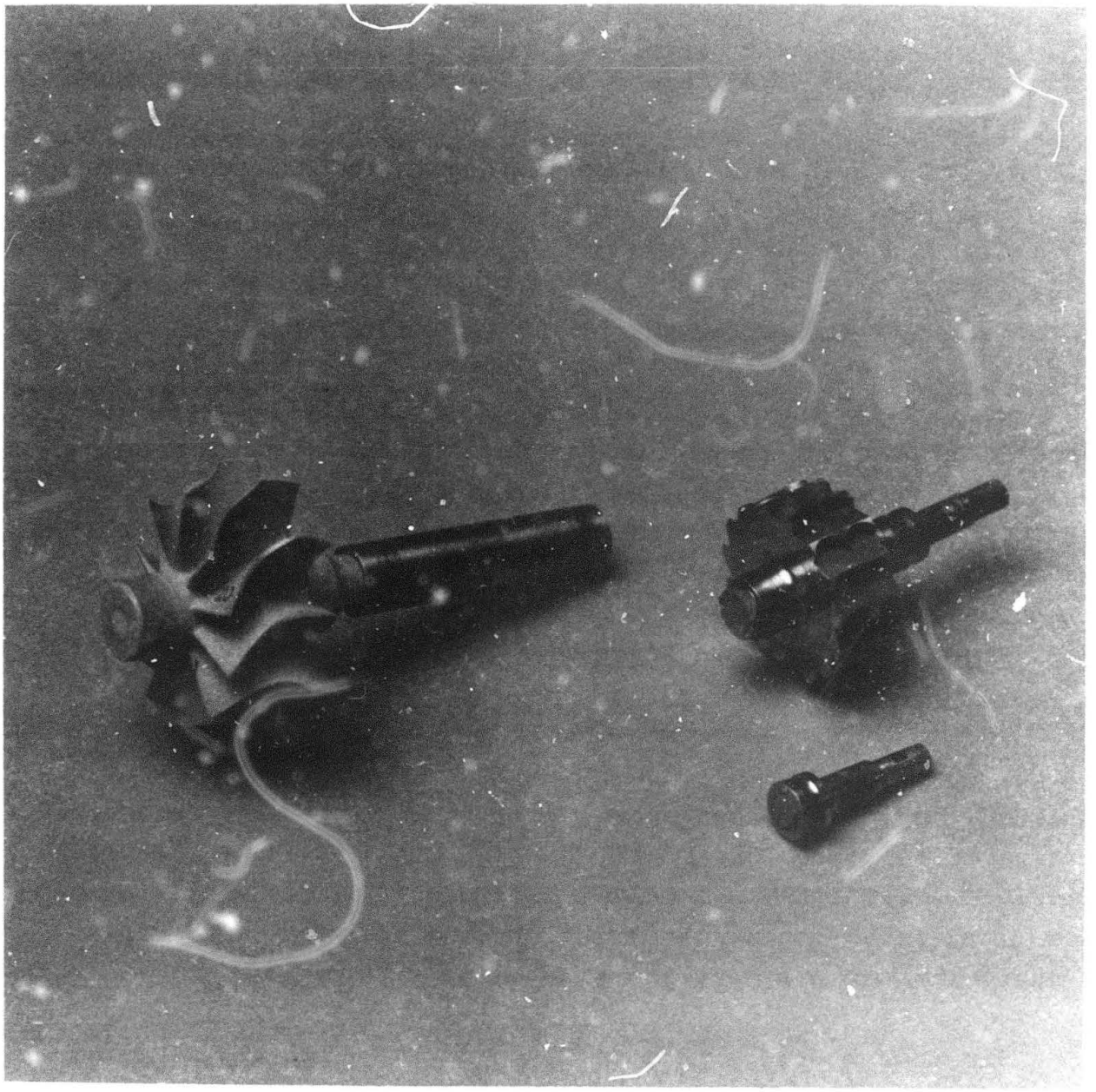

Figure 48. Ceramic and Metal Rotor after 183,000 rpm Room Temperature Spin Test.

P-87676

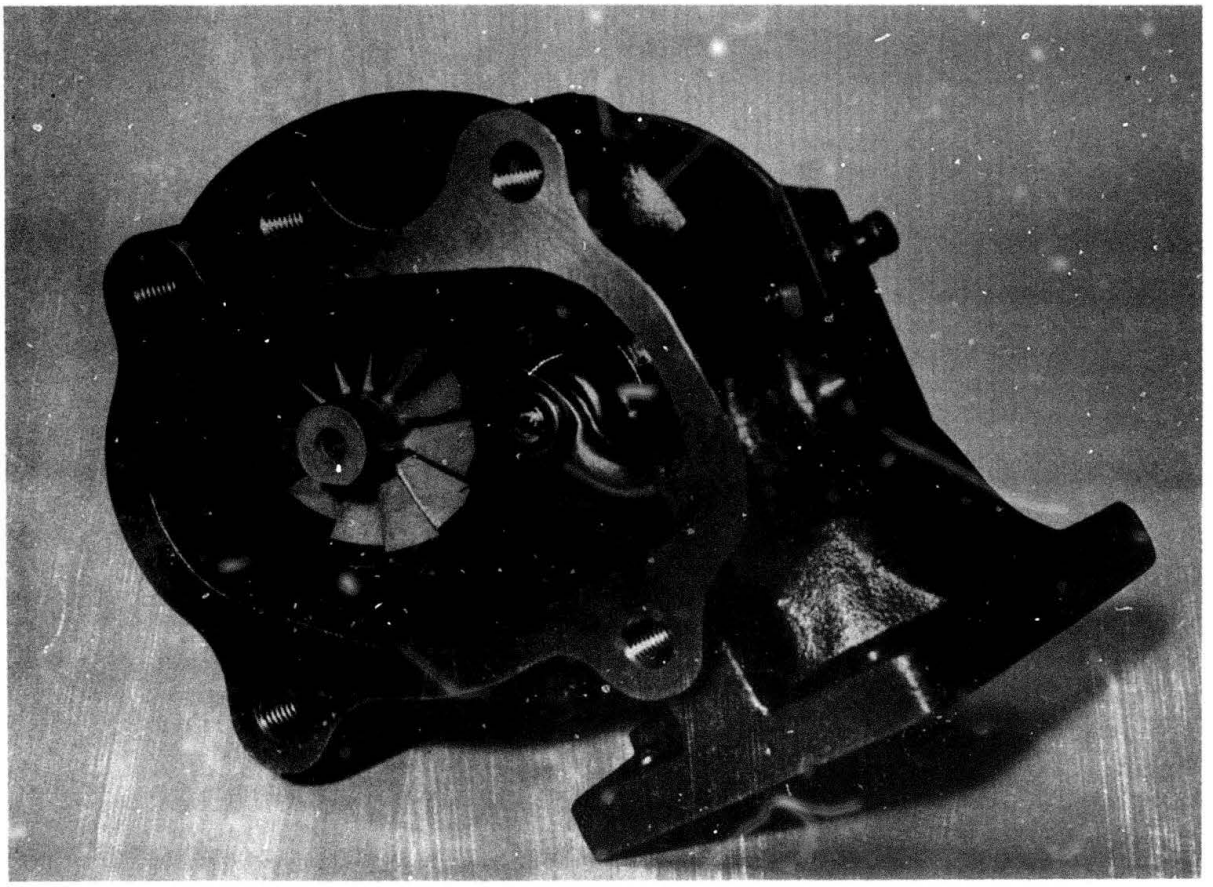

Figure 49. Ceramic Rotor in Turbocharger Test Housing.

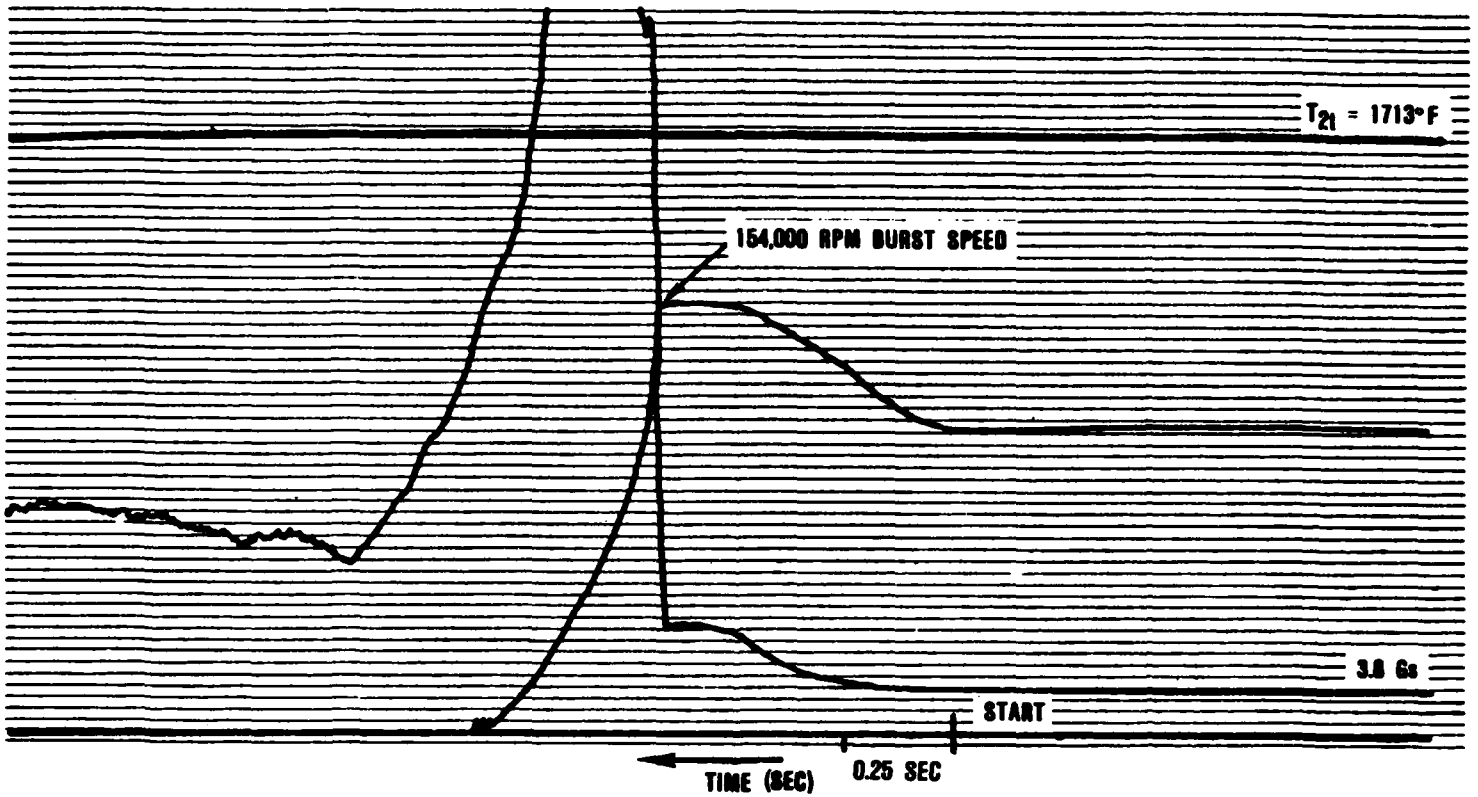

Figure 50. Burst Test Results Code 2 Rotor No. 01273-2.

rotors ranged from 143,000 to 197,000 rpm. Fractographic analysis (40x visual and scanning electron microscopy [SEM]) determined that the initial fracture origins were related to pre-existing defects that had been identified prior to testing. Figure 51 shows a typical failure origin, a pre-existing crack at the blade/hub transition. A summary of the Code 2 elevated temperature spin results are presented in Table 27.

TABLE 27. SUMMARY OF HOT SPIN RESULTS - CODE 2, T02 ROTORS

Rotor No.	Burst Speed (krpm)	Fracture Origin	Remarks
01273-2	154	Pre-existing crack at blade/ hub transition	Flaw was identified prior to test
01293-3	157	Same	Same
01293-5	160	Same	Same
01293-6	148	Same	Same
01293-8	197	Same	Same
01293-9	143	Internal Flaw?	Large crack in hub between blades was identified prior to test

Two lots of Code 7 rotor were prepared for elevated temperature spin testing at GAPCO. The shaft attachment used was a shrink-fit of INCO 907 shafts to the ceramic rotors.

Two rotors from the first lot (No. 04053-5 and 04053-7) failed during dwell at 120,000 rpm at temperature of 1730F and 1610F, respectively. The third rotor (No. 04053-10) failed at 102,000 rpm and 1360F while accelerating to dwell speed and temperature.

Initial examination of the failed rotors revealed that each had burst into numerous small pieces. Examination of the

51a. Defect Identified Before Spin Testing.

51b. Fracture Origin Identified After Spin Testing.

Figure 51. Spin Test Failures Caused by Pre-Existing Processing Flaws.

shafts in the failed region indicated that the fracture originated away from the ceramic-metal joint, probably in the hub region. An indepth fractographic analysis (40x) revealed that the three rotors failed due to flaws in the hub interior. The failure of the hub at relatively low speeds was probably related to internal flaws and/or residual silicon and is, therefore, consistant with the results reported in Section 3.

The results from the second lot of Code 7 rotors are presented in Table 28. The rotor burst results shown in Figure 52 are typical of the five rotors tested. Fractographic analysis (40x) indicated a failure origin in the hub interior probably due to the residual silicon, which appears as veins in Figure 52. The residual silicon and nonhomogenous structure of the rotor suggest that the processing of these rotors, in particular the nitriding step, was not optimized. These results are also consistant with those presented in Section 3.

TABLE 28. SUMMARY OF ELEVATED TEMPERATURE SPIN TEST RESULTS FOR CODE 7, T02 ROTORS (LOT #2)

Rotor No.	Burst Speed (krpm)	Temperature (F)	Remarks
09153-9	115	1650	Failed on way up to dwell condition
09153-16	120	1250	Failed on way up to dwell condition
09153-25	115	1550	Failed on way up to dwell condition
09153-21	120	1690	Failed on way up to dwell condition
08253-29	126	1770	Failed during acceleration from dwell

Figure 52. Code 7 Rotor No. 09153-9 After Burst Failure at 115,000 rpm and 1650F (2X).

A group of 3 fully processed Code 2 rotors with known defects were spin tested to evaluate the effect of flaws on the burst speed of the rotor. Table 29 is a summary of the major defects and the burst speeds for each rotor.

TABLE 29. RESULTS OF FLAW/BURST SPEED CORRELATION STUDY

Rotor No.	Burst Speed (Krpm)	Major Defects
01314-3	142	7 cracks at blade/hub transition
04124-15	168	1 crack at backface 8 flaw lines at blade/hub transition
04124-21	212	1 small crack at backface

Two additional materials are being evaluated by GAPCO for T02 ceramic turbocharger rotors. The elevated temperature spin test results are presented here for comparison with the results obtained on rotors developed under this program. The two materials were NGK Insulator's SN50 sintered silicon nitride and Kyocera's SN220 sintered silicon nitride. The spin test results are presented in Table 30. The results obtained on Code 2 rotors reported above are included for comparison.

TABLE 30. COMPARISON OF 1750F SPIN TEST RESULTS

Material	Rotors	Burst Speed (krpm)
Code 2 (This Program)	1	154
	2	157
	3	160
	4	148
	5	197
	6	143
	7	142
	8	168
	9	212
SN220 (Kyocera)	1	201
	2	189
	3	157
	4	197
	5	190
	6	180
	7	177
	8	155
SN50 (NGK)	1	238
	2	216
	3	188
	4	177
	5	206
	6	187
	7	174
	8	152
	9	140

6. CONCLUSIONS

- Room temperature and high temperature strengths of test bars of sintered injection-molded Si_3N_4 were significantly improved through iterative process modification and composition changes. The program goals were met with a composition containing 6 percent Y_2O_3 which had room temperature and 2250F strengths in excess of 100 ksi and 80 ksi respectively. However, a high nitrogen pressure sintering furance was required to densify this composition. A second composition containing 6 percent Y_2O_3 and 2 percent Al_2O_3 was developed which could be densified in a conventional furnance and exhibited room temperature and 2250F strengths in excess of 90 ksi and 60 ksi respectively. Based on these results, ACC has replaced the baseline material that existed at the start of the program (an 8 percent Y_2O_3 - 4 percent Al_2O_3 composition with room temperature and 2250F strengths of 76 ksi and 53 ksi respectively) with the lower additive composition.

- T02 turbocharger rotors were fabricated from the improved materials. Test bars cut from the interior of these rotors had strengths comparable to that of the injection-molded test bars

- The 3-D finite element analysis based on strength data predicted a capability of 380,000 rpm with a 0.1 percent probability of failure. The target for TO2 turbocharger production is 190,000 rpm with a 0.1 percent probability of failure. However, surface defects such as knit lines and cracks were consistently present in the rotors and contributed to a

lower burst speed during spin testing than was predicted based on the test bar strength data.

- The maximum burst speed during spin testing exhibited by rotors fabricated from the improved materials was 212,000 rpm. Rotors from other sources spin tested at GAPCO had similar results: 238,000 rpm maximum for TO2 rotors from NGK insulators, and 201,000 rpm maximum for TO2 rotors from Kyocera.

- Further fabrication development is necessary to eliminate the source of surface defects that limit rotor speed. Additional effort is also necessary to assess rotor dynamics and vibration to determine whether the turbocharger system design is influencing the spin test results.

- Since the 6 percent Y_2O_3 - 2 percent Al_2O_3 materials is an easily sintered composition with improved properties, it is replacing the earlier baseline composition in several ceramic turbocharger and automative gas turbine engine rotor development efforts at ACC.

7. REFERENCES

1. K. Styhr and J. Wimmer, "Low-Cost, Net-Shape Ceramic Radial Turbine Program," AMMRC Contract No. DAAG46-81-C-0006, Second Quarterly Report, GTEC Report 21-3991(2), August 17, 1981.

2. J.A. Mangels, "Sintering of Reaction-Bonded Silicon Nitride," in Nitrogen Ceramics II, ed. by F.L. Riley, Noordhoff International Publ. (1982).

3. C. Greskovich, "A Gas Pressure Sintering Process for Si_3N_4 Ceramics," in Nitrogen Ceramics II, ed. F.L. Riley, Noordhoff International Publ. (1982).

4. D.W. Richerson, "Effect of Impurities on the High Temperature Properties of Hot-Pressed Silicon Nitride," Bull. Amer. Ceram. Soc. 52, 560-62 (1973).

5. F.F. Lange, "High Temperature Strength Behavior of Hot-Pressed Si_3N_4: Evidence for Subcritical Crack Growth," J. Amer. Ceram. Soc., 57, 84-87 (1974).

6. G.E. Gazza, "Effect of Yttria Additions on Hot-Pressed Si_3N_4," Bull. Amer. Ceram. Soc. 54, 778-781 (1975).

7. K. Nishida and A. Tsuge, "High Strength Hot-Pressed Si_3N_4 with Concurrent Y_2O_3 and Al_2O_3 Additions," Bull. Amer. Ceram. Soc., 57, 424-426, 431 (1978).

8. F.F. Lange, "High Temperature Deformation and Fracture Phenomena in Polyphase Silicon Nitride Materials," in Nitrogen Ceramics II, ed. F.L. Riley, Noordhoff International Publ. (1982).

D.R. Clarke, "Thermodynamics of Cation-Diffusion Through an Intergranular Phase," in Nitrogen Ceramics II, ed. by F.L. Riley, Noordhoff International Publ. (1982).

APPENDIX A

STEPPED-TEMPERATURE STRESS-RUPTURE EVALUATION OF FOUR SINTERED SILICON NITRIDES

G. Quinn
Army Materials and Mechanics Research Center

Abstract

Four sintered silicon nitrides were screened for their static fatigue and creep resistance. The stepped-temperature stress-rupture test method was used for this purpose.

Introduction and Materials

Four sintered silicon nitrides were evaluated for their static fatigue and creep resistance by using the stepped-temperature stress-rupture (STSR) test method. Table A-1 lists the four materials, all of which were obtained from The Garrett Turbine Engine Company, Phoenix, Arizona. These materials were developed by AiResearch as part of a program to develop low-cost, net-shape turbine components.[1] Only a limited amount of material was made available, which precluded any testing other than STSR screening. Details of the fabrication procedures and the characterization of the four sintered silicon nitrides can be found in the progress reports of the above cited research program. None of the specimens were exposed to post processing hot isostatic pressing. These materials are a mid-1982 vintage.

Experimental Procedures

Six to eight specimens of size 2.5 x 1.5 by 25 mm were prepared for each material. The specimens were machined from large bend specimen fragments previously tested by Garrett.

Code	Starting Powder	Additives[a]	Processing	Density
2	GTE SN502 Alpha Silicon Nitride	6% Y_2O_3, 2% Al_2O_3	Sintered 1825C Nitrogen overpressure At ACC	3.21 g/cm^3
9	KBI-21-2000 Silicon Powder	6% Y_2O_3, 1% Fe_2O_3	Reaction Bonded at ACC followed by sintering with nitrogen overpressure At Ford Motor Co.	3.29 g/cm^3
11	Toshiba Alpha Silicon Nitride	6% Y_2O_3, 2% Al_2O_3	Sintered 1900C Nitrogen overpressure At ACC	3.06 g/cm^3
16	KBI-21-2000 Silicon Powder	6% Y_2O_3	Same as Code 9	3.33 g/cm^3

[a]By Wright

They were all surface ground in the longitudinal direction and had beveled chamfers.

The STSR test is a variation upon a standard stress-rupture experiment, except that a range of temperatures are applied to each specimen while it sustains a constant stress. The temperature sequence used for this study is illustrated in Figure 20 in the body of this report. Twenty 4-hour soaks at 800, 900, 1000, 1100, and 1225C in air were used. Loading was with four-point flexure fixtures with spans of 19.0 x 9.5 mm. Applied stresses were calculated from the simple elastic beam formulation. Complete details of the STSR method are in Reference 2.

Specimens that survived STSR testing intact were analyzed for creep strain. The inner gage length curvature was photographically enlarged, and the outer fiber strain calculated from the curvature. The specimens were subsequently fast fractured at room temperature in air with fixtures having spans of 31.8 and 10.4 mm. Care was taken to orient the specimens such that the portion that was in peak tension in the STSR testing was similarly loaded for the retained strength measurement.

All fracture surfaces were examined with a binocular microscope at magnifications up to 84x.

Results

The STSR results are summarized in Figure 20 in the body of this report).

Code 2

The Code 2 material exhibited the best static fatigue resistance, with only three highly stressed specimens failing

in the 900C step. Three other specimens survived the entire STSR sequence intact, and a fourth survived 7 hours at 1225C, whereupon, excessive creep deformation tripped a microswitch on the furnace. Permanent strains were negligible in the 900C failed specimens, but were significant in those which achieved 1225C. The 400, 300, 300, and 200 MPa loaded specimens had permanent outer fiber strains of 1.3, 1.03, 0.77, and 0.28 percents, respectively. All seven specimens had a uniform grey-white coloration without any unusual surface pitting or mottling. Numerous black inclusions of the order of 10 microns diameter were present, but apparently did not result in any failures.

The fracture surfaces of the 900C time-dependent failures had a fast fracture-like appearance with a mirror. Origins were either at a corner chamfer or along the tensile surface. These failures are consistent with a reduction of fast fracture strength in this material with temperature; from 641 MPa at room temperature to 441 MPa at 1232C[3].

The specimens that survived intact were fractured at room temperature for retained strength determination. Table A-2 summarizes the fractographic findings. Two low-stressed specimens had high retained strength with fracture mirrors centered upon small defects. The other two, which were under greater STSR loading, had less retained strength and failed from zones of creep cracking. This is consistent with the greater amount of deformation they had.

Code 9

Code 9 material was more susceptible to static fatigue failure. Three time-dependent failures at 900 and 1000C occurred at lower stresses than for Code 2 specimens. The room-temperature strength was not available, but the 1232C fast

TABLE A-2. CODE 2 STSR SURVIVORS.

STSR-Loading, (MPa)	Retained Strength at Room Temperature, (MPa)	Strain(%)	Fracture Origin
200	779	0.28	Surface defect in a small mirror
300	716	0.77	Surface defect in a small mirror
300	570	1.03	Creep cracked zone
400 (6.9 hours at 1225)	550	1.29	Creep cracked zone

fracture strength was 532 MPa[4]. Thus, the Code 9 time-dependent failures at 310-400 MPa are not likely due to a reduction in fast fracture strength with increasing temperature.

The specimen that broke at 1.8 hours at 900C had a corner origin which showed no evidence of slow crack growth. The specimen was a uniform dark grey in color. In sharp contrast was the distinct mottling that occurred in all specimens that were exposed to 1000C or above. The fracture origins for the two 1000C failures were at corner chamfers. A mottled oxide or transformed layer of material about 20-microns thick covered the 310-MPa specimen. No slow crack growth or creep crack markings were evident. Scanning electron microscopy would be necessary to positively identify the origin of failure, but it is likely that the oxide or transformed layer is important.

The two STSR survivors had negligible (<0.1 percent) creep strain and had high retained strengths: 724 and 761 MPa for the specimens STSR loaded to 300 and 200 MPa, respectively. The latter had a corner chamfer origin probably related to an unusually thick (~50 micron) surface layer and the former had an internal material defect.

Further testing is warranted on this material to determine if it indeed is sensitive to a phase instability at 1000C. It should be noted that HIP specimens were evaluated for its oxidation resistance in similar temperature regimes, and that no mottling or any other evidence of instability was detected[5] (see Subsection 2.6.1 in body of report).

Code 11

Six of eight specimens tested failed in a time-dependent manner. The first failure, a 300 MPa specimen at 4 minutes at 800C, was due to an unusually large (~250-micron diameter) pore. None of the other specimens had such a defect. The origins of the other time-dependent failures were difficult to identify. Usually, a poorly defined fracture mirror was present, and there were no prominent slow crack-growth or creep-cracking markings. The failures are not likely related to a reduction in fast fracture strength with increasing temperature, since the 1232C strength of this material is 530 MPa[4]. Additional stress rupture testing and more detailed fractography is necessary to identify the mechanism of time-dependent failure.

Both survivors had residual strains: 0.45 and 0.68 percents for the 200- and 300-MPa specimens, respectively. The retained strengths were high, 676 and 586 MPa. Distinctive fracture mirrors were evident in both, but SEM characterization would be necessary to specify the flaws. Of interest is that the specimen which failed on heating to 1225C had negligible creep, thus indicating that the STSR survivors accumulated all of their deformation at 1225C.

Most specimens were a uniform light grey coloration irrespective of temperature or time exposure. A mild mottling was noted on one of the two survivors. The 300-MPa specimen that failed at 3.3 hours at 1000C had a fracture origin that was a large zone which appeared as a mottling spot on the surface. This was the only instance where failure was related to apparent nonuniformity in the material.

Code 16

Code 16 material is identical to the Code 9 material except that Code 16 does not have the iron-oxide additive (Table A-1). As such, it is not surprising that its STSR performance was similar. Time-dependent failures occurred in the 800 to 1000C range and there was negligible creep deformation in any specimen, including the survivors. The retained strength of one survivor was 813 MPa.

Specimens that attained 1000C or higher exhibited pronounced mottling that was very similar to Code 9 specimens. Time-dependent fracture origins could be discerned with the binocular microscope, but scanning electron microscopy would be necessary to specifically identify their nature. However, the two 300-MPa specimens that failed in the 1000C step had crack growth-damage zones. Further testing is warranted to explore these features.

Summary

The STSR experiments revealed that the creep and static fatigue resistance vary between the four sintered silicon nitrides. None appear to offer both high creep and static fatigue resistance.

Code 2 was resistant to static fatigue failure but had significant creep deformation in the STSR survivors. The few time-dependent failures at 900C were consistent with a reduction in the fast fracture strength of the material with temperature. The Code 11 material had a similar processing additive, and it is not surprising that it also had significant creep at 1225C. Evidence indicates creep rates are substantially less at lower temperatures. Both Codes 2 and 11 materials had a uniform light grey coloration and had negligible

tendency toward mottling. Unlike the Code 2 material, Code 11 was susceptible to static fatigue failures between 900 and 1000C. This is not likely attributable to a reduction in fast fracture strength. Further testing would be necessary to identify the mechanism of time-dependent failure.

Codes 9 and 16 materials were quite different from the Codes 2 and 11 materials in that negligible creep deformation occurred. In all respects, the Codes 9 and 16 materials behaved similarly. The iron-oxide additive in Code 9 apparently had little effect on stress rupture or creep behavior. Both exhibited pronounced mottling upon attainment of 1000C or higher. There was some evidence of crack growth zones, which would account for the low (800 to 1000C) temperature failures. Additional testing is warranted to determine if some yttria phase instability may account for the stress rupture failures.

REFERENCES

1. Low-Cost, Net-Shape Ceramic Radial Turbine Program, AMMRC/Garrett Turbine Engine Company; Contract No. DAAG46-81-C-0006.

2. G.D. Quinn and R.N. Katz, "Stepped-Temperature Stress-Rupture Testing of Silicon-Based Ceramics," American Certification Society, Bulletin 57, No. 11, November 1978, pp 1057-58.

3. J. Smyth and K. Styhr, "Low-Cost, Net-Shape Ceramic Radial Turbine Program," Sixth Quarterly Progress Report, August 16, 1982.

4. J. Smyth, Private Communication.

5. J. Smyth and K. Styhr, "Low-Cost, Net-Shape Ceramic Radial Turbine Program," Fifth Quarterly Report, May 15, 1982.

DISTRIBUTION LIST

Copies

Copies	
12	Commander, Defense Technical Information Center, Cameron Station, Building 5, 5010 Duke Street, Alexandria, VA 22314
1	National Technical Information Service, 5285 Port Royal Road, Springfield, VA 22161
	Battelle Columbus Laboratories, Metals and Ceramics Information Center, 505 King Avenue, Columbus, OH 45201
1	ATTN: Mr. Winston Duckworth
1	Dr. D. Niesz
1	Mr. H. Midim (MCIC)
	Commander, Army Research Office, P.O. Box 12211, Research Triangle Park, NC 27709
2	ATTN: Information Processing Office
	Dr. G. Meyer
	Dr. F. Rothwarf
	Commander, U.S. Army Tank-Automotive Research and Development Command, Warren MI 48090
1	ATTN: Dr. W. Bryzik
1	Dr. H. Dobbs, Director
	Commander, U.S. Army Mobility Equipment Research and Development Command, Fort Belvoir, VA 22060
1	ATTN: DRDME-EM, Mr. P. Arnold
	Commander, U.S. Army Foreign Science and Technology Center, 220 7th Street, N.R., Charlottesville, VA 22901
1	ATTN: Military Tech, Mr. W. Marley
	Chief of Naval Research, Arlington VA 22217
1	ATTN: Dr. A. Diness
1	Dr. R. Pohanka
	Naval Research Laboratory, Washington, DC 20375
1	ATTN: Mr. D. Lewis
	Commander, U.S. Air Force Wright Aeronautics Laboratory, Wright-Patterson Air Force Base, OH 45433, Dr. M. Lindey
1	ATTN: AFWAL/MLLM, Dr. H. Graham
	AFWAL/MLLM, Dr. A. Katz
	AFWAL/MLLM, Mr. K. Mazdiyasni

DISTRIBUTION LIST

Copies

National Aeronautics and Space Administration, Lewis Research Center, 21000 Brookpark Road, Cleveland, OH 44135
1 ATTN: J. Accurio, USAMRDL

Department of Energy, Division of Transportation, 20 Massachusetts Avenue, N.W., Washington, DC 20545
3 ATTN: Mr. R. Schulz (TEC)
Mr. A. Chessness
Mr. C. Craig

National Research Council, National Materials Advisory Board, 2101 Constitution Avenue, Washington, DC 20418
1 ATTN: R. Spriggs
1 D. Groves

AiResearch Manufacturing Company, AiResearch Casting Company, 2525 West 190th Street, Torrance, CA 90505
1 ATTN: Mr. K. Styhr

Garrett Turbine Engine Company, Materials Engineering Dept., 111 South 34th Street, P.O. Box 5217, Phoenix, AZ 85010
1 ATTN: Dr. J. Wimmer, MS 93-393/503-4AL

SOHIO Engineered Materials (Carborundum)
P.O. Box 1054, Niagara Falls, NY 14302
1 ATTN: Mr. J. MacBeth
1 Mr. J. Hinton

Cummins Engine Company, Columbus, IN 47201
2 ATTN: Mr. T. Yonushonis
Dr. J. Patten

Synterials, Inc., 1821 Michael Faraday Drive, Reston, VA 22090
1 ATTN: Mr. R. Engdahl

Ford Motor Company, Turbine Research Department, 20000 Rotunda Drive, Dearborn, MI 48121
1 ATTN: Mr. A. McLean
1 Mr. T. Whelan
1 Mr. J. Mangels

DISTRIBUTION LIST

Copies

General Electric Company, Research and Development Center, Box 8, Schenectady, NY 12345
1 ATTN: Dr. R. Charles
Dr. C. Greskovich

Georgia Institute of Technology, EES, Atlanta, GA 30332
1 ATTN: Mr. J. Walton

GTE Laboratories, Waltham Research Center, 40 Sylvan Road, Waltham, MA 02154
1 ATTN: Dr. J. Neal
1 Dr. J. Smith

IIT Research Institute, 10 West 35th Street, Chicago, IL 60616
1 ATTN: Mr. S. Bortz, Director, Ceramics Research

Caterpillar Tractor Co., Solar Division, 2200 Pacific Highway, P.O. Box 80966, San Diego, CA 92138
1 ATTN: Dr. A. Metcalfe

Kawecki Berylco Industries, Inc., P.O. Box 1462, Reading, PA 19603
1 ATTN: Mr. R. Longenecker

Massachusetts Institute of Technology, Department of Metallurgy and Materials Science, Cambridge, MA 02139
1 ATTN: Prof. R. Coble
1 Prof. H. Bowen
1 Prof. W. Kingery

Norton Company, Worcester, MA 01606
1 ATTN: Dr. J. Penzering
1 Dr. M. Torti

Pennsylvania State University, Material Science Department, University Park, PA 16802
1 ATTN: Prof. R. Tressler

Rockwell International Corporation, Science Center, 1049 Camino Dox Rios, Thousand Oaks, CA 91360
1 ATTN: Dr. F. Lange

United Technologies Research Center, East Harford, CT 06108
1 ATTN: Dr. J. Brennan

DISTRIBUTION LIST

ies

University of Washington, Ceramic Engineering Division, FB-10, Seattle, WA 98195
1 ATTN: Prof. J. Mueller
1 Prof. A. Miller

Westinghouse Electric Corporation, Research Laboratories, Pittsburgh, PA 15235
1 ATTN: Dr. R. Bratton

NASA Lewis Research Center, 21000 Brookpark Road, Cleveland, OH 44135
1 ATTN: T. Miller

Conservation and Advanced System Programs Metals and Ceramics Division, Oak Ridge National Laboratory, Nuclear Division, P.O. Box X, Oak Ridge, TN 37830
1 ATTN: Dr. T. Schaffhauser
1 Dr. V. Tennery
1 Dr. R. Johnson

General Motors Corporation, Detroit Diesel Allison, P.O. Box 894, Indianapolis, IN 46206
1 ATTN: P. Heitman, T-15
1 H. Helms (2 cps), T-15
1 R. Johnson, T-15

General Electric Company, Aircraft Engine Group, 1000 Western Avenue, Lynn, MA 01910
1 ATTN: A. Bellin (A-37428)

Pure Carbon Incorporated, St. Marys, PA 15856
1 ATTN: W. Shobert

U.S. Army Advance Concepts & Technology Office, HQDA (DAMA-ARZ-E), Washington, D.C. 20310
1 ATTN: Dr. C. Church

1 University of Washington, College of Engineering, Roberts Hall FB-10, Seattle, WA 98195
ATTN: Prof. R. Bradt

DISTRIBUTION LIST

pies

US ARMY Materials and Mechanics Research Center,
Arsenal StreeT, Watertown, MA 07172

1 ATTN: Dr. R. Katz
1 Dr. E. Lenoe
1 Dr. G. Quinn
1 Dr. G. Gazza
1 Dr. Wright, Director
1 Dr. Chait

US ARMY Applied Technology Laboratory,
Ft Eustis, Virgina 23604-5577

1 ATT: Mr. H. Morrow
1 Mr. J. Lane